

1. Structure/function analysis of the Hsp70 cochaperone Bag-1
2. Characterization of a monocyte/macrophage-specific receptor for heat shock protein 70

## **Inaugural - Dissertation**

zur

Erlangung des Doktorgrades  
der Mathematisch-Naturwissenschaftlichen Fakultät  
der  
Universität zu Köln

vorgelegt von

**Holger Sondermann**

aus Köln

-2001-

Die vorliegende Arbeit wurde in der Zeit von Dezember 1997 bis März 2001 am Max-Planck-Institut für Biochemie in Martinsried unter Anleitung von Prof. Dr. Franz-Ulrich Hartl in der Abteilung Zelluläre Biochemie angefertigt.

**Gutachter: Priv.-Doz. Dr. Sabine Waffenschmidt**

**Prof. Dr. Thomas Langer**

**Prof. Dr. Franz-Ulrich Hartl**

**Vorsitz: Prof. Dr. Jürgen Dohmen**

Tag der mündlichen Prüfung: 12. Juni 2001

---

## Zusammenfassung

### Struktur-Funktions-Analyse des Hsp70-Kochaperons Bag-1

Molekulare Chaperone der Hitzeschockprotein 70 (Hsp70)-Familie sind konserviert von *E. coli* bis zu Säugetieren. Sie assistieren sowohl der Faltung naszierender Proteine als auch der Rückfaltung von Proteinen, die durch Streß denaturiert wurden. In Eukaryoten existieren Paraloge im endoplasmatischen Reticulum und in Mitochondrien. Strukturell sind Hsp70-Proteine aus einer amino-terminalen ATPase-Domäne und einer carboxy-terminalen Peptidbindungsdomäne aufgebaut. Im eukaryotischen Zytosol agiert Hsp70 zusammen mit verschiedenen Kochaperonen, die entweder die ATP-Hydrolyse oder die Peptidbindung beeinflussen oder eine Verbindung zum Hsp90-Chaperon-System vermitteln. Das Kochaperon Bag-1 stimuliert die ATPase-Rate von Hsp70 in Abhängigkeit von Hsp40, einem weiteren Kochaperon von Hsp70, und ist involviert in verschiedene zelluläre Prozesse wie zum Beispiel Transkription und Apoptose.

Eine stabile Domäne von humanem Bag-1M (Bag-Domäne) wurde durch limitierte Proteolyse bestimmt. Die isolierte Bag-Domäne weist die gleiche Affinität zu Hsp70 und dessen ATPase-Domäne auf wie das Bag-1-Vollängenprotein. Weiterhin steigert die Bag-Domäne die Hsp40-stimulierte ATP-Hydrolyse von Hsp70 und die Nukleotid-abhängige Substrat-Freisetzung vom Chaperon in gleichem Maße wie das Bag-1-Vollängenprotein. Kristallisation und Strukturlösung eines Komplexes bestehend aus der ATPase-Domäne von Hsc70, dem konstitutiv-exprimierten, zytosolischen Hsp70 und der Bag-Domäne führte zu einem 1.9 Å-Modell des Nukleotid-freien Komplexes. Dabei induziert die Bag-Domäne eine Konformation in Hsp70, die identisch ist mit der des bakteriellen Hsp70-Homologs, DnaK, wenn dieses den Nukleotidaustauschfaktor GrpE gebunden hat. Dieses Ergebnis etabliert Bag-1 und andere Proteine, die eine Bag-Domäne enthalten, als GrpE-ähnliche Nukleotidaustauschfaktoren von Hsp70, obwohl Bag-1 und GrpE keine Sequenzhomologien aufweisen. Diese Frage wurde bisher in der Literatur kontrovers diskutiert. Die hohe Auflösung der Komplex-Struktur erlaubte eine detaillierte Analyse der konformationellen Änderungen der Reste in der ATP-Bindetasche von Hsp70, die an der ATP-Bindung und -Hydrolyse beteiligt sind. Mutationsanalysen bestätigten die biochemischen Vorhersagen über die Relevanz der Bindung von Bag-1 an Hsp70. Außerdem wurden weitere Bag-Proteine in sämtlichen eukaryotischen Organismen durch strukturelle Sequenzvergleichsanalyse identifiziert. Das so identifizierte Bag-Protein von *S. cerevisiae*, Snl1p, wurde biochemisch analysiert, um dessen Funktion als Bag-homologen Nukleotidaustauschfaktor für Hsp70-Chaperone zu verifizieren.

### Rezeptor-vermittelte Bindung und Aufnahme von Hsp70 durch Antigen-präsentierende Zellen

Neben der zentralen Rolle bei der Proteinfaltung wurde gezeigt, daß molekulare Chaperone spezifische Immunantworten gegen verschiedene Tumorarten als auch gegen Virus-infizierte Zellen auslösen können. Die Rezeptor-vermittelte Endozytose von Chaperon-Peptid-Komplexen wird dabei als ein entscheidender Schritt diskutiert. Der molekulare Mechanismus der Chaperon-vermittelten Tumorregression ist jedoch bislang weitestgehend unverstanden.

Im zweiten Teil der vorliegenden Arbeit wurde eine auf der Durchflusszytometrie basierende Methode entwickelt, um die spezifische Bindung des humanen, zytosolischen Hsp70-Proteins an professionelle Antigen-präsentierende Zellen zu zeigen. Die

---

Behandlung der Zelloberfläche mit Proteasen resultierte im Verlust der spezifischen Bindung von Hsp70 und demonstrierte damit die Existenz eines Proteinrezeptors. Die Bindungsstellen für Hsp70 auf der Zelloberfläche konnten gesättigt werden. Die Affinität des Hsp70-Rezeptors liegt im submikromolaren Bereich. Die Bindung war insensitiv gegenüber der Anwesenheit von Nukleotid, Peptid und Kochaperonen, jedoch spezifisch für Hsp70 und Hsc70 von höheren Eukaryoten. Außerdem war die Hsp70-Bindung ausgesprochen Zelltyp-spezifisch und wurde nur an Makrophagen und Monocyten beobachtet. Die Bindung wurde nicht durch CD14 vermittelt, den Rezeptor für Lipopolysaccharide, der für Zellen dieser Abstammungslinie charakteristisch ist, und außerdem in der Chaperon-vermittelten Aktivierung von Monocyten beteiligt ist. Gebundenes Hsp70 wurde bei physiologischen Temperaturen von den Zellen endozytiert, welches zu einer vesikulären Färbung führte. Diese Ergebnisse liefern die Basis für weitere Untersuchungen der molekularen Mechanismen Chaperon-vermittelter Antigenpräsentierung, bzw. der Aktivierung von Monocyten und Makrophagen durch molekulare Chaperone.

---

## Contents

A Summary.....	8
B Introduction.....	10
B.1 Chaperone mediated protein folding.....	10
B.1.1 Protein folding <i>in vitro</i> .....	10
B.1.2 Protein folding in the cell.....	11
B.1.3 Chaperone families and folding networks.....	13
C Structure/function analysis of the Hsp70 cochaperone Bag-1.....	17
C.1 Introduction.....	17
C.1.1 Cellular function of Hsp70.....	17
C.1.2 Structure of Hsp70.....	19
C.1.3 The molecular mechanism of Hsp70 function.....	21
C.1.4 Cochaperones of Hsp70.....	22
C.1.5 The Bag protein family of Hsp70 cochaperones.....	25
C.1.5.1 Primary sequence of the Bag-1 isoforms.....	25
C.1.5.2 Cellular function of Bag-1.....	26
C.1.5.3 Other Bag proteins.....	27
C.1.6 Aim of the project.....	29
C.2 Material and Methods.....	30
C.2.1 Chemicals.....	30
C.2.2 Instruments.....	30
C.2.3 Media and buffers.....	31
C.2.3.1 Media.....	31
C.2.3.2 Buffers.....	32
C.2.4 Plasmids and bacterial strains.....	33
C.2.4.1 Plasmids.....	33
C.2.4.2 Competent <i>E. coli</i> cells using the RbCl-method.....	33
C.2.4.3 Molecular cloning using polymerase chain reaction (PCR).....	34
C.2.4.4 Site-directed mutagenesis.....	35
C.2.5 Biochemical methods.....	36
C.2.5.1 SDS polyacrylamide gelelectrophoresis (SDS-PAGE).....	36
C.2.5.2 Staining methods for protein gels.....	37
C.2.5.3 Protein expression and purification.....	37
C.2.5.4 Purification of Hsc70 from bovine brain.....	39
C.2.5.5 Determination of protein concentration in solution.....	39
C.2.5.6 Limited proteolysis and mass spectroscopy.....	40
C.2.5.7 Isothermal titration calorimetry (ITC).....	40
C.2.5.8 ATPase assay.....	41
C.2.5.9 Covalent coupling of antibodies to Protein G beads.....	41
C.2.5.10 Preparation of yeast lysates.....	42
C.2.5.11 Western blotting.....	43
C.2.5.12 Pull downs using His <sub>6</sub> -tagged proteins bound to NiNTA beads.....	43
C.2.5.13 Substrate release assay.....	44

---

C.2.6 X-ray crystallographic Methods .....	46
C.2.6.1 Theory of X-ray diffraction.....	46
C.2.6.2 Structure determination using X-ray diffraction.....	51
C.2.6.3 Protein crystallization.....	51
C.2.6.4 Data collection and data reduction.....	53
C.2.6.5 Structure solution .....	54
C.2.6.6 Model building and refinement .....	55
C.2.6.7 Analysis and presentation of structure models.....	56
C.3 Results .....	57
C.3.1 Domain structure of Bag-1M and Hsc70 .....	57
C.3.2 Characterization of the isolated Bag domain .....	57
C.3.4 Crystallization, data collection and processing .....	62
C.3.5 Crystal structure of the Hsc70 ATPase/Bag complex.....	67
C.3.6 Mutational analysis of the Bag/Hsc70 interaction .....	70
C.3.7 Characterization of the Bag protein Sn11p from <i>S. cerevisiae</i> .....	74
C.4 Discussion .....	79
C.4.1 Structural comparison of Bag-1 and GrpE.....	79
C.4.2 Molecular mechanism of Bag-1 function on Hsp70 .....	81
C.4.3 Bag-1 function in protein folding <i>in vitro</i> and <i>in vivo</i> .....	82
C.4.4 <i>S. cerevisiae</i> as a model system for analyzing Bag-1 function <i>in vivo</i> .....	84
D Characterization of a monocyte/macrophage-specific receptor for Hsp70.....	86
D.1 Introduction.....	86
D.1.1 Mononuclear phagocytes and dendritic cells .....	86
D.1.2 Antigen presentation .....	87
D.1.3 Heat shock proteins in cellular immunity .....	88
D.1.4 Aim of the project .....	91
D.2 Material and Methods .....	92
D.2.1 Chemicals .....	92
D.2.2 Instruments .....	92
D.2.3 Buffer .....	93
D.2.4 Plasmids and bacterial strains .....	93
D.2.5 Mammalian cell culture and cell lines .....	93
D.2.5.1 Cell lines.....	94
D.2.5.2 Isolation of fresh peripheral blood cells.....	94
D.2.5.3 Generation of primary dendritic cells .....	95
D.2.6 Protein expression and purification.....	95
D.2.7 Hsp binding and uptake.....	96
D.2.8 Confocal microscopy .....	97
D.3 Results.....	98
D.3.1 Cell-specific binding and uptake of Hsp70 .....	98
D.3.2 Saturable Hsp70 cell surface binding by a proteinaceous receptor .....	101
D.3.3 Specific binding of mammalian but not bacterial Hsp70 to ANA-1 cells .....	102
D.3.4 Localization of bound and internalized Hsp70 by confocal microscopy.....	104
D.3.5 Receptor-mediated binding of Hsp70 to PBMCs but not PBLs .....	105
D.3.6 Loss of Hsp70 binding properties upon differentiation to dendritic cells.....	108
D.4 Discussion.....	110
E References .....	112

---

F Appendix.....	134
F.1 Amino acid sequences of Hsc70 and Bag-1M.....	134
F.1.1 Amino acid sequence of rat Hsc70 .....	134
F.1.2 Amino acid sequence of human Bag-1M .....	134
F.2 Abbreviations.....	135
F.3 Publications .....	138
F.4 Published Meeting Abstracts .....	138
F.5 Unpublished Meeting Abstracts .....	138

## A Summary

### Structure/function analysis of the Hsp70 cochaperone Bag-1

Molecular chaperones of the heat shock protein 70 (Hsp70) family are conserved from *E. coli* to mammals and assist the folding of nascent proteins as well as the refolding of proteins denatured under stress. In eukaryotes, Hsp70 paralogs exist in the endoplasmic reticulum and mitochondria. Structurally, all family members contain an N-terminal ATPase domain and a C-terminal peptide binding domain. In the eukaryotic cytosol, Hsc70 acts together with various cochaperones which either influence ATP hydrolysis or the peptide binding state of Hsp70, or functionally connect Hsp70 to the Hsp90 chaperone system. The cochaperone Bag-1 stimulates the ATPase rate of Hsp70 in a Hsp40 dependent manner, and functions in cellular processes such as transcription and control of apoptosis.

A stable domain of human Bag-1 was defined by limited proteolysis. The domain had the same affinity for the ATPase domain of Hsp70 as the full length proteins, as measured by isothermal titration calorimetry. Furthermore, the domain is fully functional in stimulating the ATPase rate of Hsc70, and in nucleotide-dependent release of polypeptide substrate from the chaperone. Crystallization and structure solution of the complex of the fragment of Bag-1 and the ATPase domain of Hsc70 led to a 1.9 Å model of the nucleotide-free complex. Interestingly, Bag-1 induced a conformational change in Hsp70 identical to that induced in the bacterial Hsp70 chaperone DnaK by the cochaperone GrpE. This suggests that like GrpE, Bag-1 may act as a nucleotide exchange factor for Hsp70, although there is no sequence similarity between the two cochaperones. The high resolution of the structure allowed an analysis of the conformational changes of residues which would contact the nucleotide providing insight into the molecular mechanism by which nucleotide exchange is achieved. Mutational analysis confirmed the biochemical predictions. Various Bag homologs were predicted based on the presence of key residues involved in mediating the interaction of the Bag domain with Hsp70. The proposed *S.cerevisiae* Bag protein, Snl1p, was analyzed biochemically confirming its function as a Bag homolog.

### Receptor-mediated binding and uptake of Hsp70 by antigen presenting cells

Besides their important role in protein folding, chaperones have been shown more recently to mediate specific immune responses against various tumors as well as virally infected cells, a process proposed to involve receptor-mediated endocytosis of chaperone-peptide complexes. However, the molecular mechanism behind this chaperone-mediated anti-tumor response is only poorly understood.

In the second part of this thesis, a flow cytometry-based assay was established to analyze the specific binding of mammalian cytosolic, stress-inducible Hsp70 and constitutively expressed Hsc70 to the cell surface of professional antigen presenting cells. Treatment of the cell surface with proteases resulted in loss of binding, demonstrating the existence of a proteinaceous receptor. Binding was saturable and occurred with sub-micromolar affinity. Hsp70 binding was highly cell-type specific and was restricted to cells from the monocyte/macrophage lineage. However, the binding was apparently not mediated by CD14, the LPS receptor, which was reported to be involved in Hsp70-mediated activation of macrophages and monocytes. Bound Hsp70 was internalized into an intracellular, vesicular compartment. These results provide the basis for a molecular dissection of the pathway of Hsp70-mediated antigen presentation.





## B Introduction

### B.1 Chaperone mediated protein folding

Proteins are central to all biological processes such as metabolism, motility, intra- as well as intercellular communication and transport, and maintenance of cellular structure. All these processes rely on highly specific molecular recognition mechanisms, which are manifested in the three-dimensional fold of proteins. Proteins are synthesized as linear polypeptide chains, which in theory could adopt an enormous number of different conformations, but *in vivo* their native, active structure is usually well defined and attained efficiently. The aim of protein folding research is to understand how this highly selective process is achieved and maintained.

#### B.1.1 Protein folding *in vitro*

In the late 1960's, Anfinsen performed key experiments on protein refolding *in vitro*, monitoring the gain of activity of purified, heat-denatured Ribonuclease A as a measure of productive folding (Taniuchi and Anfinsen, 1969). His experiments demonstrated that the information necessary for reaching the native, folded state lies in the amino acid sequence of the folding protein itself, as folding occurred spontaneously without the aid by additional factors (Anfinsen, 1972; Anfinsen, 1973). The folding reaction was reversible and proceeded with biologically relevant kinetics (usually within seconds) (Schechter et al., 1970).

The Levinthal paradox illustrates in a striking manner the complexity of the folding problem. Given a protein consisting of 100 amino acids and assuming that each amino acid only adopts the two most stable conformations of its main chain ( $\alpha$  and  $\beta$ ) (Ramachandran and Sassiexharan, 1968; Branden and Tooze, 1991), there would be  $10^{30}$  different conformations the chain could adopt. An unbiased, random folding process leading to the native structure, i.e. to a defined structure among the  $10^{30}$  possible ones, would take over a billion years, even if a single conformational change would take only

$10^{-11}$  sec (Levinthal, 1968; Levinthal, 1969), a conundrum that became known as the Levinthal paradox. As a possible solution, it was suggested that folding occurs along a vectorial route via folding intermediates containing increasing amounts of native-like structural elements (Baldwin, 1996; Privalov, 1996; Ptitsyn, 1998). This idea of a defined folding pathway was suggested to minimize the number of conformations that must be reached during the folding process. In the following years, folding intermediates were detected for several proteins, including apomyoglobin, ribonuclease A, barstar and lysozyme (Scheraga et al., 1984; Udgaonkar and Baldwin, 1990; Radford et al., 1992; Barrick and Baldwin, 1993; Agashe et al., 1995; Jamin and Baldwin, 1996; Matagene et al., 1997; Wildegger and Kiefhaber, 1997).

More recently, experiments demonstrating the existence of multiple folding pathways for a given protein have led to a more complex view of protein folding reactions. Rather than following a defined pathway, the folding process is described by an energy landscape or folding funnel with a vast array of down-hill routes to the native state (Baldwin, 1995; Dobson et al., 1998). Typically, the native state of a protein can be described thermodynamically as the free energy minimum of all possible structures (the bottom of the folding funnel). Populated intermediates could be either transient states (local energy minima) or kinetically trapped states (misfolded states) (Radford, 2000; Schultz, 2000). Whether a denatured protein is prone to intramolecular aggregation or reaches the native state efficiently depends on the rate of the folding process, that is how fast a globular structure is reached in which hydrophobic surfaces are minimally exposed. How a given amino acid sequence encodes a defined three-dimensional structure is not yet understood precisely.

### B.1.2 Protein folding in the cell

Protein folding *in vitro* differs substantially from protein folding in a living cell. The high complexity of the latter process is due to the very high concentration of macromolecules in the cell (about 300 g/l) providing a crowded environment. This results in different thermodynamic properties of partially folded proteins and in stronger competition of unproductive side reactions (aggregation) with the productive folding pathway compared to the situation *in vitro* (Hartl, 1996; Ellis, 1997). The *in vivo* situation

is complicated further by an intimate coupling of biosynthesis and folding since the rate of folding is much faster ( $t_{1/2} < 1$  sec) than the translation rate (4-20 amino acids per sec). Emerging polypeptides at the ribosome either fold cotranslationally or have to be protected from aggregation and misfolding until translation is complete (Netzer and Hartl, 1998). Other restrictions in parameters such as ionic strength, temperature and pH within the cell limit the possible folding pathways additionally.

In the past decade, a cellular machinery of various proteins, called molecular chaperones, has been identified and studied. These proteins capture nonnative structures of other proteins, assist their proper folding but are themselves not components of the final biologically active structure (Hartl, 1996; Bukau and Horwich, 1998). To do this, chaperones recognize exposed hydrophobic surfaces of nascent or misfolded polypeptides which will be buried in the native state (Dobson et al. 1998). Binding and release of bound polypeptide substrates by chaperones is often achieved by ATP-driven conformational changes, permitting multiple rounds of interactions between substrates and the folding machinery. Nevertheless, chaperones do not provide an input of structural information in the folding process and hence chaperone action is in agreement with Anfinsen's findings that the primary sequence determines the native fold (Anfinsen, 1973). It was suggested that chaperones provide an environment in which the productive pathway leading to the native structure, the thermodynamic free energy minimum in the folding landscape, is favored and the accumulation of kinetically trapped intermediates is minimized. Chaperones are not folding catalysts in that they typically increase the yield but not the rate of a folding reaction, and can even slow down folding kinetics in some cases. This is in contrast to folding catalysts like peptidylprolyl isomerases or protein disulfide isomerases, which catalyze isomerization reactions required for folding.

Besides their function in *de novo* protein folding, molecular chaperones can refold proteins that have become misfolded because of some denaturing stress on the cell. Consistent with this, chaperone expression is upregulated upon cellular stress (heat shock, oxidative stress, etc.), i.e. under conditions that increase the danger of misfolding or aggregation. In addition to protein folding, chaperones are involved in several other cellular processes, e.g. protein targeting, degradation, and signal transduction (Ellis, 2000).

Despite these sophisticated chaperone mechanisms, there are special cases where mutant proteins with aberrant stability or folding remain misfolded persistently. In recent

years, it has been realized that the basis for several diseases (e.g. Creutzfeld-Jakob, Alzheimers or Huntingtons disease) lies in a conformational change or aggregation of proteins (Cohen, 2000; Dobson, 1999; Wanker, 2000).

### B.1.3 Chaperone families and folding networks

During translation, the polypeptide chain of a nascent protein appears at the ribosome exposed to the cytosol. Folding into a stable tertiary structure is only possible once a domain has been translated. Hydrophobic surfaces will be exposed during protein synthesis until the full information for its tertiary structure has been translated. Especially on polysomes, the local accumulation of aggregation-prone surfaces would be problematic for the cell if efficient chaperone machines did not exist (Goodsell, 1991).

Prevention of aggregation of nascent chains is achieved by binding of chaperones and other factors to exposed hydrophobic surfaces. In bacteria, there are two ribosome-bound factors that recognize newly synthesized polypeptide chains, namely the peptidylprolyl isomerase trigger factor and the 70 kDa heat shock protein (Hsp70) homolog DnaK (Deuerling et al., 1999; Teter et al., 1999). The situation in eukaryotes is less well established. In yeast, Ssb proteins, specialized Hsp70 proteins, bind to nascent chains on the ribosome (Pfund et al., 1998). With increasing polypeptide length, chaperones of the Hsp40/DnaJ and Hsp70/DnaK family bind to exposed hydrophobic stretches in bacteria and higher eukaryotes (Langer et al., 1992; Frydman et al., 1994).

The Hsp70 family represents the most highly conserved of the heat shock proteins being at least 45% identical in sequence between the most distantly related species (Bukau and Horwich, 1998). It includes constitutively expressed and inducible members in several cellular compartments (e. g. Hsc70 and Hsp70 in the mammalian cytosol, Ssa in the yeast cytosol, BiP/Grp78 in the endoplasmic reticulum, and mitochondrial Hsp70). Hsp70 proteins are very abundant accounting for as much as 1-2% of total cellular protein (Herendeen et al., 1979). Most of the biochemical work has been carried out with the bacterial chaperone DnaK. Nevertheless, it is believed that the eukaryotic Hsp70s in principle function in a similar manner. Henceforth, the general term 'Hsp70' will be used for all members of this family; when appropriate, the distinction will be made between the different mammalian homologs, especially the constitutive (Hsc70) and inducible

(Hsp70) homologs. The mechanism and function of Hsp70 and Hsp40 will be described in more detail in the following chapters.

In addition to their association with nascent chain-binding chaperones, slow-folding proteins with a tendency to aggregate (10-30% of all bacterial proteins; Horwich et al., 1993; Ewalt et al., 1997) can interact with another chaperone system which provides a sequestered environment for folding, the barrel-shaped chaperonins. Representatives in eukaryotes are the cytosolic TRiC/CTT and the mitochondrial Hsp60, but the best-characterized chaperonin is the bacterial protein GroEL. GroEL is composed of 14 subunits with a molecular weight of 60 kDa each (Langer et al., 1992). The subunits assemble into two rings forming a cylinder-shaped structure with two central cavities (Braig et al., 1994). In contrast to Hsp70 proteins, which bind linear sequences, the chaperonins recognize collapsed folding intermediates (molten globules) (Hayer-Hartl et al., 1994). The cochaperone GroES (Hsp10 in mitochondria) closes the GroEL cavity and the substrate molecule is completely encapsulated by the chaperone complex. The cavity provides a hydrophilic environment in which the protein can fold into its native structure in one or more rounds of interaction with the chaperone system (Martin et al., 1993; Mayhew et al., 1996). Thereby, substrate binding and release is regulated by the ATPase activity of GroEL.

The eukaryotic chaperonin works independently of a GroES cofactor but it is likely that its general mechanism is comparable to GroEL/ES. Helical extensions at each subunit are suggested to fulfil the function of the cochaperone (Klumpp et al., 1997). Nevertheless, substrate-specificity seems to be more restricted for the eukaryotic chaperonins. So far, only actin and tubulin have been identified as substrates *in vivo*. There is also a recently identified factor, Prefoldin/Gim, probably working in concert with the chaperonin system (Vainberg et al. 1998; Leroux and Hartl, 2000).

A scheme of the protein folding pathways in the cytosol of prokaryotes and eukaryotes is presented in Figure 1 (modified from Bukau et al., 2000). As indicated, only two systems, the Hsp70/DnaK and chaperonin systems, are capable of promoting folding proteins as opposed to simply preventing aggregation. In some cases these also work cooperatively. All other chaperone families mentioned in the next paragraphs bind to (partially) unfolded proteins and prevent their aggregation but require specific interactions with Hsp70/DnaK or the chaperonins to promote refolding. Others work downstream of Hsp70, e.g. Hsp90, and possess a more specialized function.

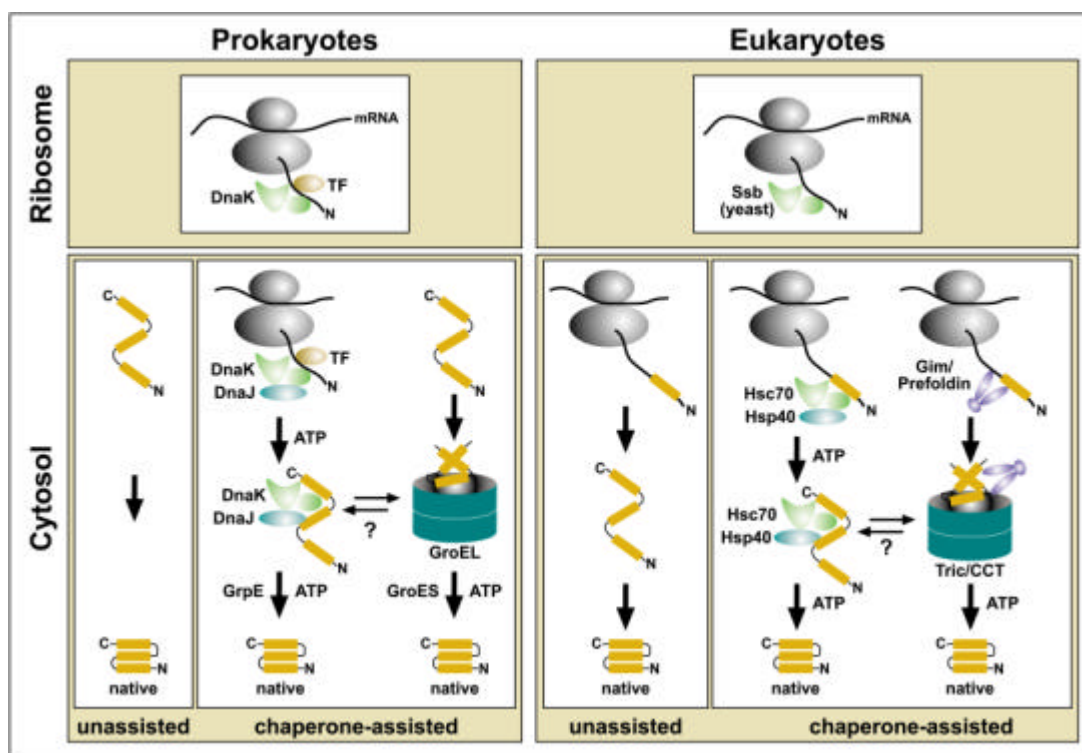


**Figure 1.** Overview of protein folding pathway in the prokaryotic and eukaryotic cytosol. (modified from Bukau et al., 2000). Gim, genes involved in microtubule biogenesis; TF, trigger factor; TRiC/CCT, cytosolic chaperonin TCP-1.

The 90 kDa heat shock protein (Hsp90) family is a chaperone system acting downstream of Hsp70/Hsp40 with a more restricted role in protein folding. Although the function of the bacterial homolog, HtpG, has remained enigmatic, the function and mechanism of the mammalian Hsp90 is reasonably well established. Hsp90 consists of three domains: a N-terminal ATPase domain, a middle domain, and a C-terminal dimerization domain (Stebbins et al, 1997). As for Hsp70, the extreme C-terminus contains the EEVD peptide motif known to mediate binding to one of the TPR-domains of the Hsp70-Hsp90 organizing protein p60/Hop and other TPR-domain containing proteins (Scheufler et al, 2000). The N-terminal and C-terminal domain possess general chaperone activity *in vitro* (Young et al., 1997; Scheibel et al., 1998). However, Hsp90 seems to bind a more restricted subset of client proteins *in vivo* (Nathan et al., 1997), being highly specific for signal transduction molecules, e.g. steroid hormone receptors and protein kinases. It is involved in the maturation of these signalling molecules rather than possessing the function of a general chaperone (Smith, 2000).

The ATPase activity of Hsp90 is essential *in vivo* in regulating substrate binding and release by the chaperone (Obermann et al., 1998; Panaretou et al., 1998; Young and Hartl, 2000). Although crystal structures of the ATPase domain with bound ATP or ADP do not show any major differences, major conformational changes in the Hsp90 dimer have been observed by electron microscopy and biochemical assays depending on the bound nucleotide (Maruya et al., 1999; Prodromou et al., 2000). Hsp90 function furthermore relies on several cofactors depending on the client protein bound. Among these are the peptidylprolylisomerases (immunophilins and cyclophilins), p50/cdc37, p23 and the serine/threonine phosphatase 5 (Pratt and Toft, 1997; Silverstein et al., 1997; Pratt et al., 1999; Weaver et al., 2000; Young and Hartl, 2000).

The Hsp90 paralog in the endoplasmic reticulum (ER), Grp94 (also known as Gp96 and endoplasmic reticulum chaperone), is less characterized with regard to function, mechanism, and regulation in protein folding/assembly (Nicchitta, 1998). However, like Hsp70, Grp94 has a function in immunology unrelated to protein folding, which will be introduced in the second part of this thesis.

Small heat shock proteins are a class of stress-inducible molecular chaperones which bind unfolded proteins preventing aggregation (van den IJssel et al., 1999). Subsequent refolding is achieved by the Hsp70 and/or chaperonin systems. Members in the eukaryotic cytosol are Hsp12, Hsp42 and the mammalian  $\alpha$ -crystallin. The bacterial small heat shock proteins IbpA and IbpB also prevent aggregation and have been found associated with inclusion bodies.

Hsp100/Clp proteins are yet another class of chaperones. Their unique function is the disassembly of protein oligomers and aggregates which can subsequently be refolded by the Hsp70/Hsp40 system or degraded by the proteasome (Glover and Lindquist, 1998; Schirmer et al., 1996).

Besides these cytosolic factors, there exist several other more specialized chaperones in various cellular compartments, whose more detailed discussion is beyond the scope of this introduction. Among these, Calreticulin and Calnexin, chaperones resident in the endoplasmic reticulum, function in the folding and assembly pathway of secreted proteins. As described in section 2, Calreticulin also has immune stimulatory properties.



## C Structure/function analysis of the Hsp70 cochaperone Bag-1

### C.1 Introduction

The activity of molecular chaperones from several families, e.g. the Hsp60 system (including GroEL/ES and TRiC/CTT), Hsp70, and Hsp90, is dependent on ATP binding and hydrolysis. Further regulation is achieved by cofactors modulating various steps of the reaction cycle. In this chapter, the Hsp70 chaperone system will be described in detail with emphasis on its ATPase cycle and its cochaperones. This will be the basis for the structure/function analysis of Bag proteins, regulators of eukaryotic Hsp70.

#### C.1.1 Cellular function of Hsp70

As a result of its function in *de novo* protein folding and prevention of aggregation (see general introduction), Hsp70 is involved in several cellular processes in addition to protein folding, including targeting and translocation, degradation, apoptosis and stress signalling (Jensen and Johnson, 1999; Pilon and Schekman, 1999; Saleh et al., 2000; Beere et al., 2000; McClellan and Frydman, 2001). These functions are briefly outlined here.

During biogenesis at the ribosome and translocation across intracellular membranes, nascent polypeptide chains targeted to the endoplasmic reticulum or mitochondria have to be kept in a translocation competent state and additionally aggregation of the partially unfolded protein must be prevented. For post-translationally targeted proteins, this is mainly achieved by cytosolic Hsp70 proteins (Chirico et al., 1988; Deshaies et al., 1988; Murakami et al., 1988). Upon translocation across the mitochondrial and endoplasmic reticulum membrane, members of the Hsp70 family located inside the respective compartment bind to the emerging polypeptide chain and facilitate completion of translocation (Kang et al., 1990; Nguyen et al., 1991; reviewed in Pilon and Schekman, 1997).

In the cytosol, a role of Hsp70 in proteasomal degradation has been suggested (Fisher et al., 1997). Recently, a direct link between the Hsp70 machinery and the degradation machinery has been demonstrated *in vitro* (Lüders et al., 2000), based on the finding that the Hsp70 cofactor Bag-1 binds directly to the proteasome, suggesting a function of Bag-1 in degradation. Another cofactor, the Hsp70/Hsp90-binding protein CHIP, stimulates ubiquitination in live cells promoting proteasomal degradation of chaperone substrates (Meacham et al., 2001; Connell et al., 2001).

Expression of the inducible form of Hsp70 (and development of cellular thermotolerance) has been shown to correlate with resistance to apoptosis. Indeed, an involvement of Hsp70 in various stages of the apoptotic cascade has been suggested. At a very early step, Hsp70 inhibits the stress-activated signalling by the c-Jun N-terminal kinase (JNK1) by direct interaction via the peptide binding domain of Hsp70. This might influence the activation of proteins of the Bcl-2 family upstream of cytochrome c release. Other apoptosis-inhibitory effects of Hsp70 were mapped downstream of cytochrome c release, but upstream of procaspase-3 activation (Mosser et al., 1997; Beere et al., 2000; Saleh et al., 2000; Li et al., 2000). The chaperone interacts with the cytosolic apoptosome, specifically with the apoptotic protease activating factor 1 (Apaf-1) preventing procaspase-9 recruitment to the complex and inhibiting caspase activation and substrate cleavage. Finally, a function in inhibition of apoptosis by Hsp70 has been located downstream of caspase-3 (Jaattela et al., 1998).

Additionally, Hsp70 has been shown to modulate cellular stress signalling initiated by heat shock, ceramide, ethanol, irradiation, TNF $\alpha$  and ischemia (Jaattela, 1993; Simon et al., 1995; Bellmann et al., 1996; Samali and Cotter, 1996; Gabai et al., 1997; Lioassis et al., 1997; Mosser et al., 1997; Meriin et al., 1998; Sharp et al., 1999).

In a mechanistic rather than regulatory role, Hsp70 has also been implicated in releasing clathrin and associated proteins from clathrin-coated vesicles during receptor mediated endocytosis (Schlossman et al., 1984; Hannan et al., 1998; Honing et al., 1994; Sherri et al., 2001).

Recently, several classes of chaperones, namely Hsp70, Hsp90, their respective ER-paralogs, and the ER-resident chaperone calreticulin, have been shown to be associated extracellularly with tumor cells and their application as potent vaccines in tumor rejection experiments has been established. The latter will be the focus of the second part of this thesis.

### C.1.2 Structure of Hsp70

Mechanistically, Hsp70 proteins are molecular chaperones with a weak intrinsic ATPase activity. They consist of two functional domains, a highly conserved N-terminal ATPase domain and a less conserved peptide binding domain close to the C-terminus. The extreme C-terminus of eukaryotic Hsp70 is unstructured but harbors the peptide motif EEVD, a binding site for cofactors of the TPR protein family (Scheufler et al., 2000). The ATPase domain is highly conserved from bacteria to mammals. Regions with higher divergence are located at the C-terminus and the peptide binding domain. The structures of both domains of Hsp70 have been solved by X-ray crystallography but not that of the full length protein (Figure 2).

The overall fold of the ATPase domain is similar to that of actin (Flaherty et al., 1991). It can be subdivided into four subdomains, named IA (residues 1-39 and 116-188), IB (residues 40-115), IIA (residues 189-228 and 307-385), and IIB (residues 229-306) (Figure 2). The center of the heart-shaped molecule forms a nucleotide binding cleft with residues responsible for nucleotide binding and hydrolysis mainly located in subdomains IA and IIB. The N- and C-termini of the domain are located at the same site of the ATPase. The phosphate groups of the bound nucleotide are coordinated by a  $Mg^{2+}$  ion. Additionally, two monovalent potassium cations are important for optimal nucleotide hydrolysis and substrate release by coordinating  $Mg^{2+}/ADP$  and  $P_i$  in the ATPase active site (Palleros et al., 1993; O'Brien and McKay, 1995; Wilbanks and McKay, 1995).

The X-ray structure of the peptide binding domain of the *E. coli* homolog of Hsp70, DnaK, in complex with a heptapeptide (NRLLLTG) has also been determined (Zhu et al., 1996). The model is shown in the right panel of Figure 2. It consists of a  $\beta$ -sandwich subdomain (residues 393-501) comprising the peptide binding cleft. The peptide is bound in an extended conformation. Two of the peptide's leucines (Leu3 and Leu4) contribute most to the contact with the  $\beta$ -sheet region forming the peptide binding groove (mainly to the highly conserved residues Gln433, Phe426, Val436, Ile438, Ile401 and Thr403 of the  $\beta$ -subdomain of DnaK in Figure 2). A hydrophobic arch over the top of the binding channel is generated by Met404 and Ala429 that encloses the peptide backbone (to the left of the peptide in Figure 2). The C-terminus of the domain forms an all  $\alpha$ -helical subdomain (residues 509-607) composed of five helices. Connected via a short helix to the  $\beta$ -sheet subdomain, a long helix covers the peptide binding cleft serving

as a lid, followed by three shorter helices at the C-terminus. Based on alternate conformations in the crystal lattice, a hinge at residues 536-538 in the middle of the long helix of DnaK has been proposed around which the  $\alpha$ -helical lid opens and closes depending on the bound nucleotide (ATP, open; ADP, closed) (Zhu et al., 1996). The 11-degree rigid body rotation of this C-terminal lid region results in a loss of the latch-like contact of the helix with the outer loops. The helical subdomain does not contact the peptide directly. The hydrophobic arch and the lid together form a closing device for the substrate binding channel whereas the substrate binding free energy mostly relies on contributions of the central pocket (Mayer et al., 2000).

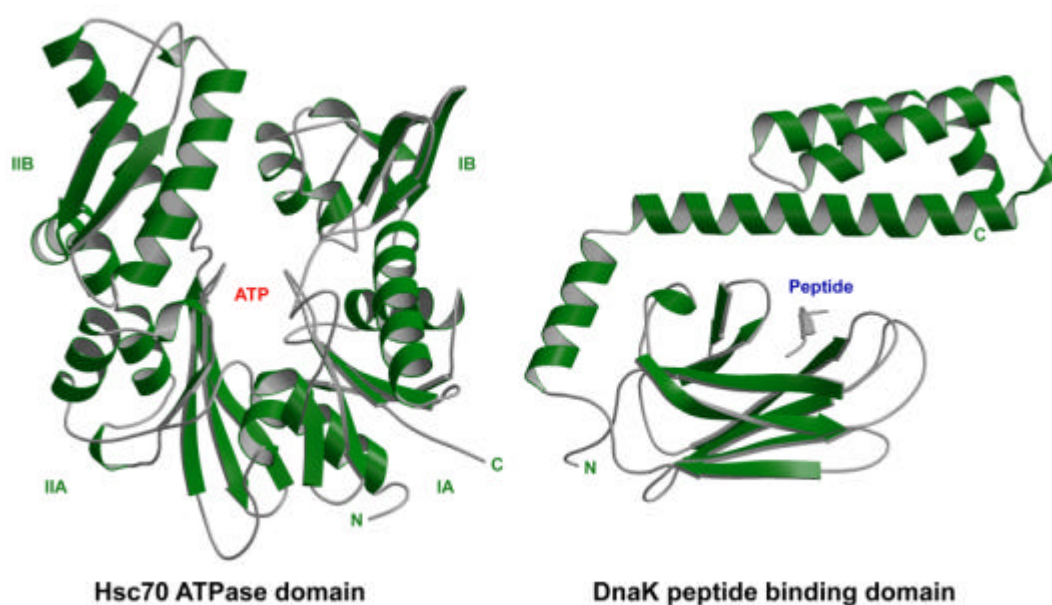


**Figure 2.** Structures of the domains of Hsp70. The N-terminal ATPase of Hsc70 with bound ATP has been solved by X-ray diffraction (PDB code 3HSC). The X-ray structure of the peptide binding domain of the *E. coli* Hsp70, DnaK, has been solved in complex with a peptide substrate (PDB code 1DKZ).

Attempts to crystallize the full length Hsp70 molecule have failed so far. This structure would be particularly interesting since there is a high degree of regulation and coordination between ATP hydrolysis and peptide binding and release as will be summarized in the next paragraph.

### C.1.3 The molecular mechanism of Hsp70 function

Chaperones of the Hsp70 family bind short stretches of unfolded proteins. In a folding reaction, substrate proteins undergo multiple rounds of Hsp70 interaction (Szabo et al., 1994; Buchberger et al., 1996). Modulation of this reaction is achieved by ATP binding and hydrolysis and several cochaperones working in concert with Hsp70. Most of the biochemical and biophysical characterization regarding Hsp70 function was carried out with the bacterial homolog, DnaK, and will be the focus of the next paragraphs. Nevertheless, the general principle of chaperone action applies also to the eukaryotic homologs (Theyssen et al., 1996; Ha and McKay, 1994; Ha and McKay, 1995; Takeda and McKay, 1996).

In principle, Hsp70 alternates between two states, the ATP-bound form characterized by low affinity for substrate and high on- and off-rates, and the ADP-bound state, characterized by high substrate affinity and slow exchange. Binding of ATP to DnaK results in an increase in the off-rate for substrate by 2-3 orders of magnitude and concomitantly leads to a 50-fold increase in the on-rate for substrate. This is also reflected by a dissociation constant for substrate 5- to 85-fold higher than the one of the ADP-bound form (Palleros et al., 1993; Schmid et al., 1994; McCarty et al., 1995; Theyssen et al., 1996). Upon hydrolysis of ATP, major conformational rearrangements within the C-terminal peptide binding domain lead to a state characterized by a low on- and off-rate for substrate. Structurally, the peptide binding cleft is in a closed conformation in the ADP-bound form, and is open when ATP is bound. Thus, ATP hydrolysis works as a pace setter for the interaction between unfolded polypeptides and the chaperone.

Nucleotide hydrolysis after peptide binding, together with conversion from the low to the high affinity state for substrate binding, is the rate limiting step in the reaction (Gao et al., 1993; McCarty et al., 1995; Karzai and McMacken, 1996; Theyssen et al., 1996). The steady-state ATPase rate ( $0.02\text{-}0.2\text{ min}^{-1}$ ) is too slow to enable efficient chaperone function and protein folding, although peptide binding already stimulates the turnover 2- to 10-fold (Flynn et al., 1989; Gao et al., 1994; Ha and McKay, 1994; Jordan and McMacken, 1995; McCarty et al., 1995; Theyssen et al., 1996). Therefore, several cofactors act in concert with Hsp70/DnaK accelerating the ATP hydrolysis cycle and thereby substrate binding and release.

#### C.1.4 Cochaperones of Hsp70

Cochaperones of the Hsp40/DnaJ family (J-domain proteins) stimulate the ATP hydrolysis step of the ATPase cycle (Liberek et al., 1991). These cochaperones are a heterogeneous group of multidomain proteins which share a conserved J-domain. J-domains are about 80 amino acids long and fold as a four helix bundle. The loop between helix 2 and 3 comprises a conserved sequence motif (HPD) suggested to be involved in the interaction of the J-domain with Hsp70 (Wall et al., 1994; Karzai and McMacken, 1996; Pellicchia et al., 1996; Qian et al., 1996; Szabo et al., 1996; Szyperski et al., 1994). The J-domain is essential for the stimulatory effect on the intrinsically low ATPase rate of Hsp70 by directly interacting with the ATPase domain, resulting in the ADP-bound state which tightly binds substrate. Some J-domain cochaperones also contact regions in the C-terminal domain of Hsp70, stabilizing the substrate-binding state. DnaJ is the main J-domain protein in the bacterial cytosol. In addition to its effect on the ATPase rate of DnaK, DnaJ also possesses an intrinsic chaperone activity sufficient to prevent aggregation of unfolded polypeptides and might be involved in delivering these to DnaK (Langer et al., 1992; Schroder et al., 1993; Gamer et al., 1996). However, this function seems not to be a general feature of J-domain proteins since such an activity has not been observed with the mammalian J-proteins (Nagata et al., 1998).

The main J-domain proteins in the mammalian cytosol are Hdj-1/Hsp40, Hdj-2, Hsj-1 and Hsj-2 (Ohtsuka, 1993; Yan et al., 1998; Cheetham et al., 1992; Oh et al., 1993). Others are found in all cellular compartments, including specialized J-domain proteins more divergent from Hsp40/DnaJ outside of the J-domain (zuotin, auxilin etc.). Differences in other parts of these proteins account for different cellular activities, but the overall stimulation of Hsp70's ATP turnover by the J-domain is in common to all of these cofactors.

In the presence of DnaJ, ATP hydrolysis by DnaK is fast enough that exchange of ADP for fresh ATP becomes the rate-limiting step in the ATPase cycle (Liberek et al., 1991; McCarty et al., 1995). In the bacterial cytosol, mitochondria and chloroplast, GrpE-like proteins facilitate nucleotide exchange enhancing the overall ATPase rate and thereby the protein folding efficiency of Hsp70 (Liberek et al., 1991; Dekker and Pfanner, 1997; Miao et al., 1997). Association of GrpE with the DnaK/ADP complex reduces the affinity of DnaK for ADP about 200-fold and accelerates the nucleotide exchange rate about 5000-fold (Packschies et al., 1997). A model of the chaperone cycle of the

DnaK/DnaJ/GrpE system is presented in Figure 3. At saturating conditions, the ATP turnover rate is stimulated several hundred fold by the presence of both DnaJ and GrpE compared to the unstimulated reaction, probably more than is necessary to support proper protein folding. Therefore, the expression of their genes is coregulated *in vivo* to ensure the optimal balance between efficient ATP turnover and protein folding within this system. The structure of a stable DnaK/GrpE complex shows DnaK in a nucleotide-free state induced by rotation of subdomain IIB in the ATPase of DnaK relative to the nucleotide-bound structure resulting in an opening of the nucleotide binding pocket upon GrpE binding (Harrison et al., 1997).

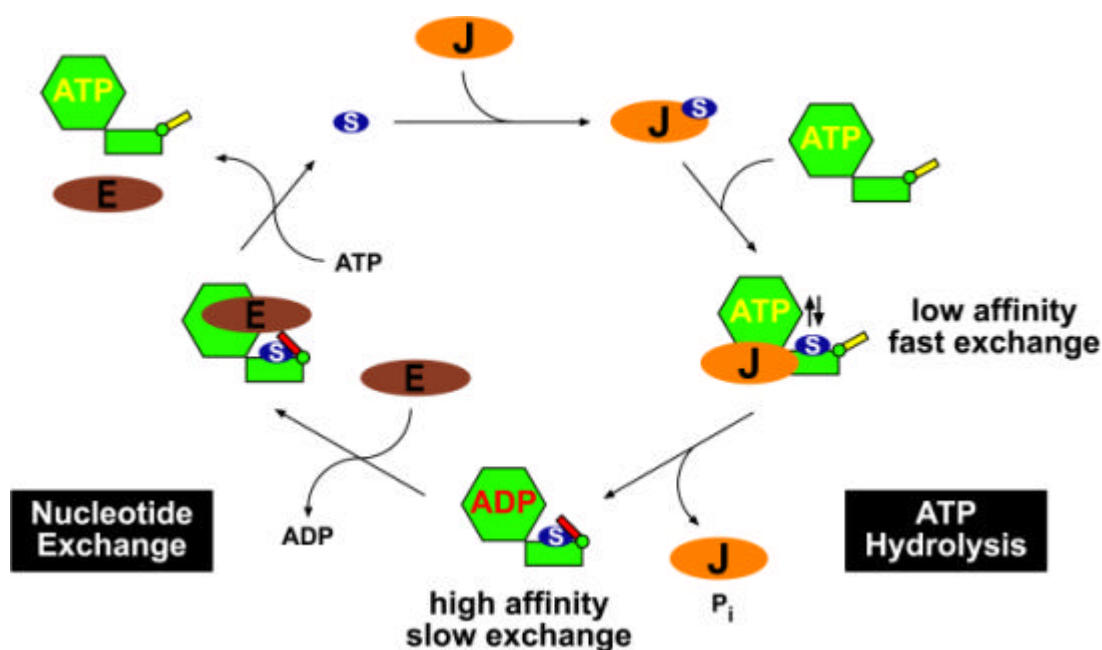


**Figure 3.** Model of the chaperone cycle of DnaK/DnaJ/GrpE. Substrate polypeptides (S) first interact with DnaJ (J), followed by transfer of the substrate to DnaK and subsequent ATP hydrolysis. DnaJ leaves the complex, and GrpE (E) associates with DnaK resulting in a release of ADP. This allows binding of ATP and release of GrpE and substrate from DnaK.

However, a eukaryotic, cytosolic GrpE homolog has not been found so far. Such a function has been proposed for the Bcl2-associated athanogene 1 (Bag-1) protein but has not been definitively proven and is rather controversially discussed in the literature (Höhfeld and Jentsch, 1997; Bimston et al. 1998). The structure and function of Bag-1 have been analyzed in the first part of this thesis. A detailed description of Bag-1 and the family of Bag proteins will be presented in the next chapters.

In the eukaryotic cytosol, further regulators and cofactors of Hsp70 proteins have been identified that are unique to this phylogenetic kingdom. A common structural motif of these are tetratricopeptide domains (Honore et al., 1992; Smith et al., 1993), highly degenerate 34 amino acid repeats (Lamb et al., 1995). The cochaperone p48/Hip binds to the ATPase domain of Hsp70 with a preference for the nucleotide-bound state of the chaperone (Höhfeld et al., 1995). It is composed of a N-terminal dimerization domain and a TPR motif which is responsible for its interaction with Hsp70. It is thought to stabilize the ADP-bound complex, thereby antagonizing the putative nucleotide exchange activity of Bag-1 (Irmer and Höhfeld, 1997; Nollen et al., 2001). Its interaction with Hsp70 was suggested to involve subdomain IIB of the ATPase (Velten et al., 2000).

The cochaperone p60/Hop binds to the EEVD motifs of Hsp70 and Hsp90 via its TPR domains (Scheufler et al., 2000), and thereby works as a adaptor for the two chaperone systems. The close proximity of the two chaperone systems might facilitate substrate transfer from Hsp70 to Hsp90 (Morishima et al., 2000; Frydman and Höhfeld, 1997).

Recently, another cochaperone belonging to the TPR protein family, CHIP (for carboxy terminus of Hsp70-interacting protein), has been identified (Ballinger et al., 1999). In addition to its TPR motif, it harbors a region similar to the proteasome-associated RING-finger protein UFD2, the Ubox, a domain characteristic for E4 ubiquitin conjugation factors. CHIP inhibits the ATPase and chaperone function of Hsp70 by an as yet unknown mechanism. *In vivo*, CHIP promotes the ubiquitination and proteasomal degradation of Hsp70- and Hsp90-bound substrates by serving as a direct link between folding and degradation (Ballinger et al., 1999; Meacham et al., 2001; Connell et al., 2001).

Another, yet less characterized cofactor of mammalian Hsp70 is HspBP1. It has been reported to inhibit ATP turnover by Hsp70 and renaturation of model substrates *in vitro* (Raynes and Guerriero, 1998). In Figure 4, the domain organization of Hsp70 is shown with the established binding regions for the various cofactors.





These are predicted to form a  $\alpha$ -helical structure. Bag-1L additionally harbors a nuclear localization sequence. Bag-1 was predicted to be all  $\alpha$ -helical and binds to Hsp70 as a monomeric protein with a 1:1 stoichiometry (Stuart et al., 1998).

#### C.1.5.2 Cellular function of Bag-1

Besides binding to the cell death inhibitor Bcl2, several other client proteins of Bag-1 have been identified mainly by the use of immunoprecipitation from cell lysates. Bag-1 binds and activates the protein kinase Raf-1 mediating stress signalling in an Hsp70-dependent manner (Wang et al., 1996; Song et al., 2001). Furthermore, it binds to several growth factor receptors, especially hepatocyte and platelet-derived growth factors (HGF and PDGF) receptors (Bardelli et al., 1996), the retinoic acid receptor (Liu et al., 1998), and the glucocorticoid receptor (Kullmann et al., 1998). Some of these interactions may be indirect via an interaction with Hsp70 which cannot be excluded based on the techniques applied. Nevertheless, all these interactions enhance the protection from apoptosis by inhibiting retinoic acid-induced cell death, by increasing the anti-apoptotic potential of HGF and PDGF, and by negative regulation of glucocorticoid receptor action, respectively. Downregulation of the glucocorticoid receptor was shown to involve a nuclear localization of Bag-1 in complex with the hormone-bound receptor mediated by the TRSEEX repeats dependent on the number of repeats (Schneikert et al., 1999). Although the effect of Bag-1 on cell death has been established, the mechanism of action remains enigmatic.

Bag-1M was also shown to have rather unspecific DNA binding properties thus stimulating transcription upon overexpression in cells (Zeiner et al., 1999). Heat stress induces a relocalization of Bag-1M to the nucleus. DNA binding and transcriptional enhancement is dependent on an N-terminally located motif consisting of basic amino acids, but is independent of the Bag domain which mediates the interaction with Hsp70.

The effect of Bag-1 on Hsp70, especially its ATPase activity, has been discussed controversially. Several lines of evidence exist which point towards a nucleotide exchange factor activity for Bag-1. It was originally observed to stimulate the steady state ATPase rate of Hsp70 only in the presence of Hsp40 and accelerate the release of bound ADP (Höhfeld and Jentsch, 1997). Others did not observe such an effect but proposed an activity similar to a J-domain-mediated acceleration of the ATPase however uncoupling

nucleotide hydrolysis from substrate release (Bimston et al., 1998). In the latter study, a Hsp40-independent stimulation of the Hsp70 ATPase rate by Bag-1 was observed without acceleration of nucleotide exchange. Addition of Hsp40 to the assay resulted only in an additive effect. The discrepancy between the two observations may be explained by the use of purified proteins from different sources (proteins expressed in insect cells and *E. coli*, respectively).

Furthermore, there has been a controversy about the effect of Bag-1 on substrate binding by Hsp70. In a native gel assay for analysis of substrate/chaperone complexes, it has been shown that Bag-1 prevents ATP-dependent substrate release from Hsp70 (Bimston et al., 1998). Yet, using gel filtration for the analysis of such complexes or immunoprecipitation, the opposite effect has been demonstrated for Bag-1, namely the dissociation of substrate/Hsp70 complexes in a ATP-dependent manner (Lüders et al., 2000; Zeiner et al., 1997).

The effect of Bag-1 on protein folding is as yet unclear since positive and negative effects have been observed *in vitro* and *in vivo* depending on the experimental setup and Bag-1 isoform used (Takayama et al., 1997; Kanelakis et al., 1999; Terada and Mori, 2000; Nollen et al., 2000; Nollen et al., 2001; Lüders et al., 2000). Nevertheless, the effect seems to be distinct from the one of GrpE on protein folding by the DnaK/DnaJ system. In the latter case, GrpE is necessary for proper folding whereas Bag-1 seems to be dispensible for at least some Hsp70 chaperone actions (Minami et al., 1996).

Recently, an association of Bag-1 with the proteasome has been demonstrated *in vitro* suggesting a link between the protein folding and degradation machinery (Lüders et al., 2000). Nevertheless, the molecular basis and implications for the situation in the cell remain to be established.

### C.1.5.3 Other Bag proteins

Several other human Bag-1-related proteins have recently been identified by yeast two-hybrid and  $\lambda$ -phage cDNA screening (Takayama et al., 1999), including the human proteins Bag-2, Bag-3, Bag-4, and Bag-5, but also Bag proteins in the invertebrate *C. elegans* and the fission yeast *S. pombe*, all containing a conserved C-terminal domain

responsible for Hsp70 binding but with diverse N-termini. Figure 5 shows a schematic representation of the mammalian Bag proteins.

The other mammalian Bag homologs lack the ubiquitin-like domain but contain different domains, e.g. a WW-domain in the case of Bag-3 (also known as CAIR-1/Bcl-2-binding protein Bis). WW-domains are protein-protein interaction domains similar to Src homology 3 (SH3) domains (Bork and Sudol, 1994; Zarrinpar and Lim, 2000). Furthermore, Bag-3 was first identified by virtue of its synergistic effect on Bcl2-mediated prevention of apoptosis (Lee et al., 1999). Bag-3 was found in a ternary complex with Hsp70 and phospholipase C- $\gamma$  which is released from Bag-3 upon EGF stimulation of the cells. Binding between phospholipase C- $\gamma$  and Bag-3 is mediated by PxxP motifs in Bag-3 which are recognized by the SH3 domain of the lipase (Doong et al., 2000). The exact role of Hsp70/Bag-3 complexes remains to be established but the divergent N-termini of homologs of the Bag family indicate specialized cellular functions or a certain targeting of Bag proteins.

So far, no Bag proteins have been identified in *D. melanogaster*, *A. thaliana* and *S. cerevisiae*.

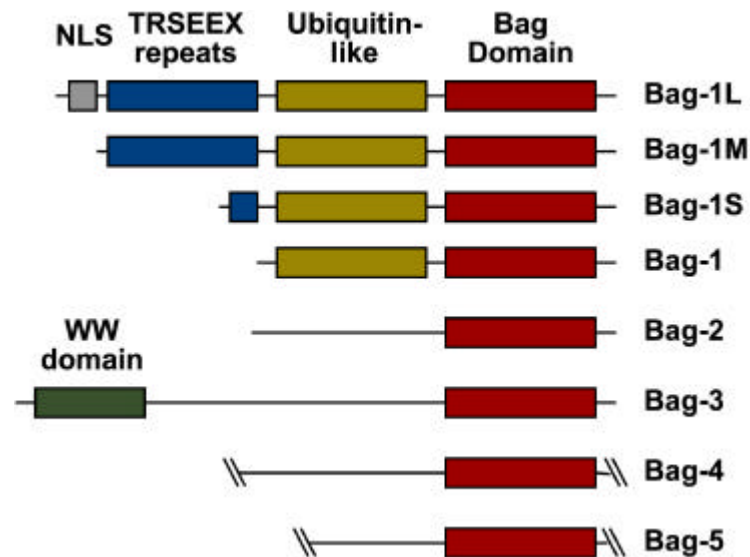


**Figure 5.** The family of mammalian Bag proteins.

### C.1.6 Aim of the project

The main focus of the project was the mechanism by which the cochaperone Bag-1 regulates Hsp70. At the beginning of the work, contradictory results had been published regarding Bag-1 function. Specifically, it was unclear whether Bag-1 acts as a nucleotide exchange factor for Hsp70 or modulates a different step of the Hsp70 ATPase cycle.

Unlike previous work addressing this question, a structural approach was taken to analyze the function of Bag-1 in the Hsp70 ATPase cycle. Thus, the immediate experimental goals were the identification of folded domains of Bag-1 and Hsp70 that would crystallize as a stable complex, and the solution of the molecular structure of this complex using X-ray diffraction data. The structure of the Hsp70/Bag-1 complex was to be compared with the known structures of Hsp70/DnaK with bound nucleotide, or in complex with the bacterial nucleotide exchange factor GrpE. Once a hypothesis about the Bag-1 mechanism of action was developed from the structural model, this hypothesis was to be tested experimentally by site-directed mutagenesis and biochemical assays. Finally, the structural information was also to be used to identify as yet unknown members of the Bag family of cochaperone proteins.

## C.2 Material and Methods

### C.2.1 Chemicals

All chemicals were of quality *pro analysi* and were purchased from *Fluka* (Buchs, Switzerland), *Merck* (Darmstadt, Germany), *Sigma-Aldrich* (Steinheim, Germany) and *USB* (Cleveland, USA) if not stated otherwise. Solutions were prepared with deionized, double-distilled and sterile-filtered water. Concentrations in percent of liquids are given as (v/v) and of solid chemicals as (w/v).

*Amersham* (Buckinghamshire, England):  $\alpha^{32}\text{P}$ -ATP.

*Roche/Boehringer Ingelheim* (Mannheim, Germany): ADP, ATP, Ampicillin.

*Green Hectares* (Wisconsin, USA): Rabbit reticulocyte lysate.

*Life Technologies/GibCo* (Karlsruhe, Germany): T4 ligase buffer.

*New England Biolabs (NEB, Beverly, USA)*: DH5 $\alpha$  and BL21pLysS *E. coli* cells, restriction enzymes and buffers, VENT DNA polymerase and thermopol buffer, T4 DNA ligase.

*Perkin Elmer* (Weiterstadt, Germany): ABI Prism Big Dye cycle sequencing kit.

*Promega* (Mannheim, Germany): TNT T7 Coupled Reticulocyte Lysate System.

*Roche* (Mannheim, Germany): Expand Long Template PCR Kit.

*Stratagene* (La Jolla, USA): QuickChange Site-Directed Mutagenesis Kit.

### C.2.2 Instruments

*ADSC* (Povay, USA): Quantum-4 CCD detector.

*Beckman* (Munich, Germany): Centrifuges J-6B, Avanti J-25, GS-6R, and Optima LE-80K ultracentrifuge with 45Ti rotor, UV-VIS-spectralphotometer DU 640, pH meter  $\Phi$ 34.

*BioRad* (Hercules, USA): Econo columns, gel electrophoresis system for protein and DNA gels.

*Charles Supper Company* (USA): Double mirror focusing optics system 7616.

*Eppendorf* (Cologne, Germany): Centrifuges 5415C and 5417R.

*European Synchrotron Radiation Facility (ESRF, Grenoble, France)*: Synchrotron station ID14-4 (EMBL).

*Fuji* (Stamford, USA): Phosphoimager Fuji Film FLA-2000.

*Hampton Research* (Laguna Niguel, USA): PEG ion screen, siliconized cover slides, VDX crystallization plates.

*Heath Scientific Co Ltd.* (Bletchley, England): MicroCal VP Isothermal Titration Calorimeter.

*MarResearch* (Hamburg, Germany): Image Plate MAR300, MARCCD detector.

*Millipore* (Eschborn, Germany): Amicon Centriprep concentrators, Milli-Qplus PF, sterile filters 0.22  $\mu$ M Millex-HA.

*Misonix Inc.* (New York, USA): Sonicator Ultrasonic Processor XL.

*Olympus* (Hamburg, Germany): Stereomicroscope SZH10.

*Perkin Elmer* (Weiterstadt, Germany): GenAmp 2400 thermocycler.

*Pharmacia* (Freiburg, Germany): FPLC system ÄKTAexplorer100, columns HiLoad 26/60 Superdex 75 and Superdex 200, Fast Desalting column HiPrep 26/10, Resource Q.

*Precision Scientific* (Chicago, USA): Precision incubator 815-BOD.

*Qiagen* (Valencia, USA; Hilden, Germany): NiNTA Superflow matrix, Plasmid Midi kit, QIAprep Spin Mini prep kit, QIAquick PCR purification and gel extraction spin kit.

*Rainin* (Woburn, USA): Gilson pipettes P2, P10, P100, P200, P1000.

*Rigaku* (Berlin, Germany): Rotating anode X-ray generator RU-200.

*Savant* (via *Life Science Int.*, Frankfurt, Germany): Slab gel dryer SGD 2000.

### C.2.3 Media and buffers

#### C.2.3.1 Media

- Luria-Bertani (LB) medium: 10 g/l Bactotryptone  
5 g/l Bactoyeast extract  
5 g/l NaCl  
(for plates, medium was supplemented with 15 g/l agar and antibiotics)

- M9 medium: 200 ml M9 salt stock solution  
2.0 ml 1M MgSO<sub>4</sub>  
20 ml 20% glucose solution  
0.1 ml 1M CaCl<sub>2</sub>  
ddH<sub>2</sub>O to 1 l final volume.
  - M9 salts stock solution: 64 g Na<sub>2</sub>HPO<sub>4</sub> x 7 H<sub>2</sub>O  
15 g KH<sub>2</sub>PO<sub>4</sub>  
2.5 g NaCl  
5.0 g NH<sub>4</sub>Cl  
ddH<sub>2</sub>O to 1 l final volume.
- Terrific Broth (TB) medium: 12 g/l Bactotryptone  
23.9 g/l Bactoyeast extract  
8 ml/l glycerol  
2.2 g/l KH<sub>2</sub>PO<sub>4</sub>  
9.4 g/l K<sub>2</sub>HPO<sub>4</sub>
- YPD medium: 20 g/l Difco peptone  
10 g/l Bactoyeast extract  
ddH<sub>2</sub>O to 1 l final volume, adjust pH to 5.8.  
Add glucose (dextrose) to 2% final.

### C.2.3.2 Buffers

- ATPase buffer: 20 mM HEPES-KOH pH 7.6, 50 mM KCl, 5 mM MgAc<sub>2</sub> (prepared as 10x stock solution).
- Buffer B: 25 mM HEPES-KOH pH 7.5, 100 mM KAc, 5% glycerol.
- Buffer G: 25 mM HEPES-KOH pH 7.5, 100 mM KAc, 5 mM MgAc<sub>2</sub>.
- Buffer C: 25 mM HEPES-KOH pH 7.5, 100 mM KAc, 1% NP40, 1% Na-deoxycholate, 0.1% SDS.
- NiNTA wash A: 25 mM KH<sub>2</sub>PO<sub>4</sub>, 500 mM KCl, 20 mM imidazole, pH 8.0.
- NiNTA wash B: 25 mM KH<sub>2</sub>PO<sub>4</sub>, 500 mM KCl, 20 mM imidazole, pH 6.0.
- NiNTA elution buffer: 12.5 mM KH<sub>2</sub>PO<sub>4</sub>, 250 mM KCl, 500 mM imidazole, pH 7.5.
- TB1: 100 mM RbCl<sub>2</sub>, 50 mM MnCl<sub>2</sub>, 30 mM KAc, 10 mM CaCl<sub>2</sub>, 15% glycerol, pH 5.8 (adjusted with 0.2 M HOAc); sterile filter.
- TB2: 75 mM CaCl<sub>2</sub>, 10 mM RbCl<sub>2</sub>, 10 mM MOPS (or PIPES), 15% glycerol, pH 6.5 (adjusted with KOH); sterile filter.
- TBE (10x stock): 890 mM Tris base, 890 mM boric acid, 20 mM EDTA.
- TEV buffer: 50 mM Tris-HCl pH 8.0, 5% glycerol, 20 mM NaCl.
- TLC running buffer: 0.5 M formic acid, 0.5 M LiCl.



## C.2.4 Plasmids and bacterial strains

## C.2.4.1 Plasmids

The following plasmids have been used for recombinant expression of native proteins (Table 1):

**Table 1. Plasmids used in this study.**

ORF	Vector	Restrict. sites	Reference
bag-1M human	pProEx HTa*	KasI/HindIII	this study
bag-1M(151-263) human	pProEx HTa*	KasI/HindIII	this study
bag-1M(151-263) human E212A	pProEx HTa*	KasI/HindIII	this study
bag-1M(151-263) human E219A	pProEx HTa*	KasI/HindIII	this study
bag-1M(151-263) human R237A	pProEx HTa*	KasI/HindIII	this study
hsp70 human	pProEx HTa*	EcoRI/XhoI	this study
hsc70 human	pProEx HTa*	KasI/XhoI	this study
hsc70 human	pET3a	NdeI/BamHI	Minami et al., 1996
hsc70 human R261A	pET3a	NdeI/BamHI	this study
hsc70(5-381) bovine	pProEx HTa*	KasI/XhoI	this study
hsp40 human	pQE9**	-	Minami et al., 1996
sn11 <i>S. cerevisiae</i> (40-160)	pProEx HTa*	KasI/XhoI	this study
sn11 <i>S. cerevisiae</i> (49-160)	pProEx HTa*	KasI/XhoI	this study
Tobacco etch virus (TEV) protease	-**	-	Parks et al., 1994

\*: N-terminal His<sub>6</sub>-purification tag, cleavable with TEV protease  
 \*\*: N-terminal His<sub>6</sub>-purification tag

C.2.4.2 Competent *E. coli* cells using the RbCl-method

Competent cells were prepared as described (Hanahan, 1983). LB medium (55 ml) was inoculated with a single colony of the desired bacterial strain and grown to an OD<sub>600</sub> of 0.22-0.5 by incubation at 37°C under shaking. Cells were chilled on ice. Cells were pelleted by centrifugation for 20 min at 1000xg at 4°C and resuspended in 7 ml ice-cold TB1 buffer. TB1 buffer (19 ml) was added and suspensions were mixed well. After incubation for 5 min on ice, cells were centrifuged as before and resuspended in 2 ml ice-cold TB2 buffer. Cell suspensions were chilled on ice for 15 min, and were aliquoted into prechilled tubes (100 µl/tube). After 15 min on ice, aliquots were flash-frozen in liquid nitrogen, and stored at -80°C.

## C.2.4.3 Molecular cloning using polymerase chain reaction (PCR)

Plasmids produced during this study were cloned using polymerase chain reaction (PCR) methods followed by restriction digestion and ligation. The standard PCR protocol is summarized in table 2.

Reaction mixture	Reaction		
1.2 µg primer I (sense)	1 <sup>st</sup> cycle:	95°C	3 min
1.2 µg primer II (antisense)	25 cycles:	95°C	1.5 min
10 µl 10x Thermopol buffer ( <i>NEB</i> )		50°C	1 min
80 ng template DNA		72°C	1 min/kb
250 µM dNTPs	last cycle:	72°C	10 min
1 µl VENT DNA polymerase ( <i>NEB</i> )		4°C	
ddH <sub>2</sub> O to 100 µl final volume			

The amplified PCR products were analyzed by agarose gel electrophoresis (1% agarose in TBE buffer supplemented with 10 µg/ml ethidiumbromide) and purified by anion exchange chromatography (QIAquick PCR purification kit, *Qiagen*) following the manufacturers' instructions. Purified PCR products and the target vector were digested over night at 37°C in a 50 µl reaction volume containing the appropriate 10x restriction buffer (*NEB*) and 2 µl of each restriction enzyme (*NEB*). The vector was additionally dephosphorylated with 5 Units calf intestinal phosphatase for 1 hour. All reactions were stopped by heat treatment (65°C for 30 min). DNA fragments were separated by preparative agarose gel electrophoresis and purified from agarose slices using anion exchange chromatography (QIAquick Gel extraction kit, *Qiagen*) following the manufacturers' instructions. Ligation reactions containing 2 µl vector DNA, 5 µl insert DNA, 2 µl 5x ligase buffer (*Life Technologies/GibCo*), and 100 Units T4 ligase (*NEB*) were incubated over night at 16°C. 4 µl of the ligation reaction were used for transformation of chemical competent *E. coli* DH5α cells. Cells were incubated for 30 min on ice, followed by a heat shock for 70 sec at 42°C. After incubation for 2 min on ice, cells were resuspended in LB medium and incubated for 1 hour at 37°C, followed by plating on LB medium plates containing antibiotics for selection of transformants. After incubation for 20 hours at 37°C, 5 ml LB medium cultures supplemented with antibiotics were inoculated with single colonies and cultures were grown over night at 37°C. Plasmids were isolated from cell pellets using anion exchange chromatography

(Mini Prep Kit, *Qiagen*) following the manufacturers' instructions. Plasmids were analyzed by restriction digestion and analytical agarose electrophoresis.

Some coding regions were amplified using yeast genomic DNA or a human brain cDNA library as template. For these reactions, the Expand Long Template PCR System (*Roche*, Germany) was used (Table 3). Amplified DNA fragments were processed as described above.

Reaction mixture	Reaction		
1.2 µg primer I (sense)	1 <sup>st</sup> cycle:	94°C	3 min
1.2 µg primer II (antisense)	33 cycles:	94°C	10 sec
10 µl 10x buffer 1 ( <i>Roche</i> )		65°C	30 sec
200 ng template DNA	last cycle:	68°C	1 min/kb
250 µM dNTPs		68°C	7 min
1 µl polymerase mix ( <i>Roche</i> )		4°C	
ddH <sub>2</sub> O to 100 µl final volume			

For recombinant expression of native proteins, the bacterial strain *E. coli* BL21(DE3)pLysS (*Novagen*) was used. This strain contains the plasmid pLysS containing the gene for the expression of T7 lysozyme and a gene for chloramphenicol resistance. After induction with IPTG, lysozyme is expressed which helps efficient cell breakage by autolysis.

#### C.2.4.4 Site-directed mutagenesis

Site-directed mutagenesis was performed using the QuickChange System (*Stratagene*) following the manufacturers' instructions. The system allows site directed mutagenesis using double stranded DNA as a template. The application of polymerase PFU turbo together with a complementary set of sense and antisense primer, both carrying the desired mutation, generates a mutated plasmid. Methylated, nonmutated parental DNA is digested by treatment with the restriction enzyme Dpn I.

The following PCR reactions were performed for single amino acid changes (Table 4). PCR products were analyzed by agarose gel electrophoresis. Parental DNA template was digested by addition of DpnI (1 µl Dpn I in 40 µl PCR reaction) for 1 hour at 37°C. Transformation into supercompetent *E. coli* XL1-Blue cells was performed by incubation with 1 µl circular, nicked double-stranded DNA for 30 min on ice, followed by heat

shock for 45 sec at 42°C. After 2 min on ice, cells were incubated for 1 hour at 37°C in 1 ml of LB medium, and then plated on LB plates supplemented with the appropriate antibiotic. Cultures were inoculated with single colonies for isolation of plasmid DNA as described before. Success of mutagenesis was confirmed by DNA sequencing (*Medigenomix*, Munich, Germany).

**Table 4. PCR protocol for site-directed mutagenesis.**

Reaction mixture	Reaction		
125 ng mutagenic primer (sense)	1 <sup>st</sup> cycle:	95°C	30 sec
125 ng mutagenic primer (antisense)	16 cycles:	95°C	30 sec
5 µl 10x reaction buffer ( <i>Stratagene</i> )		55°C	1 min
25-100 ng template DNA		68°C	2 min/kb
250 µM dNTPs	last cycle:	68°C	20 min
1 µl PFU turbo polymerase ( <i>Stratagene</i> )		4°C	
ddH <sub>2</sub> O to 50 µl final volume			

### C.2.5 Biochemical methods

#### C.2.5.1 SDS polyacrylamide gelelectrophoresis (SDS-PAGE)

Proteins were analyzed by SDS-PAGE under denaturing, reducing conditions (Laemmli, 1970). Samples were prepared by addition of 4x concentrated sample buffer (final concentrations: 2% SDS, 0.35 M β-mercaptoethanol, 60 mM Tris-HCl pH 6.8, 10% glycerol, and 0.005% bromphenole blue). Samples were incubated for 4 min at 95°C prior to loading of the gels. For the present study, separating gels were used with 12.5% or 15% polyacrylamide, and stacking gels containing 5% polyacrylamide (Table 5). Electrophoresis was carried out at constant voltage (200 V) in electrophoresis buffer (50 mM Tris-HCl pH 8.3, 380 mM glycine, 0.1% (w/v) SDS).

**Table 5. Preparation of SDS-PAGE gels.**

% Acrylamide (AA)	Seperating Gel		Stacking Gel
	12.5%	15%	5%
30% AA/BisAA	6.8 ml	8.5 ml	0.83 ml
1.875 M Tris -HCL pH 8.8	3.5 ml	3.5 ml	-
0.6 M Tris -HCL pH 6.8	-	-	0.5 ml
ddH <sub>2</sub> O	6.4 ml	4.7 ml	3.6 ml
10% SDS	167 µl	167 µl	50 µl
10% Ammoniumpersulfate	100 µl	100 µl	50 µl
TEMED*	10 µl	10 µl	5 µl

\*: N,N,N',N'-tetramethylethylenediamine (TEMED)

### C.2.5.2 Staining methods for protein gels

After SDS-PAGE, gels were stained using a Coomassie solution (0.1% Coomassie Brilliant Blue R-250, 30% methanol, 10% acetic acid) and destained by incubation in destain solution (30% methanol, 10% acetic acid).

For a more sensitive detection, a silver staining protocol for proteins was used. The protocol of the staining procedure is listed below and was carried out at room temperature:

- 2x10 min            30% ethanol  
                          10% acetic acid
- 15 min             30 ml ethanol  
                          10 ml 4M NaAc  
                          300 µl acetic acid  
                          2 ml 25% glutaraldehyde  
                          0.1 g  $\text{Na}_2\text{S}_2\text{O}_3 \cdot 5\text{H}_2\text{O}$   
                          ddH<sub>2</sub>O to 100 ml final volume
- 5x10 min            ddH<sub>2</sub>O
- 1x15 min            0.1 g  $\text{AgNO}_3$   
                          25 µl 37% formaldehyde  
                          ddH<sub>2</sub>O to 100 ml final volume
- development        2.5%  $\text{Na}_2\text{CO}_3$  (anhydrous)  
                          40 µl 37% formaldehyde  
                          ddH<sub>2</sub>O to 100 ml final volume
- stop reaction        5% acetic acid

### C.2.5.3 Protein expression and purification

All proteins were overexpressed in *E. coli* BL21(DE3)pLysS (*Novagen*) in terrific broth (TB) medium supplemented with antibiotics (100 µg/l Carbenicillin or Ampenicillin, or 50 µg/l Kanamycin). Protein expression was induced by addition of 1 mM IPTG at an OD<sub>600</sub> of 1.0. Cells were harvested either after expression for 4 hours at 37°C or for 15 hours at 18°C by centrifugation for 1 hour at 5000xg. A selenomethionine-labeled derivative of rat Hsc70(5-381) was expressed in the methionine auxotroph *E. Coli* strain B834(DE3)pLysS (*Novagen*) grown in minimal medium M9 supplemented with 50 mg/l D,L-selenomethionine and 50 mg/l of all other amino acids but lacking methione. Induction and expression were carried out as described before. Cells were resuspended in NiNTA wash A buffer, shock frozen in liquid nitrogen, and stored at -80°C.

All purifications were carried out at 4°C using a ÄKTAexplorer100 FPLC system (*Pharmacia*). Flow rates were in accordance with the column-specific instructions. Cell suspensions were thawed in a water bath at 25°C until completion. Addition of lysozyme facilitated the lysis process. Furthermore, benzonase (*Merck*) was added. After an additional 20 min at 25°C, suspensions were sonicated for 1 min on ice. Cell debris was removed by ultracentrifugation at 80,000xg for 30 min at 4°C and filtration of the supernatants. Filtrates were incubated with NiNTA affinity matrix (*Qiagen*) for 45 min at 4°C. The resin was washed with 5 column volumes NiNTA wash A buffer and 5 column volumes NiNTA wash B buffer. Proteins were eluted from the matrix by incubation with NiNTA elution buffer for 15 min at 4°C. Eluates were either dialyzed over night against TEV buffer or buffer exchange was achieved by chromatography using a fast desalting column (*Pharmacia*). The affinity tag of the proteins was removed using tobacco etch virus (TEV) protease (1 OD<sub>280</sub> TEV protease:40 OD<sub>280</sub> His<sub>6</sub>-protein for 2 hour at 25°C, then at 4°C over night). The cleaved His<sub>6</sub>-tag and uncleaved fusion protein was removed by chromatography on NiNTA, and the cleaved product was recovered in the flow through. If necessary, proteins were further purified by anion exchange chromatography on a 6 ml Resource Q column (*Pharmacia*) via a gradient elution from 10 mM NaCl to 1 M NaCl (in Tris-HCl pH 7.5) over 15 to 20 column volumes. Fractions were analyzed by SDS-PAGE and Coomassie staining. Pooled fractions containing the desired product were concentrated using Amicon Centriprep concentrators (*Millipore*) following the manufacturers' instructions. Finally, all proteins were subjected to size exclusion chromatography on Superdex75 or Superdex200 columns (*Pharmacia*) equilibrated with buffer G. Proteins were shock-frozen in liquid nitrogen at concentrations between 5-20 mg/ml, and stored at -80°C.

For crystallization trials, a stable, nucleotide-free complex of rat Hsc70(5-381) and human Bag-1M(151-263) (the Bag domain) with a 1:1 stoichiometry was formed after chromatography on NiNTA matrix and TEV protease treatment. The complex was purified to homogeneity by chromatography on a Resource Q column (*Pharmacia*) followed by gel filtration (in 10 mM HEPES-KOH pH 7.5, 25 mM KCl, and 5 mM DTT) as described above. The complex was concentrated to 40 mg/ml by ultrafiltration. The final storage buffer contained no salts (10 mM HEPES-KOH pH 7.5, 5 mM DTT).

#### C.2.5.4 Purification of Hsc70 from bovine brain

Cow brains (500-600 g) were cleaned off to remove membranes, extra blood vessels and fat. The brains were homogenized in a blender at medium speed in 1.5 l DE52 equilibration buffer (20 mM Tris-HCl pH 7.5, 0.1 mM EDTA, and protease inhibitors). Homogenate was centrifuged at 5,000xg for 10 min. Supernant was filtered and centrifuged at 100,000xg for 30 min. Filtrate of the supernatant was mixed with 200 ml DE52 matrix (*Whatman*) and incubated for 1 h under stirring at 4°C. The mixture was poured into a column (*Pharmacia*) and washed with 1 l of DE52 equilibration buffer. Proteins were eluted with 400 ml of 150 mM NaCl, 20 mM Tris-HCl pH 7.5, and 0.1 mM EDTA supplemented with protease inhibitors. DE52 eluate was adjusted to 3 mM MgCl<sub>2</sub>, and loaded on a 25 ml ATP agarose column (C8 linkage, *Sigma*), equilibrated with 20 mM NaCl, 20 mM Tris-HCl pH 7.5, and 3 mM MgCl<sub>2</sub>. The matrix was washed with 50 ml equilibration buffer, then with 50 ml 500 mM NaCl, 20 mM Tris-HCl pH 7.5, and 3 mM MgCl<sub>2</sub>. Proteins were eluted with 150 ml equilibration buffer containing 3 mM ATP. The pooled fractions containing Hsc70 were loaded on a 20 ml hydroxyapatite column (*BioRad*) equilibrated in 20 mM KH<sub>2</sub>PO<sub>4</sub> pH 7.5. The column was washed with 100 ml of equilibration buffer. Elution was carried out with a 200 ml linear gradient of 20 mM to 300 mM KH<sub>2</sub>PO<sub>4</sub> pH 7.5. The pooled protein peak was concentrated, and aliquots were frozen in liquid nitrogen.

#### C.2.5.5 Determination of protein concentration in solution

Protein concentrations were determined using either the Bradford reagent (*Pierce*) (Bradford, 1976) and a BSA standard dilution serie measuring OD<sub>595</sub>, or by measuring OD<sub>280</sub> and applying the Lambert-Beer equation using the theoretical extinction coefficient (Pace et al., 1995; Wetlaufer, 1962). Extinction coefficients were determined using the ProtParam tool at the Expasy server (<http://www.expasy.ch>).

### C.2.5.6 Limited proteolysis and mass spectroscopy

For the determination of stably folded domains, proteins were partially proteolyzed by incubation with increasing amounts of the unspecific proteases subtilisin or proteinase K. Reactions contained 20 mM HEPES-KOH pH 7.4, 20 mM (NH<sub>4</sub>)<sub>2</sub>SO<sub>4</sub>, 10 mM MgSO<sub>4</sub>, and 50 µg protein in a final volume of 100 µl. Subtilisin was added in final concentrations ranging from 0.001 mg/ml to 10 mg/ml, proteinase K was added from 0.001 mg/ml to 1 mg/ml. Reactions were incubated for 30 min on ice. Proteolysis was stopped by addition of 4 mM PMSF (final concentration). Reactions were analyzed by SDS-PAGE followed by Coomassie staining and by mass spectroscopy (electrospray ionisation mass spectroscopy (ESI-MS) service (*MPI for Biochemistry*, Martinsried).

### C.2.5.7 Isothermal titration calorimetry (ITC)

Isothermal titration calorimetry (Wiseman et al., 1989; Pierce et al., 1999) was used to measure binding constants ( $K_D$ ) in solution and to assay the stoichiometry of complex formation between Bag-1M, Hsc/Hsp70, and their respective domains. The latter value was used to describe the fitness of the proteins used for functional assays and crystallography. During the titration of two protein solutions, the heat generated or consumed upon protein-protein interaction is measured at constant temperature. The amount of heat evolved on addition of ligand can be represented by the equation

$$Q = V_0 \Delta H_b [M]_t K_a [L] / (1 + K_a [L])$$

where  $V_0$  is the volume of the cell,  $\Delta H_b$  is the enthalpy of binding per mole of ligand,  $[M]_t$  is the total macromolecule concentration including bound and free fractions,  $K_a$  is the binding constant, and  $[L]$  is the free ligand concentration. For a ligand L binding to sites on a macromolecule, the binding constant is

$$K_a = [\text{filled sites}] / [\text{empty sites}][L]$$

and

$$\Delta G^0 = -RT \ln K_a = \Delta H^0 - T\Delta S^0$$



where  $\Delta G^0$ ,  $\Delta H^0$  and  $\Delta S^0$  are the free energy, enthalpy, and entropy change for single site binding. The parameters  $K$ ,  $\Delta H^0$ , and stoichiometry are determined directly in a single experiment by non-linear least squares fit of the calorimetric titration data.  $\Delta G^0$  and  $\Delta S^0$  may then be calculated.

Calorimetric isothermal titration measurements were carried out at  $T=25^\circ\text{C}$  by titration of 100  $\mu\text{M}$  protein with 1 mM ligand in buffer G (25 mM HEPES-KOH pH 7.5, 100 mM KAc, and 5 mM  $\text{MgAc}_2$ ) by injections of 10  $\mu\text{l}$  with a 400 sec spacing between each injection. When indicated, buffers were supplemented with 5 mM ADP or ATP (cuvette and syringe solutions). Constants ( $K_D$ ) were determined by integrating heat effects normalized to the amount of injected protein and curve fitting based on a 1:1 binding model using the Origin software package. Stoichiometry factors (N) typically ranged between 0.85 and 1.05 (syringe:cuvette).

#### C.2.5.8 ATPase assay

Rates of ATP hydrolysis have been determined as described before (Liberek et al., 1991). The ATPase activity was determined from the amount of  $\alpha^{32}\text{P}$ -ATP hydrolyzed. The final reaction mixture contained 20 mM HEPES-KOH pH 7.6, 50 mM KCl, 5 mM  $\text{MgAc}_2$ , and 2 mM ATP supplemented with 1  $\mu\text{Ci}$   $\alpha^{32}\text{P}$ -ATP with a specific activity of 400 Ci/mmol in a final volume of 30  $\mu\text{l}$ . Reactions were initiated by addition of ATP to the mixtures containing the various proteins at 3  $\mu\text{M}$  final concentration. Samples (1  $\mu\text{l}$ ) were analyzed by thin layer chromatography (TLC) on polyethyleneimine (PEI)-cellulose (*Merck*) in 0.5 M formic acid/0.5 M LiCl (1:1, v/v). TLC sheets were dried using a blow dryer. The ATP and ADP spots were quantified by phosphoimaging (*Fuji Film* FLA-2000) using the MacBas software package.

#### C.2.5.9 Covalent coupling of antibodies to Protein G beads

Antibodies against the c-myc (EQKLISEEDL) epitope were covalently coupled to Protein G sepharose (*Pharmacia*) using the following protocol. Protein G beads (1 ml) were washed three times with PBS (10 ml). Washed beads were mixed with antibody

solution (1 ml of a 1 mg/ml polyclonal serum or 10 ml of cell culture supernatant) and incubated for 1 hour at room temperature with gentle rocking. Beads were washed two times with 10 volumes of 0.2 M Na-borate pH 9.0 by centrifugation at 3000xg for 5 min. Beads were resuspended in 10 volumes 0.2 M Na-borate pH 9.0. An aliquot (10  $\mu$ l) was removed for later analysis of coupling efficiency. Solid dimethylsuberimidate (10 mM final concentration; 5.5 mg/1 ml) was added to the suspension. The solution should be approximately at pH 8.3. Beads were incubated for 30 min at room temperature with gentle rocking. Again, an aliquot (10  $\mu$ l) was removed. The reaction was stopped by incubating the beads with 10 volumes 0.2 M ethanolamine pH 8.0 with gentle mixing. Beads were washed with 10 volumes 0.2 M ethanolamine pH 8.0 and finally resuspended in PBS/0.02% Na-azide. The coupling efficiency was determined by boiling the samples removed during the procedure in SDS-PAGE sample buffer and SDS-PAGE analysis. The heavy chain of the antibody (around 55 kDa) should be seen in the sample taken before the addition of the crosslinker, and should be absent after crosslinking.

#### C.2.5.10 Preparation of yeast lysates

Yeast lysates have been prepared as described (Hartley et al., 1996). YPD medium (6x 500 ml) was inoculated with 100  $\mu$ l of a starter culture grown to stationary phase. Cultures were grown at 30°C with vigorous agitation (150 rpm) until a cell density of OD<sub>600</sub>=1 was reached (normally between 14 and 16 hours depending on the strain). Cells were harvested by centrifugation at 4400xg for 5 min at 4°C. Cells were washed with 200 ml cold sterile water and centrifuged as before. Dry cell pellets were weighed. Cells were resuspended in half volume to weight of cold lysis buffer (20 mM HEPES-KOH pH 7.4, 100 mM KAc, 2 mM MgAc<sub>2</sub>, and 2 mM DTT, supplemented with protease inhibitors). Cells were transferred to sterile 50 ml Falcon tubes kept on ice, not exceeding 12 ml per tube. Acid-washed glass beads were added to just below the meniscus, followed by an incubation for 15 min on ice. Mixtures were repeatedly agitated vigorously by hand for 30 seconds, followed by chilling on ice for 1 min. The degree of disruption was estimated microscopically. After 70-80% lysis, liquid was withdrawn with a plastic pipette and transferred to a sterile Corex tube. Glass beads were washed with 1 ml cold lysis buffer. Wash buffer and lysates were pooled with the lysate. Lysates were centrifuged at

30,000xg for 10 min at 4°C. The opaque-yellow lysate was withdrawn using a sterile, cold glass pipette without contaminating it with the top lipid layer or flocculent material. The lysate was centrifuged at 100,000xg for 30 min at 4°C. Supernatants were supplemented with 20% glycerol and frozen in liquid nitrogen in aliquots.

#### C.2.5.11 Western blotting

Immunoblotting was performed following the protocol of Towbin et al. (1979). Briefly, proteins were separated by SDS-PAGE and transferred to nitrocellulose in a tank blot system (*Biorad*) in 25 mM Tris, 192 mM glycine and 20% methanol, pH 8.4 at constant current (320 mA) for two hours at 4°C. Nitrocellulose membranes were blocked with 5% milk powder in PBS/0.1% Tween20 for 1.5 hours at room temperature or overnight at 4°C. Blots were washed 3 times with PBS/0.02%, followed by incubation with the primary antibody in PBS/0.02% Tween20 for 1 hour at room temperature. Blots were washed 5-times with PBS/0.02% Tween. Incubation with the secondary, horse-reddish peroxidase-coupled antibody in PBS/0.02% Tween20 was carried out for 30 min at room temperature. Blots were washed as before, followed by additional three washes with distilled H<sub>2</sub>O. Detection was achieved by using the chemiluminescence kit ECL (*Amersham*) followed by exposure to X-ray films (*Fuji Film*).

Primary antibodies used for detection of *S. cerevisiae* Ssa and Ssb proteins were a generous gift of Elizabeth A. Craig (Madison, USA) (Lopez-Buesa et al., 1998). Antibodies recognize the C-terminal 80 and 56 amino acids, respectively. As secondary, species-specific antibody, an goat  $\alpha$ -rabbit specific antiserum directly conjugated with horse reddish peroxidase (*Sigma*) was used.

#### C.2.5.12 Pull downs using His<sub>6</sub>-tagged proteins bound to NiNTA beads

His<sub>6</sub>-tagged proteins (60  $\mu$ g) were bound to NiNTA resin (25  $\mu$ l of a 1:1 slurry) in buffer B in micro spin columns (*MoBiTec*, Germany) for 20 min at room temperature. Beads were washed twice with buffer B supplemented with 200 mM KAc and an additional wash with buffer B. Control beads without bound proteins were processed

equally. Beads were resuspended in 200  $\mu$ l buffer B. Reactions were supplemented with 200  $\mu$ l yeast lysates. Binding was performed either in the presence of apyrase (4 Units/ml), 5 mM ATP/Mg<sup>2+</sup>, or 5 mM ADP/Mg<sup>2+</sup>. Reactions were incubated for 20 min at room temperature. Beads were washed 3-times with the respective binding buffer (buffer B, buffer B containing 5 mM ATP/Mg<sup>2+</sup>, or buffer B containing 5 mM ADP/Mg<sup>2+</sup>). Bound proteins were eluted from the resin with 2x SDS-PAGE sample buffer and analyzed by SDS-PAGE and Western blotting.

#### C.2.5.13 Substrate release assay

Hsc70 release from substrate was measured as described (Young and Hartl, 2000). The principle of the experimental setup is depicted in Figure 6.

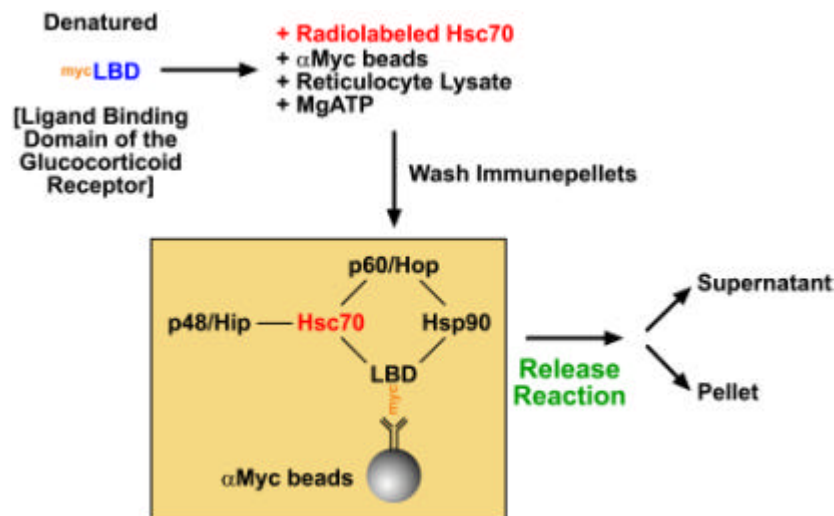


**Figure 6:** Principle of substrate release assay.

Rabbit reticulocyte lysate (RL) (*Green Hectares*) was desalted into buffer B (25 mM HEPES-KOH pH 7.5, 100 mM KAc and 5% glycerol) by chromatography on a NAP5 column (*Pharmacia*) following the manufacturer's instructions. Radiolabeled Hsc70 was generated by *in vitro* translation of Hsc70 cDNA from a T7 promoter (pET3a vector backbone) using the TNT T7 system (*Promega*). All reagents except DNA and

RNase guard were included in the system kit. Reactions were set up as follows and incubated for 90 min at 30°C:

TNT reaction:            25  $\mu$ l reticulocyte lysate (*Promega*)  
                                  2  $\mu$ l TNT reaction buffer  
                                  1  $\mu$ l T7 polymerase  
                                  1  $\mu$ l amino acid mix lacking methionine  
                                  4  $\mu$ l  $^{35}$ S-methionine  
                                  1  $\mu$ g DNA (hsc70human in pET3a)  
                                  ddH<sub>2</sub>O to 50  $\mu$ l final volume.

After 60 min of transcription/translation, purified, myc-tagged ligand binding domain of the glucocorticoid receptor (LBD) (200  $\mu$ g, kindly provided by J. C. Young) was partially denatured for 5 min in 1% SDS, 50 mM Tris-HCl pH 7.5 at room temperature. The solution was diluted 200fold into buffer C (100 mM K-acetate, 25 mM HEPES-KOH pH 7.5, 1% NP40, 1% Na-deoxycholate, 0.1% SDS). Anti-myc monoclonal antibodies, covalently coupled to Protein G Sepharose (*Pharmacia*) (50  $\mu$ l of a 1:1 slurry) were added to the partially unfolded LBD and incubated for 30 min at 25°C. Immunopellets were washed twice with 1 ml buffer B. Reactions were supplemented with radiolabeled Hsc70 from the *in vitro* translation reaction, 10 mM MgAc<sub>2</sub>, 2 mM ATP, 500  $\mu$ l buffer B, and 500  $\mu$ l desalted reticulocyte lysate (*Green Hectar*). Steady-state binding of Hsc70 and cofactors to the LBD was attained after 10 min at room temperature. The immunoprecipitation reaction was split into 10 reactions, and each aliquot was washed twice with buffer B.

For the release reaction, immunopellets were resuspended in 100  $\mu$ l buffer B containing additions as indicated. After 10 min at room temperature, beads and supernatant were separated. Supernatants were precipitated with trichloroacetic acid (12.5% final; spin for 30 min at 20,000xg at 4°C). Proteins bound to the beads were eluted with 2xSDS-PAGE sample buffer. Pellet fractions and eluates from beads were analyzed by SDS-PAGE. Quantification of the radiolabeled gel was performed by phosphorimaging (*Fuji Film FLA-2000*). Release of Hsc70 from the immunopellets was normalized to the amount of input radiolabeled Hsc70.

### C.2.6 X-ray crystallographic Methods

An adequate description of the theory of X-ray crystallography and its experimental application is too extensive to be covered in the format of this thesis. Therefore, only a summary of the diffraction theory and the different steps for X-ray analysis will be given. A more detailed description of the methods and theories can be found in textbooks by Drenth (1994), Massa (1994), McRee (1993), Giacovazzo (1992), McPherson (1982), Buerger (1977), Blundell and Johnson (1976), and Woolfson (1970).

#### C.2.6.1 Theory of X-ray diffraction

When X-rays impinge on a crystal their electromagnetic field excites the electrons within the crystal which will oscillate with the same frequency as the incident wave. Oscillating electrons scatter the radiation and they emit radiation of the same frequency as the incident radiation but with a phase shift of  $180^\circ$  (Thomson scattering). The overall intensity adds up to zero (destructive interference) if the path difference is not an integral multiple of the wavelength (see below). Periodicity is a prerequisite of constructive interference (path difference is an integral multiple of the wavelength). This requirement is given in a crystal. The wave scattered by a crystal can be described as a summation of waves, each scattered by electrons in the crystal. The aim of structure analysis by X-ray diffraction is to derive the electron density distribution as a function of the scattering information. This is achieved by Fourier transformation.

Geometric conditions that produce reflexes (constructive interference) by diffraction of X-rays at a crystal can be described by the Laue conditions:

$$\bar{a}(\bar{s} - \bar{s}_0) = h\mathbf{I} \qquad \bar{b}(\bar{s} - \bar{s}_0) = k\mathbf{I} \qquad \bar{c}(\bar{s} - \bar{s}_0) = l\mathbf{I}$$

where  $h$ ,  $k$ , and  $l$  are integer,  $\lambda$  is the wavelength of the X-rays,  $\bar{a}$ ,  $\bar{b}$  and  $\bar{c}$  are unit cell vectors,  $\bar{s}$  and  $\bar{s}_0$  are unit vectors in the direction of the impinging and diffracted ray, respectively.

Bragg described these equations in a scalar form. A set of parallel planes with the index  $hkl$  and interplanar spacing  $d_{hkl}$  produces a diffracted beam when X-rays of the

wavelength  $\lambda$  impinge upon the planes at an angle  $\theta$  and are reflected at the same angle, only if  $\theta$  meets the condition

$$2d_{hkl}\sin\theta = n\lambda$$

where  $n$  is an integer. A geometric construction of Bragg's law is shown in Figure 7. If the difference in pathlength for rays reflected from successive planes is equal to an integral number of  $\lambda$  of the impinging X-ray, then reflected rays emerge from the crystal in phase with each other, interfering constructively to produce a strong reflected beam. An interference picture characteristic for the highly ordered, crystalline system is obtained. At other  $\theta$  not fulfilling Bragg's equation, the reflected rays are out of phase and interfere destructively; no beam emerges at that angle.

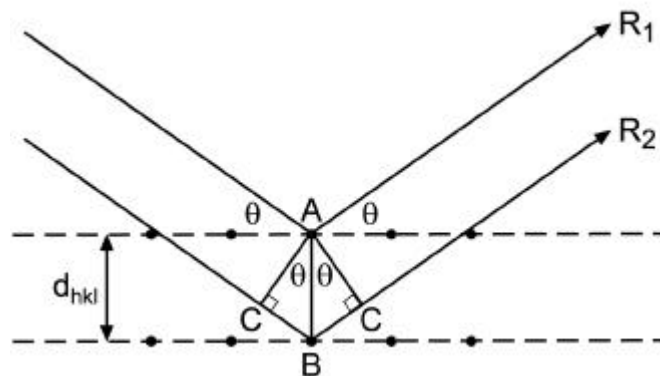


**Figure 7.** Geometric construction of Bragg's law. If the additional distance traveled by the more deeply penetrating ray  $R_2$  is an integral multiple of  $\lambda$ , then rays  $R_1$  and  $R_2$  interfere constructively. The equations  $\sin\theta = BC/AB$  and  $BC = AB\sin\theta = d_{hkl}\sin\theta$  are valid since  $ABC$  is a right triangle.

The Ewald construction transfers Bragg's law to the reciprocal space (Figure 8). The origin of the reciprocal lattice is defined as the intersection of the undiffracted ray and the Ewald sphere, a sphere with radius  $1/\lambda$ . The imaginary reciprocal lattice is in inverse relationship with the real crystal lattice. Each periodical distance between lattice planes in the real space corresponds to a vector in the reciprocal space perpendicular to the reflecting plane. The absolute value of the distance between the lattice planes in a crystal and these vectors are reciprocal to each other. If a point of the reciprocal lattice

lies on the surface of the Ewald sphere, then Bragg's law is satisfied and a reflection can be detected.

The result of a crystallographic data collection is a list of intensities for each point in the three-dimensional reciprocal lattice, the diffraction pattern of a crystal. As described above, there is an inverse relationship between the real and the reciprocal lattice. Each reflection is explicitly defined by the Miller indices ( $h$ ,  $k$ , and  $l$ ) with respect to the crystal metric. In the process of structure determination, the diffraction pattern (reciprocal space), providing parameters  $hkl$  and their intensities  $I_{hkl}$ , is converted to information about the real space.

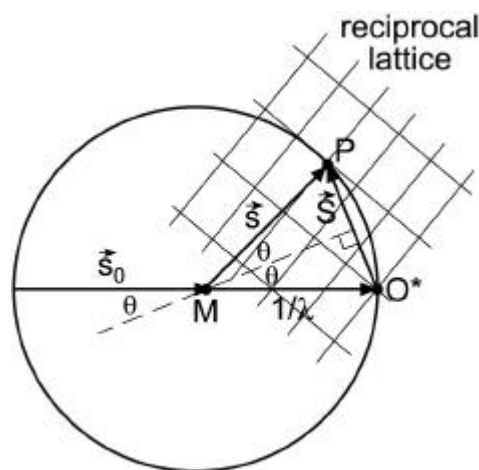


**Figure 8.** The Ewald construction as a tool to construct the direction of the scattered beam. A circle with radius  $1/\lambda$  is drawn around the crystal  $M$ . In the three-dimensional space, this will be a sphere. The origin of the reciprocal lattice is at  $O^*$ .  $\vec{s}_0$  indicates the direction of the incident beam;  $\vec{s}$  indicates the direction of the scattered beam.

Each lattice point  $P_{hkl}$  is assigned to a scattering vector  $\vec{S}$  (with  $\vec{S} = \vec{s} - \vec{s}_0$ ; see above).  $\vec{S}$  can be described with the unit cell vectors (translation vectors) of the reciprocal space  $\vec{a}^*$ ,  $\vec{b}^*$ , and  $\vec{c}^*$  with

$$\vec{S} = h\vec{a}^* + k\vec{b}^* + l\vec{c}^*$$

where the correlation of the translation vectors of the real space and the ones in reciprocal space can be expressed with



$$\bar{a}^* = \frac{\bar{b} \times \bar{c}}{\bar{a}(\bar{b} \times \bar{c})} \quad \bar{b}^* = \frac{\bar{c} \times \bar{a}}{\bar{a}(\bar{b} \times \bar{c})} \quad \bar{c}^* = \frac{\bar{a} \times \bar{b}}{\bar{a}(\bar{b} \times \bar{c})}.$$

An impinging X-ray is scattered by an electron cloud of an atom dependent on the number of electrons and their position in the cloud. The electron density at position  $\bar{r}$  is denoted by  $\rho(\bar{r})$ . The scattered wave is calculated by adding up all individual contributions within the volume of an atom by

$$f = \int_r \mathbf{r}(\bar{r}) \exp[2\mathbf{i}\bar{p}\bar{r} \cdot \bar{S}] d\bar{r}$$

where  $f$  is the atomic scattering factor and  $i$  is the imaginary number  $(-1)^{1/2}$ .

Scattering from a unit cell with  $n$  atoms at positions  $\bar{r}_j$  ( $j=1, 2, 3, \dots, n$ ) with respect to the origin of the unit cell is obtained by summation of the contribution of each atom with the origin transferred to the origin of the unit cell (the phase angles change by  $2\mathbf{i}\bar{p}\bar{r}_j \cdot \bar{S}$ ). The total scattering from the unit cell is

$$\bar{F}(\bar{S}) = \sum_{j=1}^n f_j \exp[2\mathbf{i}\bar{p}\bar{r}_j \cdot \bar{S}]$$

where  $\bar{F}(\bar{S})$  is called the structure factor, a function of the electron density distribution in the unit cell. To obtain the scattering by a crystal consisting of a large number of unit cells in each direction, the structure factors are added with respect to a single origin and is described by

$$\bar{K}(\bar{S}) = \bar{F}(\bar{S}) \times \left( \begin{array}{c} \sum_{t=0}^{n_1} \exp[2\mathbf{i}\bar{p}t\bar{h}] \\ \sum_{u=0}^{n_2} \exp[2\mathbf{i}\bar{p}u\bar{h}] \\ \sum_{v=0}^{n_3} \exp[2\mathbf{i}\bar{p}v\bar{h}] \end{array} \right)$$

where  $n_1$ ,  $n_2$ , and  $n_3$  are the number of units cells in the  $\vec{a}$ -,  $\vec{b}$ -, and  $\vec{c}$ - direction, respectively, and where  $t \cdot \vec{a} + u \cdot \vec{b} + v \cdot \vec{c}$  is the origin of an individual unit cell ( $t$ ,  $u$ , and  $v$  are whole numbers). Instead of summing over all separate atoms, an integral over all electrons in a unit cell can be used. The structure factor is then described by

$$\bar{F}(\vec{S}) = \int_{\text{unit cell}} \mathbf{r}(\vec{r})_{\text{unit cell}} \exp[2\mathbf{p}\vec{r} \cdot \vec{S}] dv.$$

With  $V$  being the volume of the unit cell and with

$$\vec{r} \cdot \vec{S} = (\vec{a} \cdot x + \vec{b} \cdot y + \vec{c} \cdot z) \cdot \vec{S} = \vec{a} \cdot \vec{S} \cdot x + \vec{b} \cdot \vec{S} \cdot y + \vec{c} \cdot \vec{S} \cdot z = hx + ky + lz,$$

$\bar{F}(\vec{S})$  can also be written as  $\bar{F}(hkl)$ :

$$\bar{F}(hkl) = V \int_{x=0}^1 \int_{y=0}^1 \int_{z=0}^1 \mathbf{r}(xyz) \exp[2\mathbf{p}(hx + ky + lz)] dx dy dz$$

$\bar{F}(hkl)$  is a Fourier transform of  $\mathbf{r}(xyz)$  and vice versa. Therefore,  $\mathbf{r}(xyz)$  can be written as a function of  $\bar{F}(hkl)$ :

$$\begin{aligned} \mathbf{r}(xyz) &= \frac{1}{V} \sum_h \sum_k \sum_l \bar{F}(hkl) \exp[-2\mathbf{p}(hx + ky + lz)] \\ &= \frac{1}{V} \sum_h \sum_k \sum_l |F(hkl)| \exp[-2\mathbf{p}(hx + ky + lz) + i\mathbf{a}(hkl)] \end{aligned}$$

Because  $I(hkl) \propto |F(hkl)|^2$  the structure factor amplitudes  $|F(hkl)|$  of the reflexion  $(hkl)$  can be derived from the intensities  $I(hkl)$  but the phase angles  $\alpha(hkl)$  cannot be measured straightforwardly. Phase information has to be assigned to each structure factor amplitude. Calculation of phase information is achieved by the structural model, an assumed electron density distribution, which will provide theoretical structure factor amplitudes  $F_{calc}$  containing the phases  $\alpha(hkl)_{calc}$ . These are transferred to the

observed amplitudes and allow a calculation of the electron density distribution under consideration of the experimental data. Methods to obtain phase information will be described briefly in the chapter 'Structure solution'.

#### C.2.6.2 Structure determination using X-ray diffraction

In Figure 9, the necessary steps of structure determination by X-ray analysis are outlined. All steps will be described briefly in the following paragraphs.

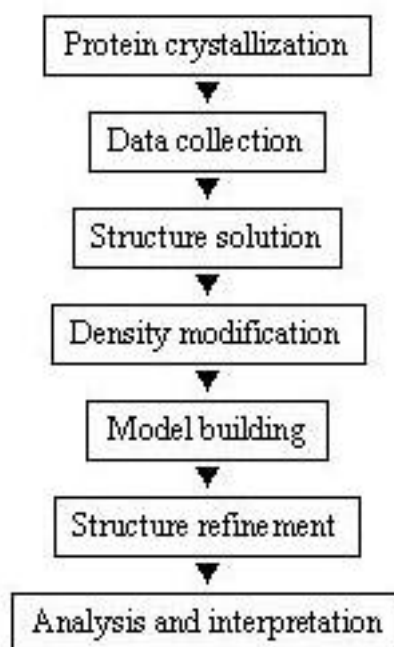


**Figure 9.** Flow chart of structure determination by X-ray analysis

#### C.2.6.3 Protein crystallization

The basis for X-ray structure analysis is the existence of suitable crystals which provide high resolution diffraction patterns. Under certain circumstances, molecules - here proteins - will enter the crystalline state from solution. Individual molecules adopt one or a few identical orientations thereby forming an orderly three-dimensional array of molecules, held together by non-covalent interactions. Prerequisite for crystallization is a crystal seed obtained by slow, controlled precipitation from an aqueous solution. Proper

conditions for optimal crystallization have to be determined empirically by testing a multi-dimensional set of condition, for example choice and concentration of precipitant, pH, temperature, protein concentration and homogeneity, ionic strength, additives such as detergents or alcohols, and sample volume (McPherson, 1990). To find suitable starting conditions, so called 'sparse-matrix screens' are used (Jancarik and Kim, 1991) which are commercially available. These screens contain a limited number of conditions which have been chosen after a statistical evaluation of known crystallization conditions. In the next steps, the starting condition is reproduced and optimized by varying the different parameters and/or including new ones. Methods for crystal growth are the sitting or hanging drop method, crystallization under oil, or crystallization by microdialysis (reviewed in Ducruix and Grige, 1992).

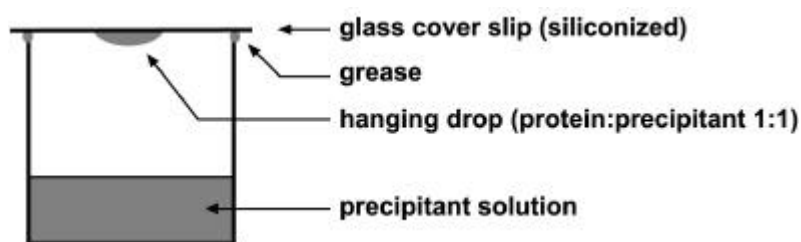


**Figure 10.** Principle of crystallization by the hanging drop method.

In the present study, protein crystallization was exclusively achieved by the vapor diffusion method in hanging drops (McPherson, 1982) (Figure 10). Purified proteins were mixed with precipitant solution in a 1:1 ratio, and the solution was suspended as a drop from a siliconized glass cover slip above the precipitant solution. The chamber was sealed with grease. Equilibrium was reached by diffusion of vapor between protein solution and precipitant solution. Sparse-matrix screens of precipitant solutions were obtained from *Hampton Research*. Protein concentrations ranged from 5 to 40 mg/ml. Optimization of starting condition for crystal growth was achieved by varying temperature, buffer and pH, salt concentration, precipitant and protein concentration. Furthermore, additives (cryoprotectant and alcohols) and seeding techniques (mainly micro-seeding) were tested.

## C.2.6.4 Data collection and data reduction

As described above, reflexes of a X-ray scattered on a crystal can be measured if the conditions described by Bragg and Laue are fulfilled. This is achieved by the oscillation of a crystal centered in a X-ray beam. During the rotation ( $\Delta\omega$  between  $0.5^\circ$  and  $2^\circ$ ), the diffraction patterns are recorded by an area detector. The goal of data collection is a set of consistently measured, indexed intensities for as many of the reflections as possible. For higher consistency of the diffraction properties of a crystal during data collections, the crystal is cooled continuously. In the present study, rotating copper anodes and synchrotron radiation were used as X-ray sources. The latter one is favorable for reasons of higher intensity and minor divergence of the radiation, and the free choice of the wavelength within in the continuous synchrotron spectrum.

After collection of diffraction patterns, the raw intensities of the reflections must be processed to improve their consistency and to maximize the number of observations which are sufficiently accurate for structure solution. This process is called 'data reduction'. The quality of data reduction is estimated by comparing symmetry-equivalent intensities which is described in the  $R_{\text{sym}}$  value (the 'reliability index').

Crystals were shock frozen in liquid nitrogen. In some cases, the drop containing crystals was overlayed with paraffin oil to improve freezing properties. Data collection was carried out on a single crystal at 100 K in a continuous stream of liquid nitrogen (*Oxford Cryostream*). Proper cryogenic conditions were achieved by co-crystallization with glycerol or xylitol. Data sets were collected at the following X-ray sources (Table 6).

X-ray source	Location	Beamline	Data set	Detector
Rotating anode RU-200 (Rigaku), mirror system (Supper)	Martinsried	-	native	Image plate MAR300
DESY	Hamburg	BW6	MAD	MARCCD
ESRF	Grenoble	ID14-4	native	ADSC Quantum-4

Data reduction was carried out using the software packages DENZO and SCALEPACK (Otwinowski and Minor, 1997).

### C.2.6.5 Structure solution

Structure solution is achieved when the first structure model has been found or, equivalent to that, the correct phase information has been obtained. For small molecules, phases can be obtained by direct methods without any further experimental analysis (Karle and Hauptmann, 1950, Harker and Kasper, 1948). For protein structures, this method is only applicable to very small molecules (< 1000 non-hydrogen atoms) and requires a very high resolution (< 1.2 Å).

For solving larger protein structures, experimental methods have been established to obtain phase information necessary for structure solution: Multiple isomorphous replacement (MIR), multiple anomalous dispersion (MAD), and molecular replacement (MR). In some cases, a combination of the different phasing methods can be applied.

In MIR experiments, heavy metal atoms (for example Hg, Pt, Au) are attached to the protein molecules in the crystal. Usually, the crystal is soaked in solutions containing heavy metal compounds (usually salts). The reflection intensities of these heavy metal derivatives of the crystals will be significantly different from the native ones. Such a crystal is called an isomorphous derivative if the unit cell parameters and the crystal packing are not different from the native crystal, a prerequisite for applying structure solution by MIR techniques. Under these conditions, the changes in reflex intensities are solely due to the incorporation of the heavy metal atoms. The position of the heavy metal atoms will be located in the unit cell of the crystal derivative by applying the patterson function with the observed differences in reflex intensities (Patterson, 1934; Patterson 1935) or by direct methods. For MIR experiments, at least two different derivatives are required for successful solution of the phase problem.

Phasing by MAD techniques depends on the presence of sufficiently strong anomalous scattering atoms in the protein structure itself. This can be achieved by incorporation of non-natural amino acid derivatives (for example selenomethionine). The technique takes advantage of the heavy atom's capacity to absorb X-rays of a specified wavelength. It results in an inequality of the intensities of symmetry-related reflections (Friedel's law,  $I_{hkl} \neq I_{-h -k - l}$ , does not hold). This inequality is called anomalous scattering (also: anomalous dispersion). Anomalous scattering can be measured at X-ray wavelength near the absorption edge of the heavy atom (the sudden drop of absorption at wavelengths just below their characteristic emission wavelength). On the other hand, absorption edges of the light atoms are not near the X-ray wavelengths, and therefore do

not contribute to the anomalous scattering. The differences in intensities are measured at wavelengths around the absorption edges of the heavy atom incorporated into the molecules. Data sets are collected at at least two different wavelengths (preferably three). MAD experiments can be performed using a single crystal and therefore, the phase information is very accurate up to the resolution limits since problems regarding isomorphism of the crystal will usually not occur.

Molecular replacement can be used as phasing technique if structural similarities indicated by sequence homology between the desired structure and an already known one can be expected (Rossmann, 1972; Huber, 1965; Rossmann and Blow, 1962; Hoppe, 1957). This method requires the correct placement of the known structure (as search model) in the unit cell of the desired crystal structure. Structure solution will be achieved by determination of the orientation and translation of the search model in the unit cell.

After determination of the experimental phases, the density maps are calculated by Fourier transformation. Improvement of the phases by density modifications is often necessary to obtain a interpretable electron density map. This is achieved by introducing boundary conditions, for example the continuity of a polypeptide chain, maxima of electron density at atom positions at high resolution (Cowtan and Main, 1993), or the observation of high electron density in proteinaceous areas and low density in solvent areas of the unit cell.

In this study, structure solution was achieved by MAD experiments on a single crystal of selenomethione-containing protein using the software package SOLVE (Terwilliger and Berendzen, 1999) followed by density modification using the program DM (CCP4, 1994).

#### C.2.6.6 Model building and refinement

After calculation of the phases, the electron density map has to be interpreted. Using the known protein sequence and other informations (for example search models from molecular replacement solutions or similar structures as template), an approximate model is built in accordance with the density. At very high resolutions, the model can be built automatically (partially or completely) using special software packages (for example

wARP (Perrakis et al., 1997)). In the refinement process, model parameters (position of atoms, temperature factors of the atoms) are optimized aiming for a maximal agreement of the structural model with the experimental information. Boundary conditions regarding stereochemical properties e.g. torsion angles and bond lengths are introduced (Engh and Huber, 1991; Branden and Jones, 1990; Konnert and Hendrickson, 1980; Jack and Levitt, 1978). Iterative cycles of model building and refinement are performed until no further optimization of the model is achieved. The quality of the model can be expressed by several statistical factors (Dodson et al., 1996; Brünger, 1992).

Model building and correction was carried out using the graphical interface O (Jones et al., 1991). The model was refined using the program package CNS (Brünger et al., 1998) in consideration of stereochemical boundary conditions. 7-10% of all reflexes were excluded from the refinement process, and were used for calculation of the  $R_{\text{free}}$  value as a criterium for model quality (Kleywegt and Brünger, 1996; Brünger, 1992). In the final stage of refinement, water molecules were introduced into the model automatically by peak analysis of the  $F_o - F_c$  difference density followed by manual inspection using the graphics interface.

#### C.2.6.7 Analysis and presentation of structure models

The structure was analyzed using the programs PROCHECK (Laskowski et al., 1993), LIGPLOT (Wallace et al., 1995), and SWISS-PDBVIEWER (Guex and Peitsch, 1997). Interaction surfaces and root mean square deviations of superpositions were calculated using CNS (Brünger et al., 1998). Presentations of the structure and its properties were obtained with the programs GRASP (for calculation and presentation of the accessible surface and its electrostatic potential) (Nicholls et al., 1993), Bobscript (Esnouf, 1999) and RASTER3D (Merrit and Bacon, 1997) for ribbons and ball-and-stick presentations.



## C.3 Results

### C.3.1 Domain structure of Bag-1M and Hsc70

A rational approach was chosen to define stably folded domains of Bag-1 since preliminary crystallization trials with the full length proteins failed (unpublished observation, Christine Schneider and Ismail Moarefi). Biochemical characterization revealed the functionality of the obtained fragments.

Recombinantly expressed human Bag-1M was used as the starting material for limited proteolysis with the unspecific proteases subtilisin and proteinase K. Incubation with increasing amounts of the enzyme resulted in the appearance of a stable protein fragment of approximately 14 kDa in both reaction series. The exact molecular weight and the domain borders were determined by electrospray ionisation mass spectroscopy followed by analysis using the software package PAWS with the obtained molecular masses and the primary sequence of Bag-1M as inputs. The fragment was identified as the C-terminal Bag-domain of Bag-1M consisting of residues 151 to 263 (see Figure 4) (data kindly provided by Christine Schneider). The respective expression construct was cloned and used for overexpression in *E. coli* cells. The fragment was purified using standard chromatography techniques. During the purification, the His<sub>6</sub>-purification tag encoded by the vector used for cloning was removed by TEV protease treatment resulting in the exact product obtained by treatment with subtilisin or proteinase K.

For crystallization and biochemical assays, the main cytosolic form of Hsp70, the heat shock cognate protein 70 kDa (Hsc70), was used. The Hsc70 ATPase domain was optimized for crystallization purposes based on the known structure. Unstructured regions were omitted from the final construct, which consists of amino acids 5 to 381 of rat Hsc70 (see Figure 4).

### C.3.2 Characterization of the isolated Bag domain

The stable Bag domain was analyzed with respect to its binding and action on Hsp70. Assays were performed addressing the binding behavior of Bag-1M and its Bag

domain to Hsp70 and the isolated ATPase domain, respectively, their influence on the ATPase rate and substrate binding of Hsp70. Bag domain activities were always compared to the respective effects observed with the full length protein Bag-1M.

Isothermal titration calorimetry (ITC) was used to measure the binding constants for the interaction of Bag-1 and Hsp70 and their respective interacting domains in solution. All proteins were expressed recombinantly and were purified as described above. The binding reactions were performed in buffer containing physiological salt concentration. Furthermore, the effect of nucleotide on binding was tested. In Figure 11, an example of an ITC measurement is shown (cuvette: 100  $\mu$ M Hsc70, syringe: 1 mM Bag-1M; both in buffer G).

Stoichiometry factors (N) typically ranged between 0.85 and 1.05 representing 1:1 binding of Hsp70 to Bag-1 and the respective domains. Furthermore, this value also reflects the functionality of the proteins used in the titration, and later on for crystallization, given the specific stoichiometry for the Hsp70/Bag-1 interaction of 1:1 (Stuart et al, 1998). The construct comprising the minimal Bag domain had the same affinity for Hsc70 or its ATPase domain as the Bag isoform Bag-1M ( $K_D$  1-3  $\mu$ M; Table 7). Binding affinities were substantially reduced (about 7- to 10-fold) in the presence of ADP or ATP in agreement with the binding characteristics of the full-length proteins (Stuart et al., 1998). Furthermore, no binding of the Bag domain to the *E. coli* homolog of Hsc70, DnaK, was observed.

**Table 7. Thermodynamic Analysis of Bag-1/Hsc70 Interaction.\***

	$K_D$ ( $\mu$ M)**	
	Bag-1M	Bag domain
Hsc70(5-381)	2.8 $\pm$ 0.2	3.6 $\pm$ 0.9 27.3 $\pm$ 1.0 [ADP]*** 25.5 $\pm$ 0.9 [ATP]***
Hsc70	0.75 $\pm$ 0.07	1.1 $\pm$ 0.1
DnaK	n.d.	no binding

\* Calorimetric isothermal titration measurements were carried out at T=25°C by titration of 100  $\mu$ M Hsc70 or its ATPase domain with 1 mM Bag-1M or Bag domain in buffer G (25 mM HEPES-KOH pH 7.5, 100 mM KAc, and 5 mM MgAc<sub>2</sub>).

\*\* indicated errors represent goodness of fit.

\*\*\* 5 mM nucleotide was present in both protein solutions.

Next, the effect of Bag-1 and the isolated Bag domain on the ATPase activity of Hsp70 was tested. The source of Hsc70 for these studies was protein purified from bovine brain, material of high purity (> 98%) and activity. Hsp40-dependent ATP hydrolysis of

Hsc70 is stimulated 10-fold in the presence of the Bag domain or Bag-1M (Figure 12A). No stimulation was observed in the absence of Hsp40. Bag-1M and Hsp40 do not possess an intrinsic ATPase activity (data not shown).

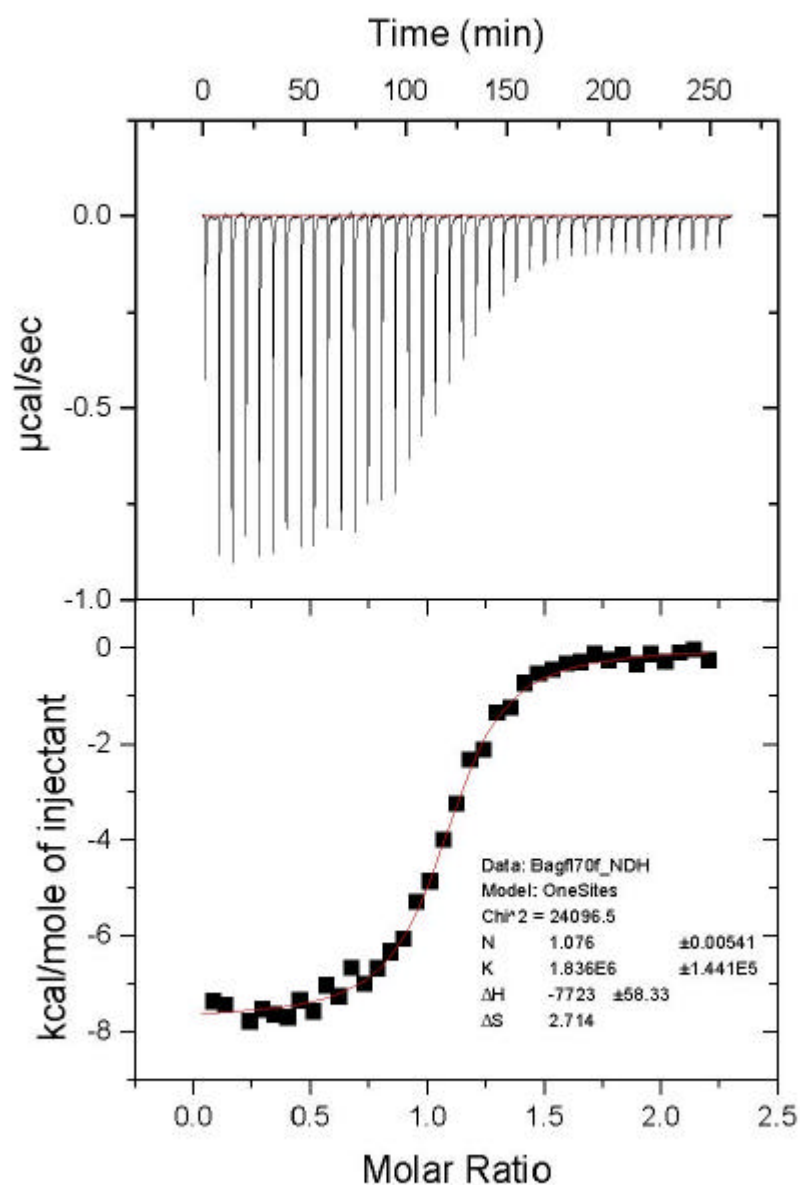


**Figure 11.** Isothermal titration calorimetry. Bag-1M (1 mM) was titrated into a solution of human Hsc70 (0.1 mM). Dissociation constants ( $K_D$ ) were determined by integrated heat effects normalized to the amount of injected protein and curve fitted based on a 1:1 binding model.

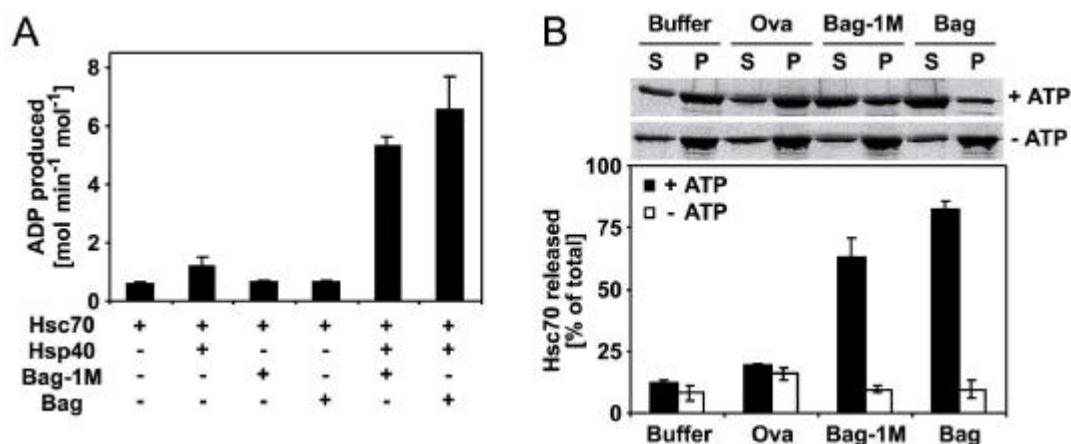


**Figure 12.** Functional characterization of Bag-1M and the Bag domain. **(A)** Bag-1M and the Bag domain stimulate the ATPase activity of Hsc70 in a Hsp40-dependent manner. Hsc70 (3  $\mu$ M) was incubated at 30°C with Hsp40 (3  $\mu$ M) and Bag-1M or isolated Bag domain (3  $\mu$ M) as indicated. The amount of ATP hydrolyzed was quantified (see Material and Methods). **(B)** Bag-1M and the Bag domain stimulate Hsc70 release from substrate polypeptide in a nucleotide-dependent manner. Release of <sup>35</sup>S-Met-labeled Hsc70 from partially denatured immobilized ligand binding domain (LBD) of the glucocorticoid receptor was measured upon incubation with ovalbumine, Bag-1M or Bag domain (5  $\mu$ M each) for 10 min at 25°C in the presence or absence of MgATP (2 mM) (see Material and Methods). S, supernatant fractions containing released Hsc70; P, pellet fractions containing LBD-bound Hsc70. Supernatants and pellets were analyzed by SDS-PAGE followed by phosphoimaging. The bar diagram shows the amounts of Hsc70 released from LBD expressed in percent of total bound Hsc70. Error bars represent standard mean deviations of three independent experiments.

Opposite effects of Bag-1 on the binding of substrate to Hsp70 have been described in the literature. On the one hand, stabilization of Hsp70/substrate complexes by Bag-1 has been observed using a native PAGE assay (Bimston et al., 1998). On the other hand, Bag-1 has been shown to promote substrate release from Hsp70 as analyzed by gel filtration and immunoprecipitations (Lüders et al., 2000; Zeiner et al., 1997). While previous immunoprecipitation experiments examined the equilibrium binding of Hsp70 to substrate, an *in vitro* assay has been recently established to specifically analyse the dissociation of chaperone/substrate complexes (Young and Hartl, 2000). Using this novel assay, the effect of Bag-1 on complexes of Hsp70 with substrates was tested. Immuno-isolated complexes of Hsp70 with a model substrate (partially denatured glucocorticoid receptor ligand binding domain, LBD) were incubated with various forms of Bag-1 cochaperones, and the amounts of Hsp70 released were quantified. In the presence of

ATP, the Bag domain and Bag-1M triggered efficient release of radiolabeled Hsc70 from the LBD, whereas little release was observed with ovalbumin (Figure 12B). This is consistent with the previously published observations from gel filtration experiments and immunoprecipitations of Hsc70/substrate complexes (Lüders et al., 2000; Zeiner et al., 1997). Bag-dependent dissociation of the Hsc70/LBD complex required ATP as Bag-1 in the absence of nucleotide did not trigger substrate release (Figure 12B). Addition of ADP or ATP alone without Bag-1 did not release Hsc70 from substrate above control reactions lacking nucleotides (Figure 13A).

Bag-1 has also been reported to compete with the cofactor p48/Hip in binding to the ATPase domain of Hsp70 and to oppose its influence on ATPase hydrolysis and protein folding by Hsp70 (Gebauer et al., 1997; Höhfeld and Jentsch, 1997; Lüders et al., 1998). p48/Hip was also present in the substrate/chaperone complexes (Figure 13B) (Young and Hartl, 2000). In this experiment, radiolabeled p48/Hip was translated to monitor and quantify its fate upon the different incubations. In parallel, the experiment was carried out with radiolabeled Hsp70, as described above (Figure 13A). Treatment of the immune pellets with control proteins or nucleotides alone did not release the cochaperone from the pellets. Efficient release of p48/Hip was only observed when Bag-1M or the Bag domain was present. This reaction was independent of nucleotide. Furthermore, Hip binding to the ATPase domain of Hsp70 was salt sensitive, comparable to other TPR-mediated interactions, e.g. that of p60/Hop with the C-termini of Hsp70 and Hsp90 (Young and Hartl, 2000).

Taken together, the Bag domain used for crystallization was fully functional with respect to binding properties and action on Hsp70 reported earlier (Höhfeld and Jentsch, 1997; Stuart et al., 1998; Lüders et al., 2000). In all assays, the isolated domain accounts for the effects of Bag-1M on Hsp70 activity.

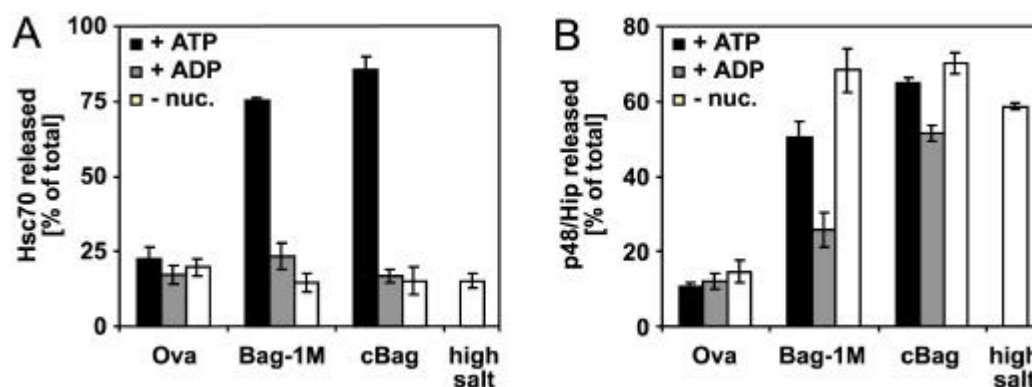


**Figure 13.** p48/Hip release from LBD/chaperone complexes. (A) Bag-1M and the Bag domain stimulate Hsc70 release from substrate polypeptide in an ATP-dependent manner. Release of  $^{35}\text{S}$ -Met-labeled Hsc70 from partially denatured LBD was assayed as before (Figure 12). (B) Bag-1M and the Bag domain stimulate p48/Hip release from Hsc70 in a nucleotide-independent manner. Release of  $^{35}\text{S}$ -Met-labeled p48/Hip from the complexes was assayed as for Hsc70 release. Error bars represent standard mean deviations of three independent experiments.

#### C.3.4 Crystallization, data collection and processing

For crystallization trials, proteins were expressed and purified as described in Materials and Methods. Complex formation between the human Bag domain of Bag-1M with the ATPase domain of rat Hsc70 (100% identical to the human primary sequence) was performed by incubating a mixture of the two proteins, using a slight excess of Bag over the ATPase domain (Bag domain:Hsc70 ATPase domain 1.5:1). The complex was further purified to homogeneity by anion exchange chromatography and gel filtration. A selenomethionine-labeled derivative of the ATPase domain was produced in the *E. coli* strain B834(DE3)pLysS, and incorporation of the heavy metal derivative was confirmed by electrospray ionisation mass spectroscopy (data not shown). Substitution of methionine by selenomethionine was quantitative (6 out of 6 sites).

**Table 8. Crystal growth conditions.**

Initial conditions (PEG ion screen)	Optimized conditions (native, in house)	Optimized conditions (native, ESRF)	Optimized conditions (SeMet-derivative)
0.2 M Na-K-tartrate 20% PEG3350*	0.05-0.1 M Na-K-tartrate 14-16% PEG3350** 20% glycerol	0.05 M NaCl 10-12% PEG3350 20% glycerol	0.05 M Na-K-tartrate 16% PEG3350 30% glycerol
and	0.1 M Tris -HCl pH 8.5	0.1 M Tris -HCl pH 8.5 5% ethanol (frozen in parafine oil)	0.1 M Tris -HCl pH 8.5 (no parafine oil)
0.2 M NaCl 20% PEG3350*			

\*: polyethylene glycol (average molecular weight 3350 Da)

Initial conditions of crystal growth were obtained by the use of the sparse-matrix screen 'PEG ion screen' (*Hampton Research*) (Table 8). Washing of a single crystal in the crystal growth medium and dissolving it in water followed by SDS-PAGE analysis and silver staining revealed that the Hsc70/Bag-1 complex had been crystallized (Figure 14B). Optimization of the crystal growth condition resulted in stable and sizeable crystals ( $0.25 \times 0.15 \times 0.15 \text{ mm}^3$ ) with good diffraction properties (Table 9; Figure 14A and C). Crystal seeds appeared after 5 days, maximum crystal size was reached after day 7 at 20°C. Crystals containing the selenometionine derivative of the ATPase domain were obtained under similar conditions, and showed similar properties with respect to growth and X-ray diffraction.

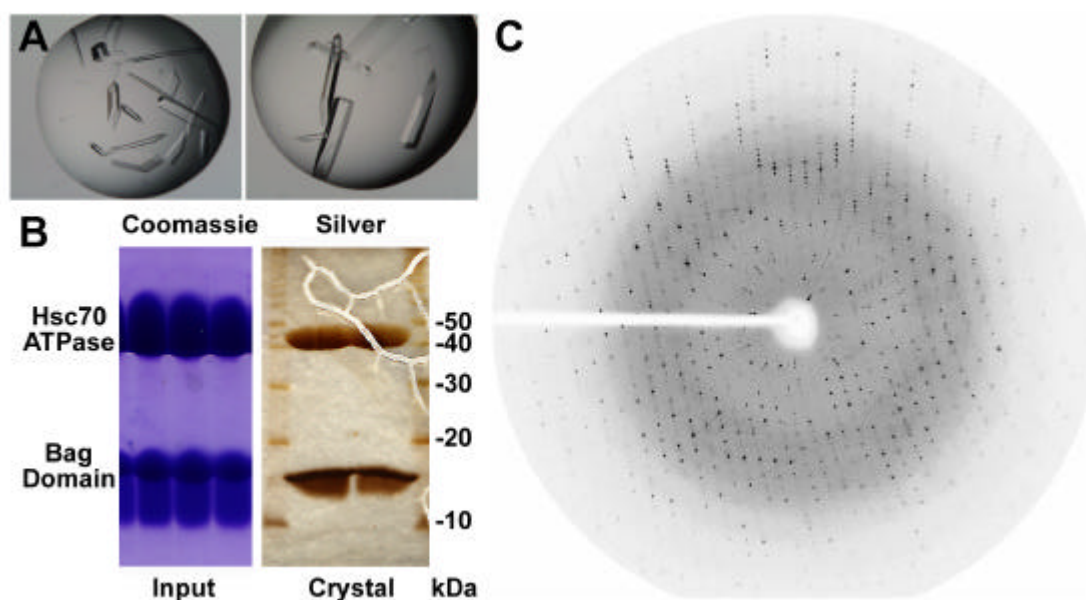


**Figure 14.** Crystals of the Hsc70 ATPase/Bag domain complex. (A) Crystals growing in 12% PEG3350, 50 mM NaCl, 20% glycerol, and 5% ethanol. Pictures were taken after 7 days of crystal growth. (B) The Coomassie-stained gel shows the complex after purification by anion exchange chromatography and gel filtration (Input). Silver-stained gels present the content of a single crystal, washed in precipitant solution and dissolved in sample buffer. (C) Diffraction pattern of a single crystal of the Hsc70 ATPase/Bag domain complex, collected at the rotating Cu anode (in house). The resolution limit shown is 2.3 Å.

A preliminary data set was measured in-house using a rotating anode as X-ray source ( $U=50 \text{ kV}$ ,  $I=80 \text{ mA}$ ,  $\text{CuK}\alpha:\lambda=1.5418 \text{ \AA}$ ) with a maximal resolution of 2.4 Å using a single crystal, shock-frozen in liquid nitrogen and constantly kept at 100 K in a nitrogen

stream during the measurement. A high resolution data set (15-1.9 Å) of a single, native crystal was collected at beamline ID14-4 at ESRF (Grenoble). The MAD data set (18-2.6 Å) was collected at beamline BW-6 at DESY (Hamburg) with consecutive measurements at three wavelengths. These have been determined by collecting fluorescence spectra at energies around the absorption edge (K-edge) of selenium ( $\lambda_1=0.9786$  (peak),  $\lambda_2=0.9792$  (inflection),  $\lambda_3=0.9500$  (remote)) (Table 9). Diffraction properties of the crystals have been improved by (repeated) annealing of the crystal in the cryostream (rearming of a flash-cooled crystal) (Harp et al., 1998). Data reduction was carried out with the software packages DENZO and SCALEPACK (Otwinowski and Minor, 1997). The space group C2 was unequivocally determined.

**Table 9. Data Collection, Phasing, and Refinement Statistics.**

Data Collection <sup>a</sup>	Native	SeMet		
Space Group		C2		
Unit Cell		a = 116.57 Å, b = 40.78 Å, c = 129.26 Å $\alpha = \gamma = 90^\circ$ , $\beta = 114.84^\circ$		
# Complexes / asym. unit		1		
X-ray source	ESRF, ID14-4 <sup>b</sup>		DESY, BW6 <sup>c,d</sup>	
Wavelength (Å)	$\lambda = 0.9287$	$\lambda_1 = 0.9786$ (peak)	$\lambda_2 = 0.9792$ (inflection)	$\lambda_3 = 0.9500$ (remote)
Resolution (Å)	15-1.95 (2-1.95)	18-2.6 (2.67-2.60)	18-2.6 (2.67-2.60)	18-2.6 (2.67-2.60)
I / $\sigma_I$	21.0 (3.6)	16.7 (5.9)	17.6 (7.0)	12.8 (7.0)
Completeness (%)	99.5 (99.6)	98.2 (97.8)	98.1 (97.4)	98.1 (97.7)
R <sub>sym</sub> (%)	5.6 (27.0)	3.3 (10.5)	3.2 (9.6)	3.2 (9.0)
<b>MAD Phasing<sup>e</sup></b>				
Anomalous scatterer		Selenium (6 of 6 sites)		
Resolution (Å)		18-2.6		
Figure of merit		0.59		
<b>Model Refinement<sup>f</sup></b>				
Resolution (Å)	15-1.9			
# reflections R <sub>work</sub> / R <sub>free</sub>	40,599/3149			
R <sub>work</sub> / R <sub>free</sub> (%) <sup>g</sup>	23.4/27.9			
# solvent molecules	359			
R.m.s.d. bond length (Å)	0.01			
R.m.s.d. angles (°)	1.4			

<sup>a</sup>Values as defined in SCALEPACK (Otwinowski and Minor, 1997); <sup>b</sup>European Synchrotron Radiation Facility in Grenoble, beamline ID14-4; <sup>c</sup>Deutsches Elektronen Synchrotron in Hamburg, beamline BW6; <sup>d</sup>Bijvoet pairs separated; <sup>e</sup>Values as defined in SOLVE (Terwilliger and Berendzen, 1999); <sup>f</sup>Values as defined in CNS (Brünger et al., 1998); <sup>g</sup>No sigma cutoffs.

Phase information and structure solution was obtained automatically using the software package SOLVE (Terwilliger and Berendzen, 1999). After solvent correction with DM (CCP4, 1994), the known structure of the ATPase domain of Hsc70 was placed into the electron density, and the structure of the Bag domain was built manually. The



structure was refined with the program package CNS (Brünger et al., 1998). All statistics of data collection, phasing and refinement are summarized in Table 9.

The somewhat high  $R_{\text{free}}$  of the final model can in part be attributed to significant radiation damage during the collection of the native data set that could only be partially corrected during data processing and scaling. The His<sub>6</sub>-tag of the Hsc70 ATPase is completely disordered and is not included in the final model. Furthermore, three loop regions in the ATPase domain and one loop in Bag were less structured and contain some residues which could only be built as alanines since there was no significant density for their side chains. Nevertheless, the geometry of the refined model is of good quality with respect to bond lengths and angles (standard deviation from the ideal values of 0.01 Å for bond length and 1.4° for bond angles) (Engh and Huber, 1991). Analysis of  $\phi$ - $\psi$ -torsion angles using a Ramachandran plot (Ramachandran and Sasisekharan, 1968) showed all amino acids in most favored and allowed regions except Gln260, a residue at the extreme C-terminus of the Bag domain (Figure 15). Nevertheless, the residue was included in the final model since the quality of the final decreased when it was omitted.

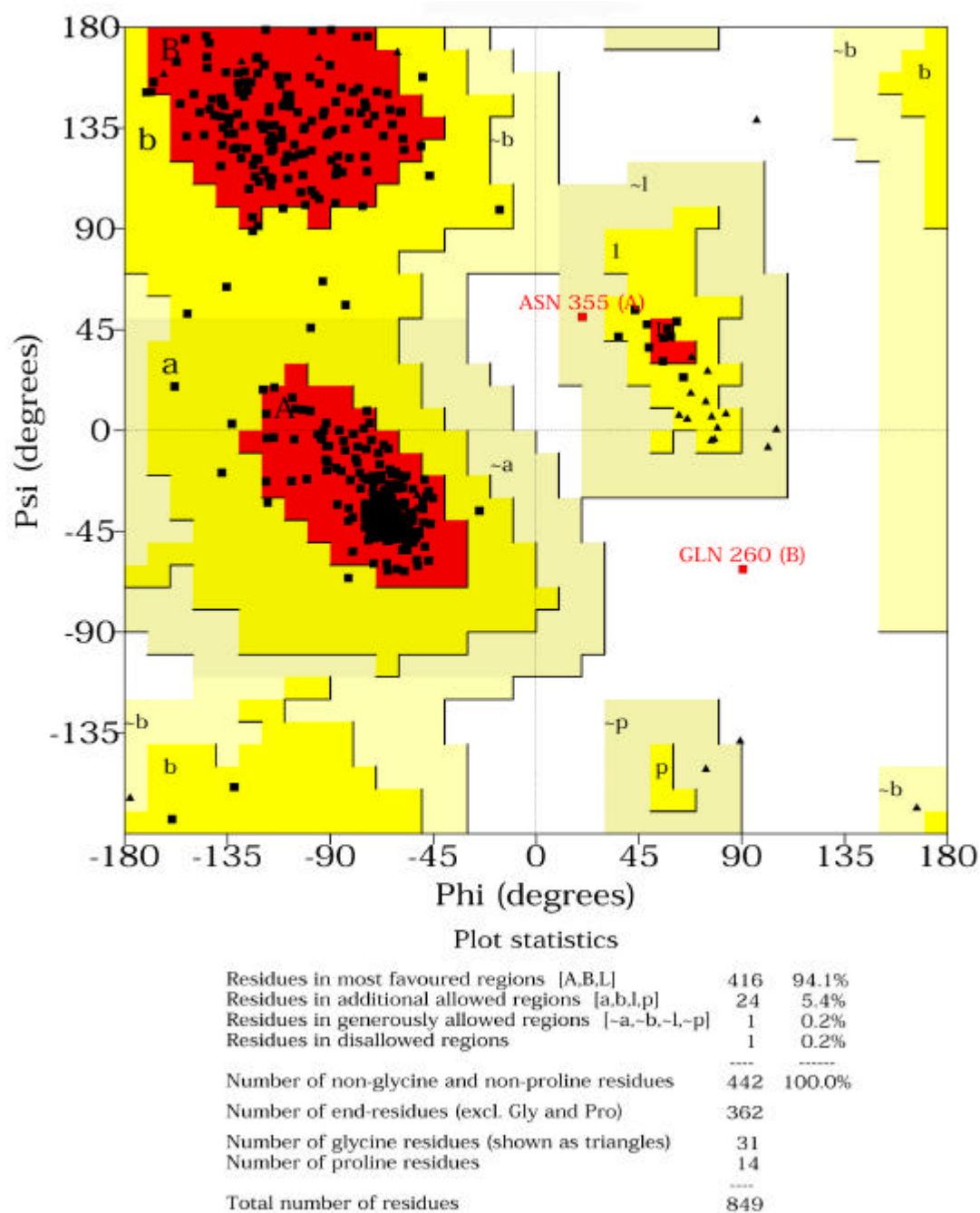


**Figure 15.** Ramachandran plot of the final model of the Bag domain/Hsc70 ATPase domain complex structure. All amino acids are in mostly favoured or allowed regions (except Gln260 of the Bag domain).

### C.3.5 Crystal structure of the Hsc70 ATPase/Bag complex

The final model of the complex between the Bag domain and the ATPase domain of Hsc70 is shown as a ribbon representation (Figure 16A) and, in the same orientation, as a representation of the accessible surface (Figure 16B). The Bag domain is monomeric and forms an anti-parallel three-helix bundle. Helices 2 and 3 contact the subdomains IB and IIB of the ATPase (Figure 16A and B) whereas helix 1 does not contact the ATPase domain. The contact within the heterodimer cannot be explained by crystal packing effects which mainly involve helix 1 of the Bag domain and areas of the ATPase domain not involved in Bag binding (data not shown). Upon crystallization, a disulfide bridge between Cys259 at the very C-terminus of the Bag domain and Cys201 was formed resulting in a short, non-regular stretch in helix 2, in an area not relevant for Hsc70 binding. However, binding of the Bag domain to Hsc70 was not affected by reducing agents as observed in binding studies (ITC in buffer supplemented with a glutathione redox system; data not shown).

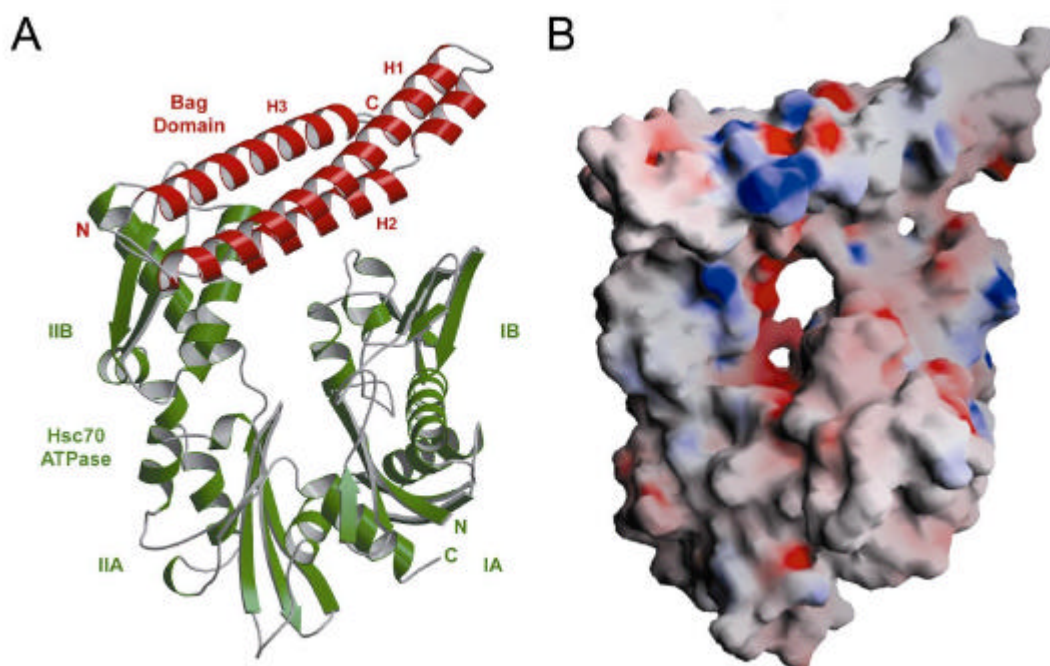


**Figure 16.** The Bag-domain/Hsc70 complex. **(A)** The backbones of the Bag domain (red) and the ATPase domain of Hsc70 (green) shown in a ribbons representation generated with the program Bobscript (Esnouf, 1999). **(B)** The electrostatic potential of the Bag domain/Hsc70(5-381) complex modeled onto the accessible molecular surface as calculated and visualized by GRASP (Nicholls et al., 1993). Red and blue indicate negative and positive charges, respectively. Orientation as in (A).

The consequence of Bag-1 binding to the Hsp70 ATPase domain is a 14-degree rotation of subdomain IIB about a hinge in the region of Leu228 and Leu309 relative to the structure of Hsc70 with ATP bound (Figure 18A and 27) (Flaherty et al., 1990). In this region, the highest root mean square deviation (rmsd) between the two structures is observed (Figure 17). The route mean square deviation (rmsd) of the superposition is shown as a function of residue number of Hsc70 as calculated with the program module from the CNS software package. Significant differences between the two structures are solely seen in residues of subdomain IIB of the ATPase. This is in agreement with a calculation of the rmsds for the different subdomains as calculated using the SwissPDB viewer program (see inset of Figure 17). Figure 18A shows the superposition of the ATP-bound and the Bag-bound ATPase. The color code represents the rmsd of the superposition. Furthermore, there was no significant density in the Bag-containing complex which could account for bound ADP or ATP (Figure 18B). All attempts to soak crystals in nucleotide-containing precipitant solutions resulted in rapid destruction of the crystals, indicating that Bag binding is incompatible with nucleotide binding. This is also supported by the affinity measurements in the presence and absence of nucleotide (Table 7).

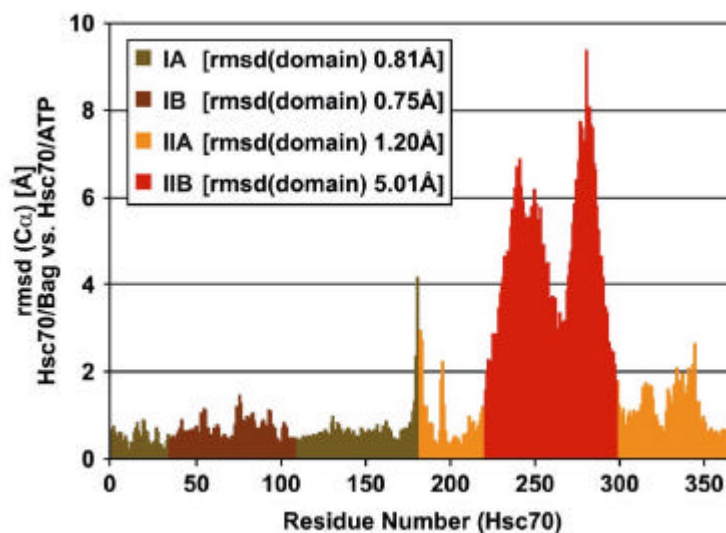


**Figure 17.** Route mean square deviation (rmsd) of the superposition of the ATPase domain in complex with ATP and the Bag domain. The bar diagram represents the rmsd values of the superposition of the two structures for each residue as calculated using CNS (Brünger et al., 1998). The inset shows the rmsd values for each subdomain as calculated with SwissPDB viewer.

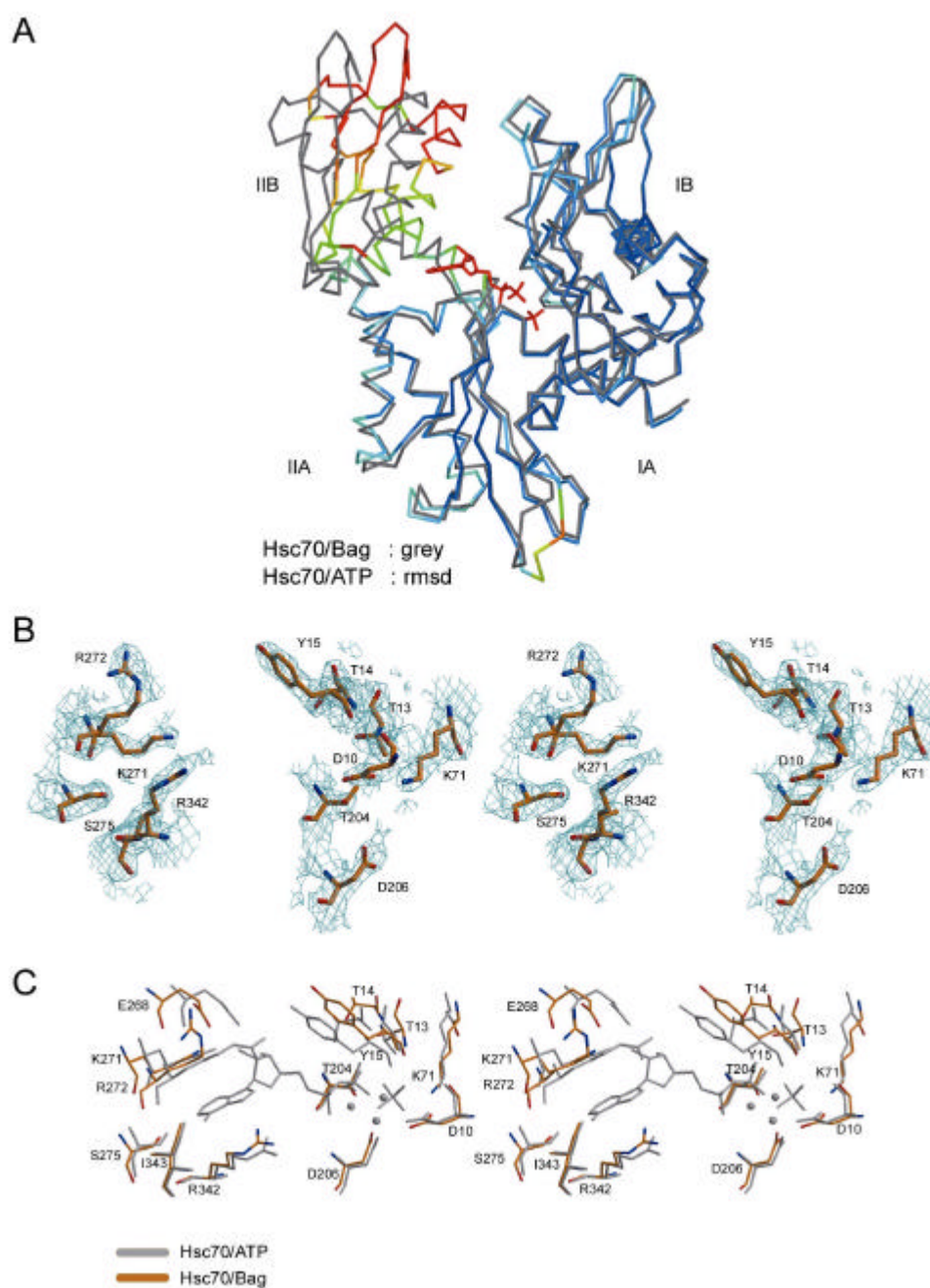


**Figure 18.** Analysis of the Hsc70 ATPase/Bag domain structure in comparison to the nucleotide-bound structure. **(A)** Superposition of Hsc70(5-381) in complex with the Bag domain (grey) with the nucleotide-bound domain of Hsc70 (rmsd) (PDB code 3HSC). The color code represents the root mean square deviation (rmsd) of the superposition calculated and visualized by SwissPDB Viewer (blue, low degree of deviation; red, high degree of deviation). **(B)** Stereoview of a 2fo-fc simulated annealing omit map of the Hsc70 region involved in ATP binding and hydrolysis calculated in the absence of the indicated residues (contour level at 1 sigma). **(C)** Stereoview of the superposition of the sidechains in Hsc70 involved in ATP binding and hydrolysis. The nucleotide-bound state is drawn in grey, the conformation of the respective residues in the Bag domain/Hsc70(5-381) complex is drawn in orange.

The high resolution crystal structure allowed the analysis of the conformational changes in positions that are critical for nucleotide binding and hydrolysis by superimposing relevant residues from Hsc70 bound to ATP (Flaherty et al., 1990) and Hsc70 bound to Bag. Figure 18B and C show Hsc70 residues responsible for ATP binding and hydrolysis in a ball-and-stick representation. A 2fo-fc simulated annealing omit map of the Hsc70 region involved in ATP binding and hydrolysis calculated in the absence of the indicated residues (contour level at 1 sigma) is also shown revealing the reliability and quality of the structural model (Figure 18B). The main changes in the ATPase domain induced by binding of the Bag domain occur in residues of subdomain IA and IIB that orient the adenosine moiety of the nucleotide (Figure 18C). The positions of other residues in the binding cleft and the residues involved in catalysis of ATP hydrolysis in subdomains IB and IIA are not significantly altered. The structural transition results in a movement of Glu268, Lys271, and Ser275 in domain IIB and Thr13, Thr14, and Tyr15 in subdomain IA away from their position in the nucleotide-bound structure. This leads to an opening of the nucleotide binding cleft. Additionally, the sidechain of Arg272 assumes an alternative conformation when compared to the nucleotide-bound state. In the latter state, Arg272 and Arg342 form a clamp that fixes the adenine ring via hydrophobic interactions and the  $\pi$ -electron system of their guanidinium groups.

### C.3.6 Mutational analysis of the Bag/Hsc70 interaction

In Figure 19A, the contacts of the Bag/Hsc70 interaction are presented in detail using the software package LIGPLOT (Wallace et al., 1995). Binding of the monomeric Bag domain to the ATPase domain is mediated by electrostatic interactions, mainly exploiting residues Glu212, Asp222, Arg237 and Gln245 in Bag-1 (Figure 19A). To further confirm the relevance of our structural model, we performed site-directed mutagenesis to produce single amino acid changes in some residues showing multiple interactions. These are shown as ball-and-stick presentation in Figure 19B.

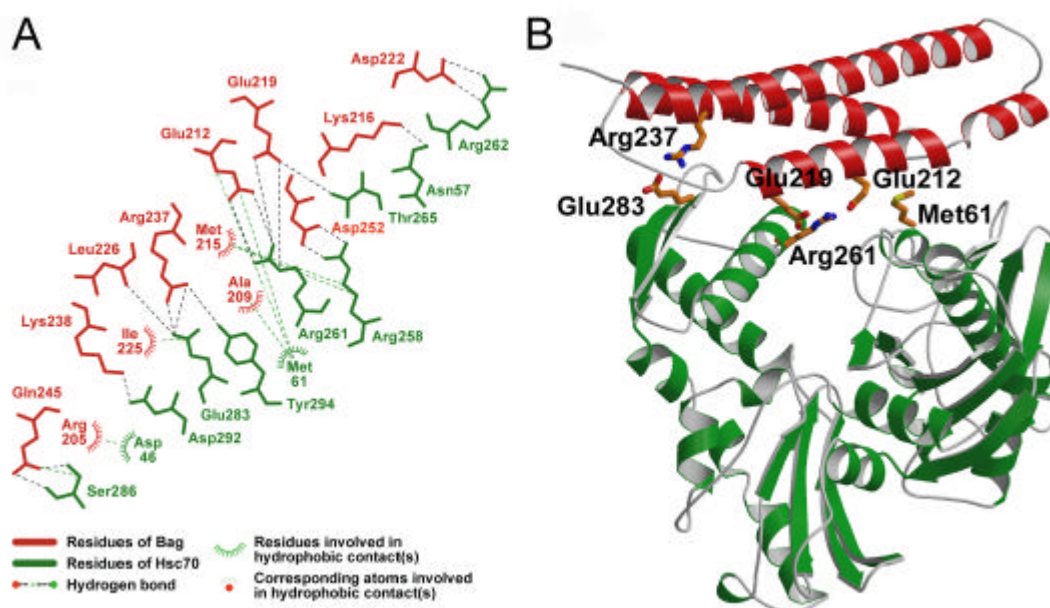


**Figure 19.** Interactions between Hsc70 and the Bag domain. (A) The diagram was produced by LIGPLOT (Wallace et al., 1995). Red: residues of Bag-1M; green: residues of Hsc70. (B) Ball-and-stick presentation of residues targeted for site-directed mutagenesis.

Mutations Glu212Ala and Glu219Ala in the Bag domain resulted in a substantial reduction (about 8-fold) in binding affinities to the ATPase domain of Hsc70 (Figure 20A). The mutation Arg237Ala affected the binding even more drastically showing a more than 10-fold reduction. The lower affinities to Hsp70 correlated with a reduced stimulation of the ATPase rate of Hsc70 (Figure 20B). Mutation of Glu212 and Glu219 still showed about 50% of the wild type activity in stimulating the ATPase rate whereas mutation of Arg237 resulted in a loss of this function matching the differential effects of the different mutations on the binding constants. The same effect was observed in the substrate release assay (Figure 21). The partial stimulatory activity of the Bag domain containing Ala-substitution in Glu212 or Glu219 on the ATPase rate was sufficient for releasing about 50% of the Hsc70 from its substrate compared to the wild-type activity (Figure 21A). This activity is still dependent on the presence of ATP. The mutant Arg237Ala was almost completely impaired in its release activity, only showing background levels comparable to control reactions using buffer alone or ovalbumin (negative control). Arg261 in Hsc70 is one of the counterresidues of Glu212 and Glu219 in Bag-1M. The mutation Arg261Ala in Hsc70 resulted in similar effects on the substrate

release activity when treated with wild-type Bag domain protein comparable to the effect of the two Bag mutants, Glu212Ala and Glu219Ala, on the release of wild-type Hsc70 from LBD (Figure 21B). There was almost no additive effect when the mutants in Glu212 or Glu219 of Bag were used together with mutant Hsc70.

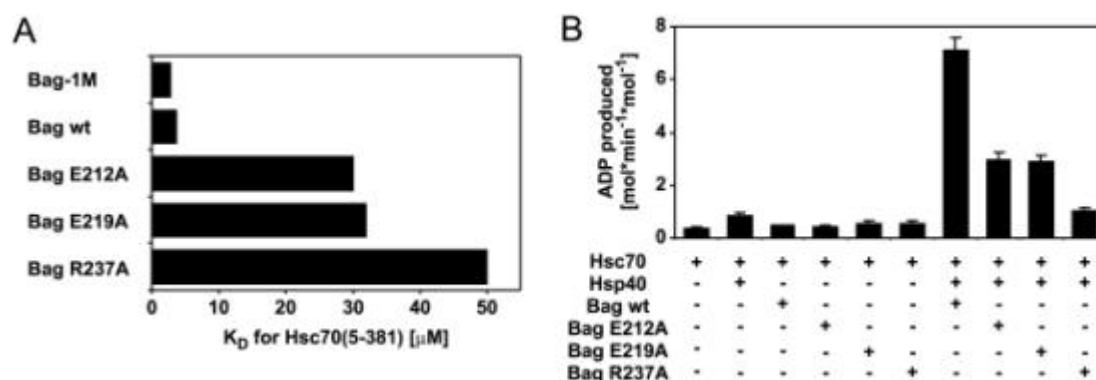


**Figure 20.** Mutants of Bag affecting the affinity to Hsc70 are impaired in stimulation of the ATPase activity of Hsc70. **(A)** Binding constants of the wild type Bag domain and mutant proteins to the ATPase domain of Hsc70 were measured by isothermal titration calorimetry as described in Material and Methods and Table 7. **(B)** ATPase rates were determined as described before (Figure 12). Error bars represent standard mean deviations of three independent experiments.

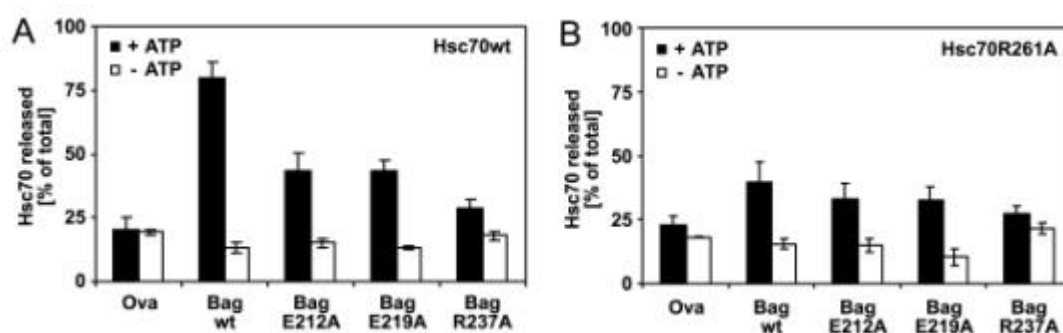


**Figure 21.** Impaired substrate release from Hsc70 correlates with reduced stimulation of the ATPase rate by Bag proteins. Release of Hsc70 from its bound substrate (LBD) was measured as described before (Material and Methods and Figure 12). **(A)** Release of  $^{35}\text{S}$ -Met-labeled wild-type Hsc70 from partially denatured immobilized LBD of the glucocorticoid receptor was measured upon incubation with the indicated proteins in the presence or absence of ATP. **(B)** Release of  $^{35}\text{S}$ -Met-labeled mutant Hsc70 (Arg261Ala) was measured as in (A). Error bars represent standard mean deviations of three independent experiments.



All residues of Bag which are involved in the interaction with Hsc70 are highly conserved in all known mammalian Bag proteins. Furthermore, they are conserved in Bag proteins from *D. melanogaster*, *C. elegans*, and *S. pombe* which have been discovered recently (Takayama et al., 1999). A structural alignment using the PSI-BLAST internet interface (<http://www.ncbi.nlm.nih.gov>) and the knowledge about the exact contact surface revealed the existence of Bag proteins in all eukaryotic species including *S. cerevisiae* and *A. thaliana*, organisms in which no Bag family members had been identified so far (Figure 22). The Bag protein in *S. cerevisiae*, Sn11p, will be the subject of further work as discussed below. Other highly conserved residues are probably involved in proper folding (e.g. packing interactions) of the Bag domain (highlighted in blue).



**Figure 22.** Structure-based sequence alignment of Bag domain proteins from different species. Conserved residues forming the interaction surface with the Hsc70 ATPase domain are highlighted in red and residues important for packing interactions are shown in blue. (Accession numbers: human Bag-1M, Q99933; human Bag-3/CAIR/BIS, AAD16122; human Bag-4, AAD16123; human Bag-5, AAD16124; *C. elegans* Bag-1, AAD16125; *S. pombe* Bag-1B, AAD16127; *S. cerevisiae* Sn11p, NP\_012248; *D. melanogaster* gene product, AAF49807; *A. thaliana* putative protein, CAB87278).

The existence of Bag proteins in all eukaryotic organisms strongly correlates with the conservation of Hsp70 within the residues responsible for Bag binding (Table 10). These residues are only conserved in the cytosolic forms of Hsp70 proteins but not in their paralogs from organelles (e.g. mitochondria or the endoplasmic reticulum) or bacterial homologs, proteins that either rely on GrpE as a nucleotide exchange factor (*E. coli* DnaK and mitochondrial Hsp70) or are thought to function independent of an exchange factor (BiP).

**Table 10. Conservation of Bag binding residues in Hsp70 proteins.<sup>a</sup>**

Bag binding residues <sup>b</sup>	Hsc70 mouse	BiP mouse	mHsp70 mouse	Hsp70 <i>C. ele.</i>	Hsp70 <i>Dros. m.</i>	Ssa1 <i>S. cerv.</i>	Ssb1 <i>S. cerv.</i>	Hsp70 <i>A. thal.</i>	DnaK <i>E. coli</i>
D46	✓	✓	✓	✓	✓	✓	P	✓	✓
N57	✓	✓	R	✓	✓	✓	✓	✓	R
M61	✓	S	T	✓	✓	✓	L	✓	T
R258	✓	✓	M	✓	✓	✓	✓	✓	D
R261	✓	Q	Q	✓	✓	✓	✓	✓	A
R262	✓	K	✓	✓	✓	✓	✓	✓	M
T265	✓	R	E	✓	✓	✓	✓	✓	L
E283	✓	✓	N	✓	✓	✓	✓	✓	D
S286	✓	✓	Y	✓	A	✓	✓	✓	L
D292	✓	✓	S	✓	✓	✓	✓	✓	✓
Y294	✓	S	N	✓	✓	✓	E	✓	H

<sup>a</sup>, Accession numbers: mouse Hsc70, P08109; mouse BiP, P20029; mouse mitochondrial Hsp70, P38647; *C.elegans* Hsp70, P09446; *D.melanogaster* Hsp70, P02825; *S.cerevisiae* Ssa1, P10591; *S.cerevisiae* Ssb1, P11484; *A. thaliana* Hsp70, P22953; *E. coli* DnaK, P04475;<sup>b</sup>, Residues of rat Hsc70 amino acid sequence involved in binding of the Bag domain (Sondermann et al., 2001).

Taken together, the Hsc70 ATPase/Bag domain structure elucidated the mechanism by which Bag proteins act on Hsp70. The functional relevance of the structural model was additionally confirmed by mutational analysis. Furthermore, structural alignments revealed the existence of Bag proteins in the cytosol of all eukaryotic species with a very high degree in conservation with respect to the established interaction surface.

### C.3.7 Characterization of the Bag protein Snl1p from *S. cerevisiae*

Because the overall homology of the *S. cerevisiae* protein Snl1p to Bag-1 is low, it did not produce a significantly high score in conventional BLAST searches. Therefore, a

characterization of its effect on Hsp70 was carried out to confirm its function as a Bag protein. Although all residues corresponding to the Hsp70-binding residues in Bag-1 are conserved, there is almost no similarity in the putative helix 1 and further upstream sequences between Snl1p and Bag-1. Snl1p harbors a predicted, single transmembrane domain at its N-terminus. The putative Bag domain is predicted to face the cytosol. By indirect immunofluorescence staining and cellular fractionation experiments, the protein was shown to be localized at the nuclear and endoplasmic reticulum membrane. In this work, homology of Snl1p to another nuclear pore transmembrane protein unrelated to the known Bag proteins had been proposed (Wente et al., 1999).

DNA encoding the cytosolic fragment of Snl1p, consisting of the putative Bag domain, was cloned into a vector for overexpression in *E. coli* using chromosomal yeast DNA as template for PCR-based cloning. Since the homology within helix 1 is poor and exact domain borders could not be unambiguously predicted, two constructs were produced varying in length at their N-termini. Proteins were overexpressed as His<sub>6</sub>-tagged fusions, and purified as described in Material and Methods. Both proteins were highly soluble.

Their effect on Hsp70 was analyzed using ATPase and substrate release assays. Both systems were heterogenic because they were based on mammalian Hsc70. Nevertheless, all residues of the interaction surface between Bag-1 and Hsp70 are conserved across the species borders (see Table 10).

Both proteins containing the cytoplasmic domain of Snl1p stimulated the ATPase rate of Hsc70 efficiently, comparable to the effect seen with the isolated Bag domain (Figure 23A) and Bag-1M (Figure 12). As seen before, this effect was highly dependent on the presence of Hsp40, and no effect of the Bag domain of Snl1p was seen when Hsp40 was omitted from the reaction. As observed with the Bag domain and Bag-1M, Snl1p also stimulated the release of Hsc70 from substrate in an ATP-dependent reaction (Figure 23B). The substrate release was as efficient as observed with the other Bag proteins.

The stimulation of the Hsc70 ATPase activity and substrate release, comparable to the effect of mammalian Bag-1, clearly establishes Snl1p as the first and probably the only Bag protein in *S. cerevisiae*. Furthermore, the primary sequence of Snl1p could be modeled on the tertiary structure of the Bag domain with the residues of helix 2 and 3

covering the full interaction surface of Bag and Hsc70 (Figure 24). This is in agreement with the structural alignment and functional similarity to other Bag proteins.

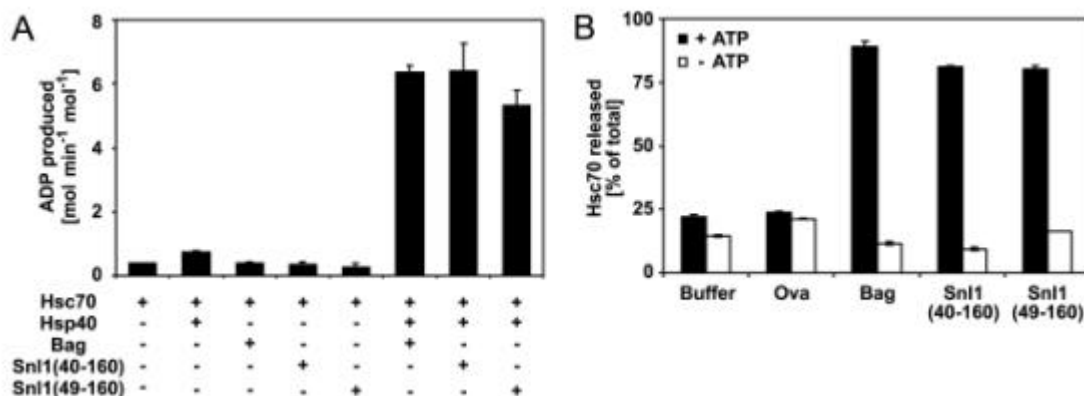


**Figure 23.** Functional characterization of Snl1p. **(A)** Snl1p and the Bag domain stimulate the ATPase activity of Hsc70 in an Hsp40-dependent manner. ATPase rates were determined as described before (see Material and Methods and Figure 12). **(B)** Snl1p and the Bag domain stimulate Hsc70 release from substrate polypeptide in a nucleotide-dependent manner. Release of <sup>35</sup>S-Met-labeled Hsc70 from partially denatured immobilized ligand binding domain (LBD) of the glucocorticoid receptor was measured as described (see Material and Methods and Figure 12). Error bars represent standard mean deviations of three independent experiments.

Since the *in vitro* experiments with Snl1p were performed in a heterogenic system, the ability of the Bag domain of Snl1p to bind the yeast homologs of Hsp70, especially the main cytosolic isoforms Ssa and Ssb, was tested. The recombinantly expressed, His<sub>6</sub>-tagged Bag domain of Snl1p, bound to NiNTA-agarose beads was allowed to interact with total yeast lysates and then recovered with associated proteins. These proteins were analyzed by SDS-PAGE, Coomassie staining or Western blotting with antibodies specific for either Ssa or Ssb proteins.

His<sub>6</sub>-Snl1p Bag domain associated mainly with two proteins (double band) from yeast lysates with a molecular weight of approximately 65-70 kDa (Figure 25). The interaction was most stable under nucleotide-free conditions (Apyrase, Apy), but was significantly weakened in the presence of either ATP or ADP. This behavior mirrors that observed with Bag-1M and Hsc70 (see above). The protein band around 45 kDa coprecipitated from the Apyrase-treated lysate is likely to be the ATPase domain of yeast Hsp70, proteolytically cleaved during the incubation periods of the pull down. Similar to the 70 kDa bands, the 45 kDa band also dissociated from the Snl1p domain in the

presence of nucleotides. Control NiNTA beads lacking the Bag domain did not bind to proteins in yeast lysates, as seen in the Coomassie-stained gel.

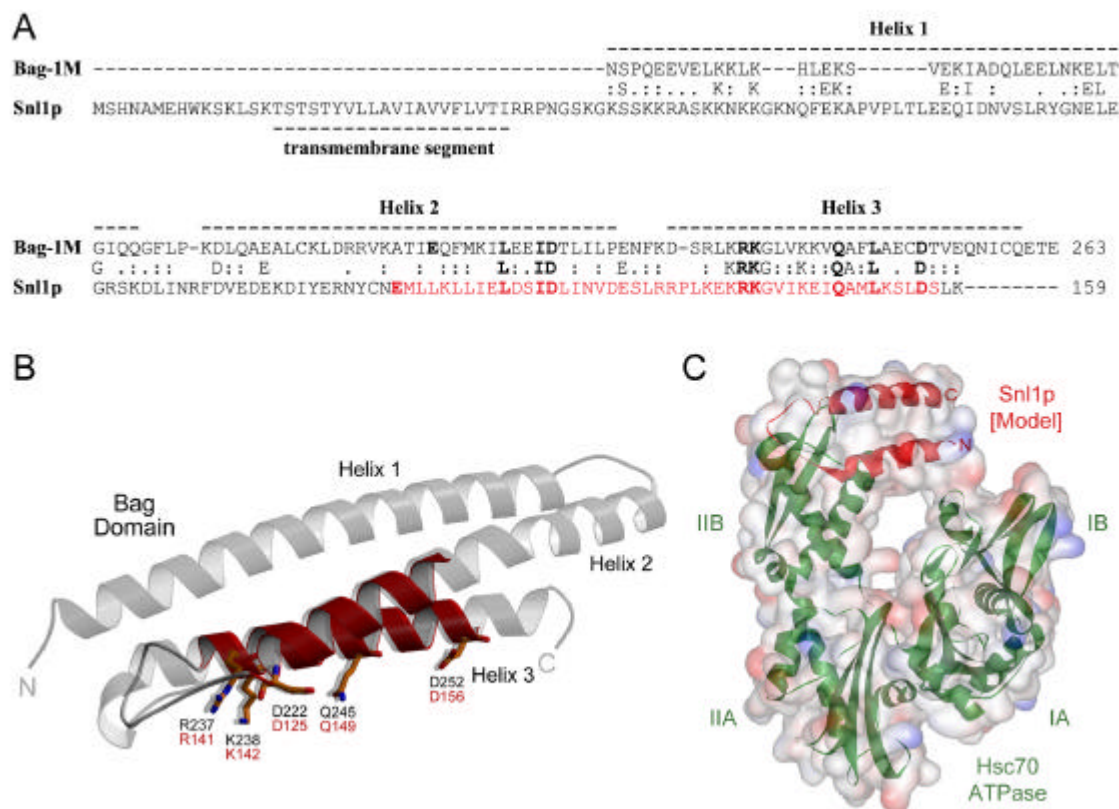


**Figure 24.** Modeling of the C-terminal domain of Sn11p on the structure of the Bag domain of Bag-1M. **(A)** Structural alignment of Bag-1M and Sn11p. Helices of Bag-1M are indicated. Residues highlighted in red indicate the modeled part of Sn11p in **(B)**. **(B)** Structural model of a subdomain of Sn11p aligning with Bag-1M. The Sn11p model was generated using the SwissModel internet interface (<http://www.expasy.ch>). Presentation was generated with the program Bobscrip (Esnouf, 1999). Black labels correspond to the sequence of Bag-1M, red labels correspond to the sequence of Sn11p. **(C)** Structural model of the ATPase domain of Hsc70 in complex with the subdomain of Sn11p modelled in **(B)**. Presentation was generated with the program WebLab viewer Pro (MSI).

The identities of the Sn11p-interacting proteins were revealed by Western blotting. A specific antibody raised against Ssa proteins, the major cytosolic isoforms of Hsp70 in yeast, clearly recognized one band of the doublet around 70 kDa. As had already been seen in the Coomassie-stained gel, the signal was strongly diminished in the presence of ATP and ADP to the level detected on the control beads. Similar results were obtained when a Ssb-specific antibody was used for detection. Ssb proteins are mainly bound to

the ribosome but there is also a free pool in the cytosol (Pfund et al., 1998) and for steric reasons, this is likely the population which interacts with Snl1p. Again, binding was strongest under nucleotide-free conditions, and substantially reduced in the presence of ATP and ADP. Nevertheless, there might be a preference for ADP over ATP since there is still more Ssb bound in the presence of ADP compared to ATP. As seen in Table 10, residues involved in Bag binding are conserved in Ssa as well as Ssb proteins; the latter sequence shows three minor changes mainly in hydrophobic contacts between Bag and the ATPase domain.

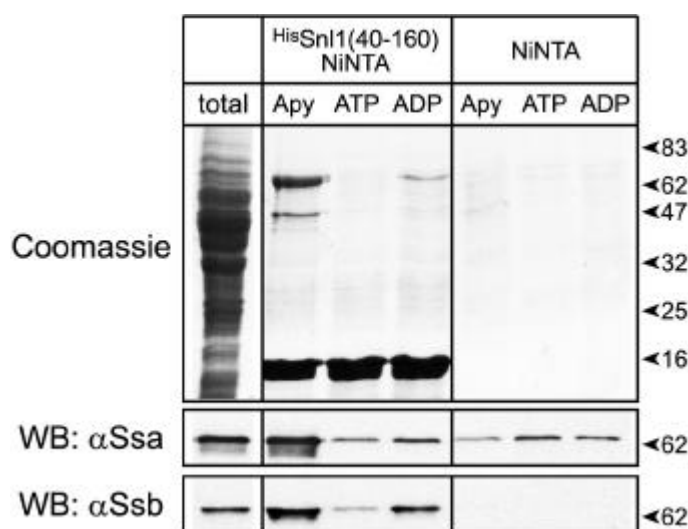


**Figure 25.** NiNTA-pull down of Ssa and Ssb proteins from yeast lysates with the His<sub>6</sub>-tagged Bag domain of Snl1p as bait. Proteins (60 μg) were bound to NiNTA resin in buffer B for 20 min at room temperature. Beads were washed twice. Control beads without bound proteins were processed identically. Reactions were supplemented with yeast lysates. Binding (20 min at room temperature) was performed either in the presence of Apyrase (4 Units/ml), 5 mM ATP/Mg<sup>2+</sup>, or 5 mM ADP/Mg<sup>2+</sup>. Beads were washed 3-times with the respective binding buffer. Bound proteins were eluted from the resin with 2x SDS-PAGE sample buffer and analyzed by SDS-PAGE and Western blotting using Ssa- and Ssb-specific antibodies.

In summary, the Snl1p could be clearly identified as a Bag protein in *S. cerevisiae*. It has the same effect on the ATPase rate of Hsp70 and the regulation of substrate binding by the chaperone as observed with Bag-1M and its Bag domain. Furthermore, it strongly interacts with Ssa and Ssb proteins, the major isoforms of Hsp70 in the yeast cytosol. This interaction is sensitive to both ATP and ADP, ruling out a substrate-like interaction of Hsp70 with Snl1p.

## C.4 Discussion

In the present study, the crystal structure of the Hsc70 ATPase domain in complex with the Bag domain of Bag-1M was solved to a resolution of 1.9 Å. The Bag domain forms an anti-parallel three-helix bundle inducing a conformational switch in the ATPase that is incompatible with nucleotide binding. Biochemical analysis of the functional effect of Bag-1 on Hsp70 confirms the functional relevance of the structural model. The structure provides a detailed view of the action of Bag-1 on Hsp70 clarifying the controversy whether Bag-1 is a nucleotide exchange factor of Hsp70. Furthermore, yet unidentified Bag proteins were predicted to exist in all eukaryotic organisms including *A. thaliana* and *S. cerevisiae*. The Bag protein of *S. cerevisiae*, Snl1p, was further characterized *in vitro*, and was confirmed to function as a Bag protein.

While this thesis was written, a study was published identifying patches of surface residues in Hsc70 involved in Bag-1/Hsc70-interaction by using peptide libraries (Petersen et al., 2001). Also, the Bag domain structure solved by nuclear magnetic resonance (NMR) techniques was published (Briknarová et al., 2001). NMR chemical shift experiments marking the ATPase-interacting surface of the Bag domain are in agreement with the crystal structure presented here.

### C.4.1 Structural comparison of Bag-1 and GrpE

A comparison of the present structure with the one of the ATPase domain of the *E. coli* Hsp70 homolog DnaK with its well established nucleotide exchange factor GrpE is shown in Figure 26. Although the Bag domain and GrpE of *E. coli* are structurally unrelated (Figure 26A and B), they interact with the same subdomains, IB and IIB, of their respective Hsp70 ATPase domains. However, in contrast to the Bag domain, GrpE forms a dimer that mainly employs a  $\beta$ -strand subdomain, in addition to contacts from its  $\alpha$ -helical region, to bind to the ATPase domain of DnaK (Figure 26B and Figure 27B) (Harrison et al., 1997).

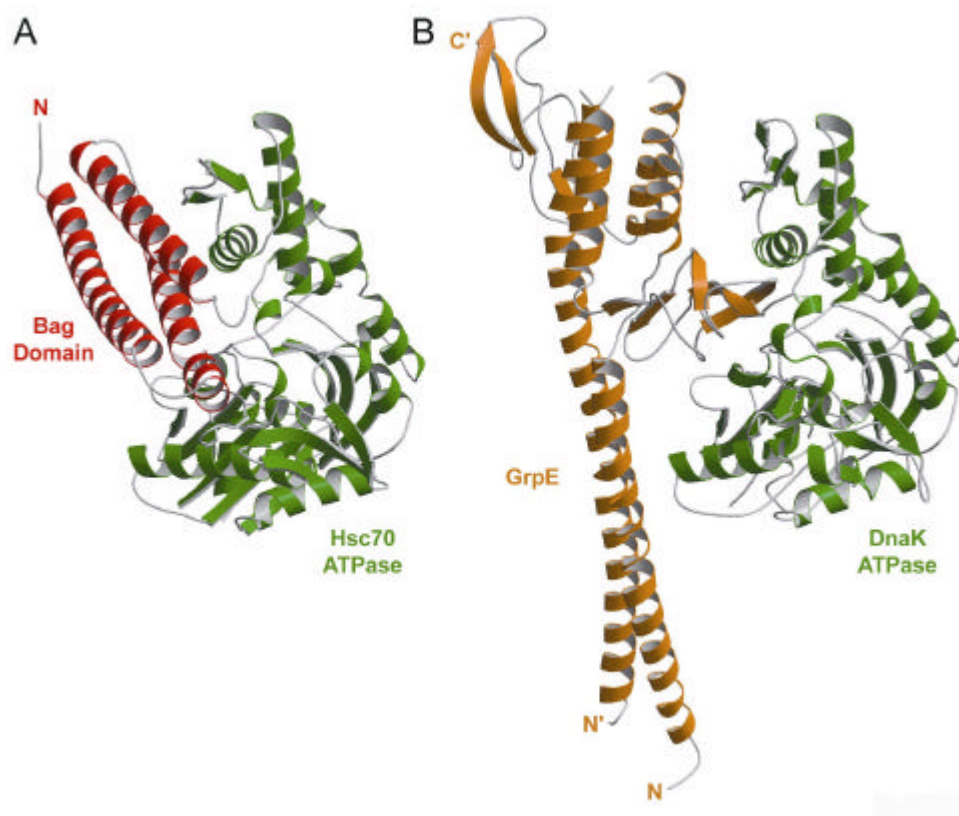


**Figure 26.** Structural comparison of Bag domain/Hsc70 (A) and DnaK/GrpE complexes (B). The ATPase domains of Hsc70 and DnaK are colored green, the Bag domain red and GrpE yellow.

Hydrophobic contacts from the  $\beta$ -strand region of GrpE reach deep into the nucleotide-binding cleft and contribute significantly to the tight interaction of the two proteins. In Figure 27, a LIGPLOT analysis is shown of both complex structures, again highlighting the different modes of binding of Bag-1 and GrpE to their respective ATPase domains of Hsp70. Bag mainly binds to the ATPase via hydrogen bonds, whereas the GrpE binding to DnaK is dominated by hydrophobic interactions. Different residues are contacted in the Hsp70 ATPase domains of the two complexes. GrpE additionally interacts with a loop in DnaK that is not conserved in eukaryotic cytosolic forms of Hsp70 (Figure 28B). In addition, it has been suggested that the long, extended helices of GrpE also contact the peptide binding domain of DnaK, influencing peptide binding in a direct manner. However, there is no indication that Bag-1M has a similar effect since the affinities of the full length protein and the isolated C-terminal Bag domain to Hsc70 are not substantially different.



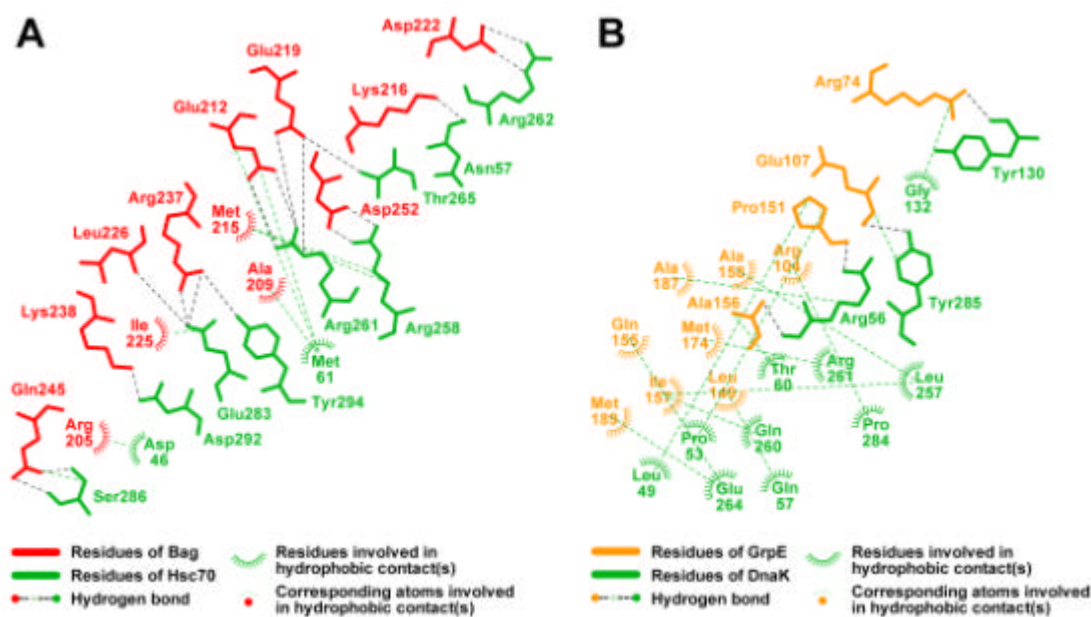


**Figure 27.** Comparison of the mode of interaction in the complexes of Hsc70/Bag-1 and DnaK/GrpE. The diagrams were produced by LIGPLOT (Wallace et al., 1995). (A) Red: residues of Bag-1M; green: residues of Hsc70. (B) Yellow: residues of GrpE; green: residues of DnaK.

#### C.4.2 Molecular mechanism of Bag-1 function on Hsp70

The consequence of Bag-1 binding to the Hsp70 ATPase domain, a 14-degree rotation of subdomain IIB about a hinge in the region of Leu228 and Leu309 relative to the structure of ATP-bound Hsc70, is shown in Figure 28A. For comparison, the superposition of the DnaK/GrpE complex with the Hsc70/Bag structure is presented in Figure 28B. The color gradient from blue to red indicates the degree of deviation between the structures (blue: low rmsd, red: high rmsd). Despite striking structural differences between the Bag domain and GrpE, the conformation of the Hsc70 ATPase in complex with Bag is remarkably similar to the conformation of the ATPase domain of DnaK in complex with GrpE (Harrison et al., 1997). In both cases, this conformation is incompatible with high affinity nucleotide binding. Thus, the eukaryotic Bag domain has evolved convergently to induce a nucleotide release mechanism that has been conserved in Hsp70 proteins. It remains to be established, whether this conserved switch is exploited by as yet unidentified additional exchange factors.

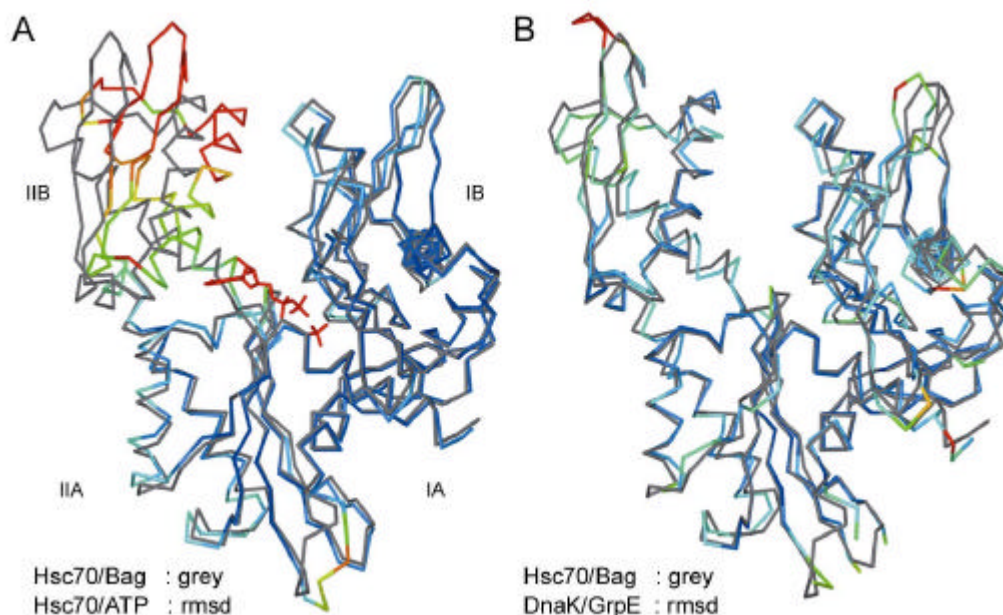


**Figure 28.** Nucleotide exchange mechanism of Bag and GrpE proteins. Superposition of Hsc70(5-381) in complex with the Bag domain with the nucleotide-bound domain of Hsc70 (PDB code 3Hsc) (**A**) and with the ATPase domain of DnaK in complex with its nucleotide exchange factor GrpE (PDB code 1DKG) (**B**). Colour code represents the root mean square deviations (rmsd) of the superpositions calculated and visualized by SwissPDB Viewer (blue, low degree of deviation; red, high degree of deviation). A loop region in domain IIB of DnaK not present in Hsc70 is seen in red (maximal rmsd).

A similar mechanism has been described for the protein Sos, the nucleotide exchange factor of the GTPase Ras (Boriack-Sjodin et al., 1998). In both cases, efficient release and rebinding of nucleotides is achieved by a conformational change that is induced in the enzyme by insertion of two  $\alpha$ -helices from the exchange factor into the nucleotide binding cleft.

#### C.4.3 Bag-1 function in protein folding *in vitro* and *in vivo*

From the structural studies, it is now evident how Bag-1 and most likely all other Bag proteins act on Hsp70 proteins, and that they function as nucleotide exchange factors. Nevertheless, the cellular function of Bag proteins especially with respect to protein folding still remains to be clarified. Present studies available in the literature, carried out *in vitro* and *in vivo*, fail to produce a clear picture of the influence of Bag action on Hsp70-mediated protein folding. In the cytosol, the high level of ATP (approximately 2

mM ATP) and a substoichiometric concentration of ADP (approximately 0.2 mM) will induce a release of Bag proteins from Hsp70 resulting in an ATP-bound form of Hsp70; Hsp40-dependent and/or peptide-stimulated nucleotide hydrolysis will convert Hsp70 to its ADP-bound form.

Under the conditions applied so far, stoichiometric amounts of Bag-1 to Hsp70 and superstoichiometric concentrations of ATP have been used which will effectively shift the equilibrium to ATP-bound Hsp70 as Bag proteins are very potent nucleotide exchange factors (see Figure 12). In the Hsp70 reaction cycle, this state is characterized by a high on- and off-rate for substrate, a circumstance which might be counterproductive for protein folding assuming that a substrate will need a certain time to be bound to the chaperone in order to be productively folded. This is also reflected in the results of the substrate release assays in this and other studies (Lüders et al., 2000; Zeiner et al., 1997) where Bag-1 and the Bag domains dissociate chaperone/substrate complexes in an ATP-dependent manner. An opposite effect observed in another study, namely prevention of ATP-dependent substrate release from Hsp70 by Bag-1, might be explained by the different experimental setup (nucleotide-free native gel electrophoresis) and source of purified proteins used (Bimston et al., 1998).

*In vitro* experiments carried out at different stoichiometries of Hsp70 and Hsp40 to Bag-1 suggest a differential, concentration-dependent effect of nucleotide exchange on protein folding with positive regulation at lower, physiological concentration of Bag-1 (Kanelakis et al., 1999; Terada and Mori, 2000). In cultured cells, overexpression of Bag-1 under a strong constitutive promoter interferes with the refolding of heat-inactivated luciferase (Nollen et al., 2000). This is consistent with the concentration-dependent effect of Bag-1 observed *in vitro*, in that high levels of Bag-1 relative to Hsp70 are counterproductive for protein folding. It is possible that with lower levels of overexpression, Bag-1 may in fact enhance Hsp70-dependent protein folding. However, it is more likely that the normal cellular concentrations of Bag-1 and other cochaperones are optimal for protein folding, and that any artificial change of the level of these would be deleterious.

Bag binding is incompatible with p48/Hsp70 binding to Hsp70. p48/Hsp70 is reported to stabilize the nucleotide bound form of the chaperone, therefore working as a counterbalance of Bag proteins (Nollen et al., 2001; Kanelakis et al., 2000). Bag binding to a complex of Hsp70 and p48/Hsp70 releases the latter from Hsp70 effectively even in the

absence of nucleotide, whereas substrate release from Hsp70 by Bag-1 is highly dependent on the presence of ATP (Figure 13). One can imagine a mechanism by which p48/Hip binds to the ATPase of Hsp70 in a manner that mechanically ‘clamps’ subdomain IIB thereby preventing an opening of the nucleotide binding pocket. This might slow down the spontaneous release or exchange of nucleotide. Modelling studies and competition experiments suggested a binding site for p48/Hip at subdomain IIB close to or overlapping with the Bag binding site on this domain (Velten et al., 2000; Gebauer et al., 1997).

In a cellular context, Bag proteins probably act in specific processes such as protein degradation, apoptosis or cellular signalling rather than being general nucleotide exchange factors for Hsp70 in *de novo* protein folding. Their involvement in specific cellular processes is achieved by different N-terminal domains of the various Bag proteins, such as the ubiquitin-like domain in Bag-1 and the WW domain in Bag-3 which might target Bag proteins to specific locations or functional complexes within the cell. In addition to the different binding modes of Bag and GrpE to Hsp70/DnaK, this is another striking difference between Bag proteins and the bacterial nucleotide exchange factor, GrpE, the latter being essential for proper folding of substrates by the DnaK/DnaJ system (Ang and Georgopoulos, 1989).

#### C.4.4 *S. cerevisiae* as a model system for analyzing Bag-1 function *in vivo*

Yeast might be a suitable experimental system to address the cellular function of Bag proteins. In particular, the benefits of *S. cerevisiae* are the ease of genetic manipulation and the availability of a fully sequenced genome. Because Sn1p is the only Bag protein in *S. cerevisiae*, defects in the protein will not be immediately complemented by pre-existing Bag isoforms, as would be the case in mammalian cells. Sn1p may be involved in a limited number of cellular processes, as it is not essential and is localized at the nuclear and endoplasmic reticulum membrane. It has been proposed that Sn1p contributes to nuclear pore biogenesis, based on its ability to alleviate defects caused by expression of mutant nuclear pore proteins (Ho et al., 1998). However, the biochemical data presented in this thesis suggests that Sn1p may fulfil its cellular function by regulating Ssa (cytosolic Hsp70 in *S. cerevisiae*), and therefore that Ssa may be involved

in nuclear pore assembly. Thus, substitution of wild-type Snl1p with a mutant unable to regulate Ssa should lead to specific phenotypes related to nuclear pore biogenesis. The mechanism by which Snl1p relieves the nuclear pore phenotypes could also be addressed by determining whether the mutant pore proteins are stabilized by the refolding activity of Ssa together with Snl1p, or are more effectively cleared by degradation.

Most of the Bag proteins in all organisms harbor a protein-protein interaction domain in addition to the Hsp70-binding Bag domain, for example a ubiquitin-like domain in Bag-1, a WW domain in mammalian Bag-3, or the transmembrane domain of Snl1p in *S. cerevisiae*. It is likely that these domains target the Hsp70-regulatory function of the Bag domain to specific complexes or intracellular locations. In case of Snl1p, the importance of its endoplasmatic reticulum and nuclear membrane localization is not known. This may be experimentally tested *in vivo* by analyzing nuclear pore biogenesis in yeast overexpressing Snl1p lacking the transmembrane domain.

It has been suggested that the Bag domain itself is capable of binding client proteins (Song et al., 2001) in addition to binding directly to the ATPase domain of Hsp70. From the structure presented in this thesis, it is probable that a client protein binding surface would involve the non-conserved helix 1 of Bag proteins. The lack of conservation within this region suggests that the various Bag proteins may have different substrate specificities. This possibility could be addressed in yeast by analyzing the nuclear pore phenotypes after overexpression of the Snl1p transmembrane domain fused to the Bag domain of the mammalian homologs, which will still interact with Ssa via the highly conserved binding surface. If these chimeric Bag proteins can rescue the nuclear pore defects as well as Snl1p, client protein binding by the Bag domains is likely to be promiscuous and not specific for a limited subset of client proteins.

The distinct phenotypes of nuclear pore defects which can be rescued by Snl1p overexpression and the ease of genetic manipulation in *S. cerevisiae* may allow a detailed analysis of these and other aspects of Bag function *in vivo*.

## **D Characterization of a monocyte/macrophage-specific receptor for Hsp70**

### **D.1 Introduction**

The immune system of all vertebrates and some invertebrates is designed to recognize and respond to foreign antigens. In such a reaction, antigens are presented by almost all cell types on cell surface molecules, major histocompatibility complex (MHC) class I and II, to specialized effector cells of the immune system. Subsequently, these cells react with a cascade of defense mechanisms against invading microbes or virally infected cells which bear the foreign antigens. Activated effector cells also trigger mechanisms to heal injured tissues.

#### **D.1.1 Mononuclear phagocytes and dendritic cells**

Mediators of the mammalian immune response reside in the blood. All blood cells originate from a single stem cell type in the bone marrow. Differential maturation pathways lead to lymphoid progenitor cells, from which natural killer cells, B- and T-cells arise, and to myeloid progenitor cells, precursors of all other blood cells. Among the latter, professional antigen presenting cells (APCs) from the monoblastic lineage, such as monocytes and macrophages, are particularly important in antigen presentation since they phagocytose and react to foreign particles very efficiently. This is achieved by a wide selection of various receptors mediating uptake and sensing of foreign antigens. One of them, CD14, is a common marker for monocytes, the first cell type which enters the peripheral blood from the bone marrow, and for macrophages, which are matured monocytes residing within the tissues. CD14 is a receptor for lipopolysaccharides (LPS), a cell wall component of microbes. Upon ligand binding, it triggers release of tumor necrosis factor  $\alpha$  (TNF $\alpha$ ) and other cytokines activating macrophages for an innate immune response.

Dendritic cells, first visualized as Langerhans cells in the skin, capture and process antigens in the periphery, migrate to lymphoid tissues and control lymphocyte function (Banchereau and Steinmann, 1998). In that, they are very potent antigen presenting cells and initiators of immune responses. Upon uptake of foreign antigens they differentiate into their mature form expressing costimulatory factors for a strong immune response. Immature dendritic cells can be generated *in vitro* from peripheral blood monocytes but are distinct from them in several aspects. Maturation *in vitro* is achieved by treatment of immature dendritic cells with TNF $\alpha$  and/or LPS.

### D.1.2 Antigen presentation

MHC class I and II provide a continuously updated display of the intracellular and environmental protein composition, respectively. The MHC class I presentation of antigens operates in almost all cells providing a mechanism for monitoring viral infections and tumors (Pamer and Cresswell, 1998). In the classical pathway, cytosolic proteins are hydrolyzed to short peptide fragments mainly by the proteasome, the cytosolic degradation machinery of the cell. Subsequently, the resulting peptides, usually 8 to 10 residues in length, are translocated by the transporter in antigen processing (TAP) into the endoplasmic reticulum and become bound by newly synthesized MHC class I proteins comprising a polymorphic  $\alpha$  chain harboring a transmembrane domain, non-covalently bound  $\beta_2$  microglobulin and a peptide. The MHC class I/peptide complexes then reach the cell surface via the secretory pathway (Rock and Goldberg, 1999; Cresswell et al., 1999; Lehner and Cresswell, 1996). Usually peptides are derived from autologous proteins and therefore are tolerated by the immune system. Only if foreign peptides are displayed, either derived from viral polypeptides or mutated gene products such as those appearing in cancer, CD8-expressing cytotoxic T-lymphocytes (CTLs) will recognize the peptide/MHC complex and kill the peptide-presenting cell. Presented self-antigens are not recognized except under abnormal conditions (i.e. in autoimmune diseases) due to the lack of the complementary T cell receptor on the CTLs or as a result of silencing of autoreactive CTLs.

In contrast, the MHC class II pathway presents exogenous antigens to the effector cells. MHC class II molecules consist of polymorphic  $\alpha$  and  $\beta$  chains, and are present on

mononuclear phagocytes, dendritic cells, B lymphocytes, endothelial cells and the thymic epithelium. CD4-expressing cells, mostly helper T cells, are responsive to peptide presented on MHC class II complexes. Mechanistically, extracellular antigens are taken up by antigen presenting cells via receptor-mediated endocytosis, phagocytosis, and macropinocytosis. The antigens are proteolytically processed in the lysosomes and loaded onto MHC class II molecules which then will reach the plasma membrane by exocytosis (Watts, 1997; Germain, 1994). The peptides derived from extracellular proteins usually do not leave the vesicular structures and therefore do not appear in the cytosol.

Recently, there is increasing evidence for a pathway termed cross-priming or cross-presentation, in which peptides derived from extracellular proteins appear on MHC class I molecules and are recognized by CTLs (Rock, 1996; Carbone et al., 1998; Yewdell et al., 1999). Cross-presentation is mainly achieved by professional APCs such as macrophages and dendritic cells. After uptake from the extracellular space, antigens reach the cytosol by an as yet unknown pathway. The mechanism is size-dependent ( $\leq 30$  kDa) as measured by cytosolic staining of unspecifically internalized labeled dextran beads of different relative molecular masses and the appearance of a 30 kDa degradation fragment of internalized BSA (Rodriguez et al., 1999). Furthermore, transport is selective for proteins not normally resident in the lysosomal/endosomal compartment. Further processing of antigens appears to follow the typical MHC class I pathway, that is proteolysis by proteasomes in the cytosol, translocation into the ER by TAP transporters, and normal MHC class I assembly. Cross-priming is the result of another property of molecular chaperones and heat shock proteins (Hsps), namely their role and use as tumor rejection antigens (Reed and Nicchitta, 2000; Yewdell et al., 1999).

### D.1.3 Heat shock proteins in cellular immunity

The role of molecular chaperones and heat shock proteins (Hsps) in mediating the folding of newly-synthesized proteins and the refolding of stress-denatured proteins is well established (see general introduction). Hsp70 has further been reported to generally enhance MHC class II presentation upon overexpression in macrophages (Panjwani et al., 1999) by an as yet unknown mechanism. It is also selectively accumulated in exosomes of dendritic cells (Théry et al., 1999).



In addition, molecular chaperones and Hsps have a role in eliciting specific MHC class I immune responses against various tumor-derived and viral antigens that is not yet well understood (Srivastava et al., 1986; Nieland et al., 1996). Hsp/peptide complexes isolated from tumors were shown to mediate immunoprotection against that tumor in mice and may thus prove useful as therapeutic agents in anti-tumor vaccination (Przepiora and Srivastava, 1998). Similarly, MHC class I anti-viral responses have been generated with Hsp/peptide complexes. Thus far, three cellular chaperones have been identified as potent peptide carriers in these vaccination approaches, namely Grp94 (the ER paralog of Hsp90), calreticulin (an ER-specific chaperone), and cytosolic Hsp70 (Udono and Srivastava, 1994; Basu and Srivastava, 1999; Nair et al., 1999). Historically, Grp94 was the first of these discovered to act as a tumor rejection antigen in chemically induced sarcomas in mice (Srivastava et al., 1986). Other chaperones such as cytosolic Hsp90 or BiP (the ER paralog of Hsp70) are less active (Udono and Srivastava, 1994). *In vitro*, these proteins can induce specific CTL responses against bound peptides (Suto and Srivastava, 1995), with a few micrograms of Hsp/peptide complex being sufficient to elicit a potent response (Chandawarkar et al., 1999). *In vivo*, vaccinations with these proteins reduce the size and number of seeded tumors. Immune-active Hsp/peptide complexes can be isolated from tumor tissue, or reconstituted *in vitro* from purified components (Moroi et al., 2000; Blachere et al., 1997). The antigenic peptides introduced in chaperone complexes are ultimately presented on MHC class I molecules of APCs by an unknown mechanism that involves peptide uptake by endocytosis (Suto and Srivastava, 1995). Recently, receptor-mediated binding and uptake of Grp94 by APCs, e.g. dendritic cells and macrophages and B cells, followed by presentation of the bound peptides on MHC class I has been reported (Arnold-Schild et al., 1999; Wassenberg et al., 1999; Singh-Jasuja et al., 2000). Binder and colleagues lately identified CD91 as a receptor for Grp94 on the surface of a mouse macrophage cell line (RAW264.7) and on primary monocytes (Binder et al., 2000). Such a receptor has not been described for Hsp70/Hsc70. To obtain evidences for the existence of such a receptor was the focus of the work presented here.

Subsequent to internalization, alternative routes have been described for presentation of the chaperone-bound antigens depending on the structural context of the antigenic peptide. An engineered Hsp70 binding sequence fused to an antigenic peptide in different manners (C- or N-terminal fusions) determined whether Hsp70-mediated

loading of antigenic peptide onto MHC class I involved the classical pathway, involving proteasomal degradation and TAP-dependent ER-translocation, or via an as yet unknown mechanism in early endosomes (Castellino et al., 2000). An endosomal loading mechanism has also been suggested for Grp94-bound antigens after uptake, since a colocalization of Grp94 with MHC class I molecules in early endosomes has been observed (Arnold-Schild et al., 1999). On the other hand, depletion of cellular ATP and blockage of the secretory pathway with the specific inhibitor Brefeldin A abolish the effective presentation of Hsp70-bound peptides on MHC class I molecules suggesting the classical loading pathway as the predominant mechanism, independent of processing in the acidic, lysosomal compartment (Suto and Srivastava, 1995). Upon uptake, Grp94 further induces maturation of dendritic cells and downregulation of its receptor (Singh-Jasuja et al., 2000).

A different mode of uptake, probably unrelated to the one described before, has been described for pre-B cells, antibody-producing effector cells from the lymphoid lineage of blood cells. Hsp70 internalization by these cells occurs with very fast kinetics resulting in an intracellular staining suggesting a direct translocation across the plasma membrane. Furthermore, this process seems to be less restricted regarding the size of the protein, but specific for Hsp70 (Fujihara and Nadler, 1999). The uptake of Hsp70 by pre-B cells is unrelated to the uptake observed with APCs and does not lead to MHC class I presentation. The exact mechanism of translocation remains to be established.

As a more general immunostimulatory effect, Hsp70 and mitochondrial Hsp60 can induce monocytes and macrophages to produce proinflammatory cytokines (Asea et al., 2000; Chen et al., 1999; Moroi et al., 2000). This cellular response is dependent on the expression of CD14 and toll-like receptors (Asea et al., 2000; Kol et al. 2000; Ohashi et al., 2000). *In vivo*, increased expression of Hsp70 during tumor cell killing leads to the infiltration of immature dendritic cells and macrophages into the tumor tissue and induces an innate immune response at the site of cell death. Immature dendritic cells treated with the lysates of Hsp70-overexpressing tumor cells are inhibited in their maturation and thus maintain the capability for efficient phagocytosis and antigen processing (Todryk et al., 1999). Whether the chaperone-specific activation of APCs is distinct from the receptor-mediated uptake of chaperone/peptide complexes remains to be analyzed.

It is possible that Hsps released from cells act as part of the normal immune surveillance system, reaching the extracellular space upon necrosis of cells and probably

also apoptosis. Given a limited efficiency of the KDEL retention mechanism for ER luminal proteins, it is also possible that small amounts of Grp94 and BiP may constantly be secreted from cells in complex with a variety of antigenic peptides that have been transported from the cytosol into the ER lumen for presentation on MHC class I. A specific binding of TAP-translocated peptides to Grp94 and calreticulin has been demonstrated suggesting a peptide loading mechanism for these chaperones (Lammert et al., 1997; Spee and Neefjes, 1997). Furthermore, the reported association of Grp94- and Hsp70-related antigens with the cell surface of certain tumor cells (Altmeyer et al., 1996; Multhoff et al. 1995) has been suggested to stimulate a natural killer cell response against the tumor (Multhoff et al., 1997), but may be unrelated to Hsp-mediated antigen presentation.

#### D.1.4 Aim of the project

The goal of this project was to reach a better understanding of the molecular basis of chaperone-mediated tumor immunity. At the beginning of the work the existence of an Hsp70-specific receptor for endocytosis of chaperone/peptide complexes on antigen presenting cells had been proposed but not formally demonstrated.

The main aim was to establish an assay for the specific binding of Hsp70 to the cell surface of antigen presenting cells and the characterization of its binding properties, which would then serve as the basis for the identification of such a receptor. The assay was to be used to characterize the expression pattern and binding specificity of the receptor. Criteria for ligand specificity, in particular competition with homologs from the Hsp70 family and other chaperones, nucleotide effects, and peptide binding states were to be addressed.

## D.2 Material and Methods

Several materials and methods used have been already introduced in Chapter C but were also applied in this part of the present thesis. In order to avoid redundancy, only techniques will be described in the following which are unique to this part.

### D.2.1 Chemicals

All chemicals were of quality *pro analysi* and were purchased from *Merck* (Darmstadt, Germany) or *Sigma-Aldrich* (Steinheim, Germany) if not stated otherwise. Plastic ware for cell culture was purchased from *Greiner* (Frickenhausen, Germany).

*Amersham* (Buckinghamshire, England): Cy3 protein labeling kit.

*Biochrom KG Seromed* (Berlin, Germany): DMEM, VLE-RPMI 1640 medium, fetal calf serum (low endotoxin), L-glutamine, penicillin/streptomycin.

*Biowhittaker* (Walkersville, USA): Limulus Amebocyte Lysate (LAL) Complete Test Kit QCL-1000 (Endotoxin determination).

*Life Technologies/GibCo* (Karlsruhe, Germany): human recombinant granulocyte/macrophage-colony stimulating factor (GM-CSF), human recombinant interleukin 4 (IL-4), human tumor necrosis factor  $\alpha$  (TNF $\alpha$ ).

*Molecular Probes* (Leiden, Netherlands): Alexa488 protein labeling kit.

*Nycomed* (Oslo, Norway): Lymphoprep, Nycoprep.

*Pharmingen* (San Diego, USA): R-phycoerythrin (PE)-conjugated mouse anti-human monoclonal antibody  $\alpha$ CD1a (clone HI149) and PE-IgG<sub>1</sub> isotype control, fluorescein isothiocyanate (FITC)-conjugated mouse anti-human  $\alpha$ CD83 (clone HB15e) and FITC-IgG<sub>1</sub> isotype control, 7-Amino-actinomycin D (7-AAD, Via-Probe).

### D.2.2 Instruments

*Becton Dickinson* (San Jose CA, USA): FACSCalibur flow cytometer with CellQuest software.

## D.2.3 Buffer

- PBS: 137.0 mM NaCl, 2.7 mM KCl, 8.4 mM Na<sub>2</sub>HPO<sub>4</sub> · 2H<sub>2</sub>O, 1.5 mM KH<sub>2</sub>PO<sub>4</sub>, adjust with HCl to pH 7.4.
- PBA: PBS, 1% (w/v) BSA, 0.02% (w/v) sodium azide.
- PBMC wash buffer: 1% (w/v) BSA, 0.13% (w/v) EDTA, 0.9% (w/v) NaCl

## D.2.4 Plasmids and bacterial strains

The following plasmids have been used for recombinant expression of native proteins (Table 11):

**Table 11. Plasmids used in this study.**

ORF	Vector	Purification tag	Restriction sites	Reference
human hsp70	pProEx HTa	His <sub>6</sub> (N-term.)	EcoRI/XhoI	this study
GST	pGEX6P	-	-	Pharmacia
mouse BiP	-	His <sub>6</sub> (C-term.)	-	Ingrid Haas
human hsp40	pQE9	His <sub>6</sub> (N-term.)	-	Minami et al., 1996
human p60TPR1S	pProEx HTa	His <sub>6</sub> (N-term.)	EheI/HindIII	Scheufler et al., 2000

## D.2.5 Mammalian cell culture and cell lines

All cells were cultured in 'Very low endotoxin' (VLE)-RPMI 1640, supplemented with 10% FCS, 2 mM L-glutamine and antibiotics (100 U/500 ml penicillin and 100 µg/500 ml streptomycin) (Seromed/Biochrom, Germany) at constant temperature, humidity and atmosphere (37°C, 5% CO<sub>2</sub> and 95% air).

## D.2.5.1 Cell lines

The following cell lines were used in this study (Table 12):

Name	Species	Type	Reference
ANA-1	mouse	macrophage	Cox et al., 1989
Raw264.7	mouse	macrophage	Ralph and Nakoinz, 1977
Jurkat	human	T lymphocyte	Schneider et al., 1977
DC10	human	dendritic cell	Shen et al., 1997
THP-1	human	monocyte	Tsuchiya et al., 1980
U937	human	monocyte	Sundstrom et al., 1976
70Z/3	mouse	pre-B lymphoblast	Bach et al., 1979
293	human	kidney epithelial	Graham et al., 1977

## D.2.5.2 Isolation of fresh peripheral blood cells

Human peripheral blood lymphocytes (PBLs) and monocytes (PBMCs) were isolated from a healthy donor. Fresh blood was diluted into PBS (1:1) and overlaid on top of a Lymphoprep cushion (*Nycomed*). After centrifugation at 500xg for 30 min, the interfaces containing the PBL- and PBMC-population were separated and mixed with FCS. After additional washing with PBS the cells were transferred into binding buffer PBA (PBS, 1% (w/v) BSA, 0.02% (w/v) sodium azide).

Alternatively, monocytes were isolated using a Nycoprep gradient (*Nycomed*) resulting in a highly enriched PBMC population consisting of more than 95% CD14<sup>+</sup> cells. The PBLs were removed during the isolation procedure. Specifically, fresh blood was supplemented with 0.1 volumes of 6% dextran and incubated for 40 min at room temperature. The plasma depleted of erythrocytes was centrifuged through a Nycoprep cushion (*Nycomed*) for 15 min at 800xg. The interface containing the monocytes was washed four times with wash buffer (1% (w/v) BSA, 0.13% (w/v) EDTA, 0.9% (w/v) NaCl) by centrifugation at 400xg for 10 min and subsequent resuspension in wash buffer. Finally, cells were resuspended in binding buffer PBA and directly used in the binding assay. For other experiments, PBMCs were resuspended in freshly prepared VLE-RPMI 1640 medium and used for generation of primary dendritic cells.

### D.2.5.3 Generation of primary dendritic cells

Freshly purified human peripheral blood monocytes (Nycoprep gradient) were resuspended in VLE-RPMI medium additionally supplemented with 400 U/ml GM-CSF and 400 U/ml IL-4 and seeded into 24-well plates with 1 ml culture volume per well. Medium was carefully changed at day 2 and 4. For maturation of primary dendritic cells, cells were treated with 1000 U/ml LPS and/or 0.3 ng/ml TNF $\alpha$  for two additional days. Differentiation from PBMCs to dendritic cells were monitored by detection of CD1a cell surface expression, and maturation was controlled by expression of CD83 on the cell surface using FITC- and PE-conjugated monoclonal antibodies, respectively. Unrelated antibodies were used as isotype control.

### D.2.6 Protein expression and purification

The cDNA of human Hsp70 (*Mojave Therapeutics*, New York, USA) was amplified by PCR and cloned into the prokaryotic expression vector pProExHTa (*Life Technologies/GibCo*) encoding a N-terminally His<sub>6</sub>-tagged protein. All recombinant proteins were expressed in *E. coli* BL21(DE3)pLysS cells grown in terrific broth supplemented with 100 mg/l carbenicillin (*Sigma*) at 18°C for 12 hours after induction with 0.5 mM IPTG at OD<sub>600</sub>=1.5. Cell lysates were prepared by repeated freeze-thawing and subsequent addition of lysozyme (*Sigma*) and Benzonase (*Merck*) followed by sonication and centrifugation at 100,000xg for 30 min at 4°C. Recombinant Hsp70 was purified by NiNTA chromatography followed by anion exchange chromatography on MonoQ (*Pharmacia*) and gel filtration on Sephacryl S-200 (*Pharmacia*), equilibrated with PBS.

Human Hsp40 was expressed and purified using the plasmid pQE-9/Hsp40 as described (Minami et al., 1996). GST was expressed from pGEX6P vector (*Pharmacia*) and purified by glutathione-Sepharose chromatography. Hsc70 from bovine brain and liver and DnaK from *E. coli* were purified as described (Minami et al., 1996).

The Hsp70 proteins used were functionally active as determined by their ability to bind the unfolded polypeptide reduced carboxymethylated  $\alpha$ -lactalbumin (RCMLA) (Palleros et al., 1991) and to hydrolyze ATP in a manner sensitive to stimulation by the cochaperone Hsp40 (Liberek et al., 1991; Minami et al., 1996). Analytical gel filtration

was performed to exclude the appearance of aggregated Hsp70 protein before and after fluorescent labeling (data not shown).

Protein concentrations were determined by Bradford assay (*Pierce*). Endotoxin contamination of all proteins was measured by quantitative chromogenic Limulus Amebocyte lysate assay (*BioWhittaker*) following the manufacturers' instruction.

Proteins were labeled using the protein labeling kit Alexa488 (*Molecular Probes*) or Cy3-labeling (*Amersham*) following the manufacturers' instructions. FITC-labeled transferrin was commercially available (*Molecular Probes*).

#### D.2.7 Hsp binding and uptake

After two days of continuous culture, cells grown to sub-confluency ( $1.5 \times 10^6$  cells/ml) were gently washed off the culture flask. Cells were centrifuged at 500xg, 4°C for 5 min and resuspended in PBA for binding assays (4°C) or in complete medium containing FCS for uptake experiments (37°C).  $5 \times 10^5$  cells were incubated for 45 min at 4°C or 37°C with 1  $\mu$ M Alexa488-labeled ligand in the presence or absence of 20-fold excess of unlabeled competitor in a final volume of 500  $\mu$ l. Cells were washed twice with 1 ml of ice-cold PBA, and finally resuspended in ice-cold PBS containing 1 g/ml propidium iodide, then directly subjected to flow cytometry analysis using a FACSCalibur (*Becton Dickinson*). In some experiments, cells were treated with 1.5 mg/ml Pronase dissolved in PBS for 30 min on ice before or after the binding assay. Proteolysis was stopped by washing cells twice with ice-cold PBA. Propidium iodide staining was used to restrict the analysis to viable cells.

Cell surface binding of Alexa488-labeled proteins was quantified using the geometric mean fluorescence value that represents an average fluorescence weighted to the number of cells emitting at each fluorescence intensity in the range of  $10^0$ - $10^4$ . Values were normalized to 100% binding of Hsp70 with 2 to 5% of gated cells in the control (autofluorescence).



### D.2.8 Confocal microscopy

Microscopic studies have been carried out in collaboration with Felix Wieland and Thalia Becker (BZH Heidelberg, Germany).

Cells were resuspended in medium containing 10% FCS. After incubation for binding with 100 nM Hsp70 or GST and 20 nM transferrin for 45 min on ice, cells were washed 4 times with 1 ml PBS and finally resuspended in 0.2 ml complete medium. Cells were either directly seeded onto sterile glass cover slips coated with poly-L-lysine for 10 min or after additional incubation for 30 min at 37°C, followed by fixation with 3% paraformaldehyde for 20 min and mounting onto slides.

Microscopy was carried out with a confocal microscope, Leica TCSSP, at 63-fold magnification.

## D.3 Results

### D.3.1 Cell-specific binding and uptake of Hsp70

A flow cytometry-based assay system was established to investigate the binding and uptake of human cytosolic Hsp70 by ANA-1 cells, a macrophage cell line, and by Jurkat cells, a T lymphocytic cell line. Recombinant Hsp70 was labeled fluorescently with the dye Alexa488 under physiological conditions in PBS with two molecules of Alexa488 being coupled per molecule of Hsp70 (data not shown). Essentially identical cell binding results were obtained with a variety of Hsp70 and Hsc70 preparations, either expressed as recombinant proteins or purified from bovine tissue sources. Cells were incubated in the presence of labeled Hsp70 with or without unlabeled competitor proteins at low temperature (4°C) to inhibit nonspecific endocytosis. Binding analysis was carried out by measuring the fluorescence intensity on the cell surface after washing out unbound material. Propidium iodide staining was used to restrict the analysis to viable cells (usually more than 95% of total).

ANA-1 macrophage cells bound Hsp70 specifically (Figure 29). The addition of a 20-fold excess of unlabeled Hsp70 competed the binding of fluorescent-labeled Hsp70 significantly, indicated by highly reduced fluorescence intensities of the cell surfaces (Figure 29A). The same molar excess of the protein glutathione S-transferase (GST) (Figure 29B) and several His<sub>6</sub>-tagged proteins unrelated to Hsp70 (data not shown) were without effect. Competition of labeled with unlabeled Hsp70 was incomplete with about 25% of bound Hsp70 not being competable. This issue will be addressed below in detail. Furthermore, Hsp70 binding was cell-type specific; it was observed with ANA-1 cells but not with Jurkat cells (Figure 29C and D). Other cells tested with this assay included various monocytic/macrophage cell lines (RAW264.7, THP-1, U937), a dendritic cell line (DC-10), a pre-B cell line (70Z/3), and kidney cells (293), and none of them showed any specific Hsp70-mediated cell surface staining (data not shown). There was no detectable ATP- or ADP-dependence of Hsp70 binding to ANA-1 cells (see Figure 33A). Moreover, Hsp70 binding was undiminished in the presence of a molar excess of peptide C (KLIGVLSSLFRPK) which binds with high affinity to the C-terminal polypeptide-

binding domain of Hsp70 (Figure 33A) (Flynn et al., 1989). Because Hsp70 binding to ANA-1 cells is cell-type specific, nucleotide independent and not competitive with peptide, it cannot be explained by a chaperone-like interaction of Hsp70 with unfolded cell-surface proteins in general. Instead, a more specific mode of binding is suggested.

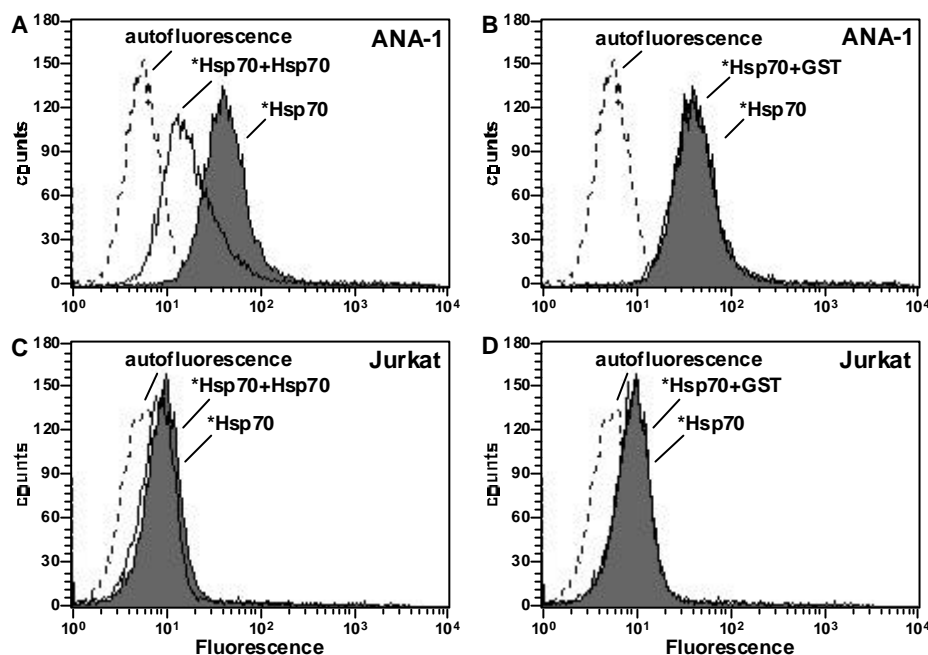


**Figure 29.** Specific binding of Hsp70 to murine ANA-1 macrophages, but not to Jurkat cells.  $5 \times 10^5$  ANA-1 cells (A, B) or Jurkat cells (C, D) were incubated at  $4^\circ\text{C}$  for 45 min in PBA with  $1 \mu\text{M}$  Alexa488-labeled Hsp70 (\*Hsp70) in the presence or absence of  $20 \mu\text{M}$  unlabeled Hsp70 (A, C) or GST (B, D) as a competitor. Intensity of surface fluorescence (x-axis) is plotted against cell counts. Representative results of at least three independent experiments are shown.

To determine whether the observed binding of Hsp70 to the surface of ANA-1 cells (Figure 29A and B; Figure 30A) was due to a non-specific association of fluorescently labeled proteins with these cells, binding assays were carried out with Alexa488-labeled GST and Alexa488-labeled transferrin as control proteins. Transferrin was used as a positive control because this protein binds to the ubiquitously expressed transferrin receptor. Binding of labeled GST to the cell surface was not observed (Figure 30B). However, transferrin showed similar properties of binding to ANA-1 cells as Hsp70. Unlabeled transferrin inhibited the binding of the labeled protein, whereas GST did not compete (Figure 30C). Transferrin did not compete for the binding of labeled Hsp70 (data not shown).

Binding reactions with ANA-1 cells were also carried out at physiological temperature where bulk endocytosis occurs (Figure 30D-F). Specific competition of binding and uptake of Hsp70 and transferrin by the unlabeled proteins was again observed. However, non-specific endocytosis predominated under these conditions (Figure 30D-F), as indicated by the uptake of GST which did not bind specifically to the cell surface.

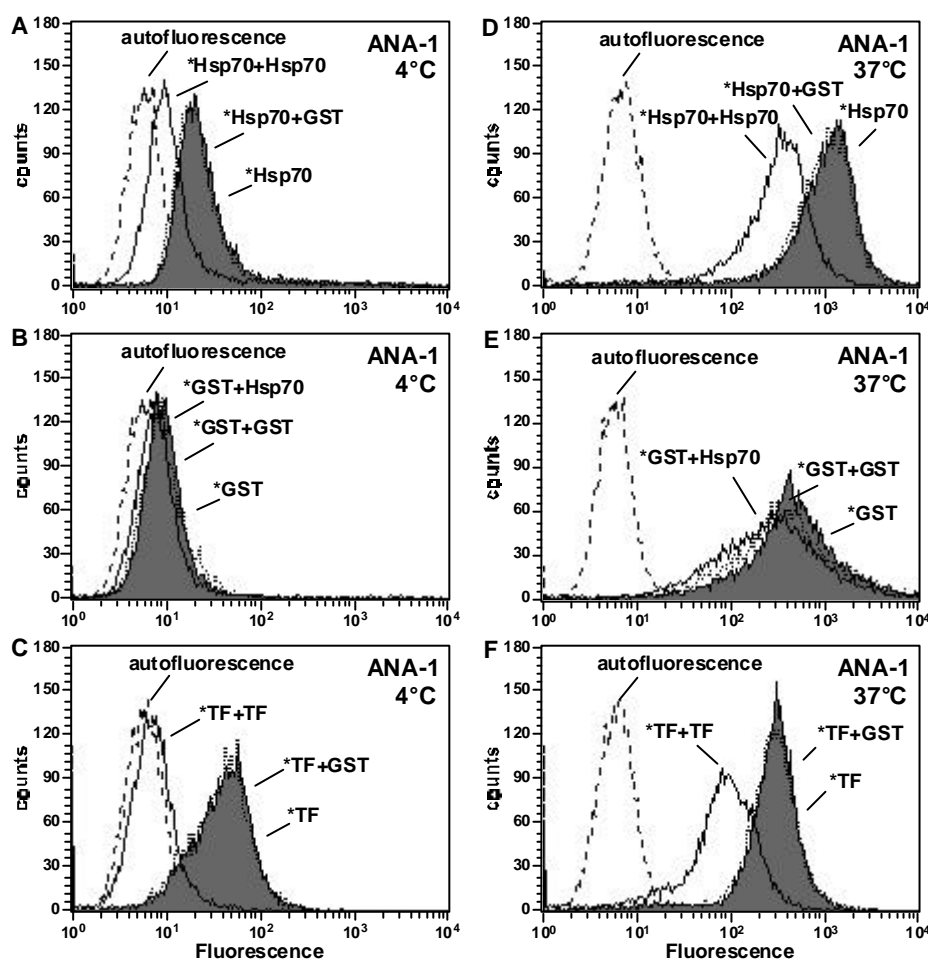


**Figure 30.** Specific binding and uptake of Hsp70 by murine ANA-1 macrophages. ANA-1 cells were incubated with labeled Hsp70 (\*Hsp70) (A and D), labeled GST (\*GST) (B and E), or labeled transferrin (\*TF) (C and F) either at 4°C (A, B, and C) or at 37°C (D, E, and F) in the presence or absence of the respective unlabeled ligand as specific competitor, or GST as an unspecific competitor. Cells were analyzed as described in Figure 29.

## D.3.2 Saturable Hsp70 cell surface binding by a proteinaceous receptor

To determine whether surface binding of Hsp70 is mediated by a proteinaceous receptor, ANA-1 cells were incubated with the protease Pronase prior to Hsp70 binding. This treatment reduced the binding of labeled Hsp70 to the same extent as did the addition of excess unlabeled Hsp70 in reactions with control cells (Figure 31A), indicating that specific binding of Hsp70 is mediated by proteinaceous sites. The same reduction in the amount of bound Hsp70 was obtained when Pronase treatment was performed after the binding reaction (Figure 31B), indicating that under the conditions used (binding at 4°C), specifically bound Hsp70 remained at the cell surface. In contrast, the noncompetable binding of fluorescent labeled Hsp70 is probably not mediated by specific protein-protein interactions and may be due to a direct interaction of the fluorescence dye with the membrane.

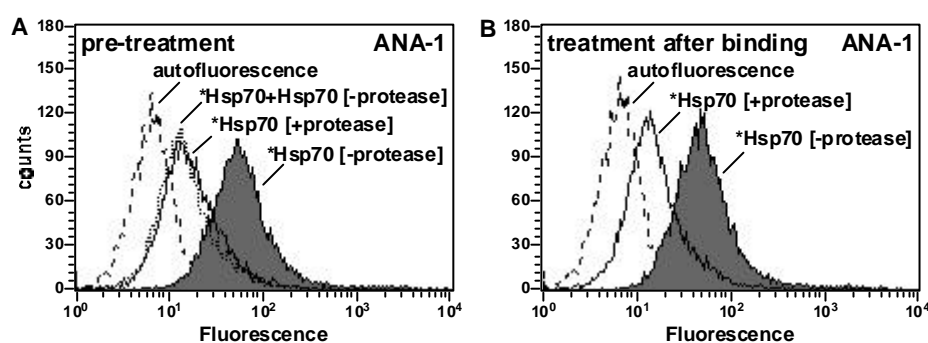


**Figure 31.** Protease-sensitivity of Hsp70 binding to the cell surface of ANA-1 macrophages. **(A)**  $5 \times 10^5$  cells were treated with 1.5 mg/ml Pronase for 30 min on ice, washed twice with PBA, and then incubated with Alexa488-labeled Hsp70 (\*Hsp70) (see Figure 29). Fluorescence intensities were measured by flow cytometry. **(B)** Protease treatment as in **(A)** was performed after binding of \*Hsp70.  $5 \times 10^5$  cells were treated with 1.5 mg/ml Pronase for 30 min on ice after binding of \*Hsp70. Mock treatment without protease was carried out as control. Cells were washed twice with PBA and then analyzed as in **(A)**. Comparable results were obtained in three independent experiments.

The above results strongly suggested that Hsp70 was recognized by a proteinaceous receptor expressed by the ANA-1 cells. Such receptor-mediated binding was expected to be saturable and to have a reasonably high affinity. To test these predictions, we investigated the concentration-dependence of Hsp70 binding to determine the binding mode and approximate affinity of the receptor-ligand interaction. ANA-1 cells were incubated with 0.2  $\mu$ M of fluorescence-labeled Hsp70, added either alone or in

combination with a 20-fold molar excess of unlabeled Hsp70 to determine the level of non-specific binding. As expected, competition for binding was optimal at the lowest concentration of labeled Hsp70 used where the ratio of specific to non-specific binding was maximal (Figure 32A). The difference curve obtained by subtracting non-specific binding indicates that specific Hsp70 binding is saturable and occurs with an apparent  $K_D < 100$  nM (Figure 32B). The shape of the binding curve suggests that Hsp70 either binds to a single type of receptor or, less likely, to different receptors with binding properties that are indistinguishable by this assay. The exact number of Hsp70 receptor sites remains to be determined but their density is approximately 10-fold lower than that of the transferrin receptor (Huebers and Finch, 1987) and thus should be in the range of 10,000 per cell.

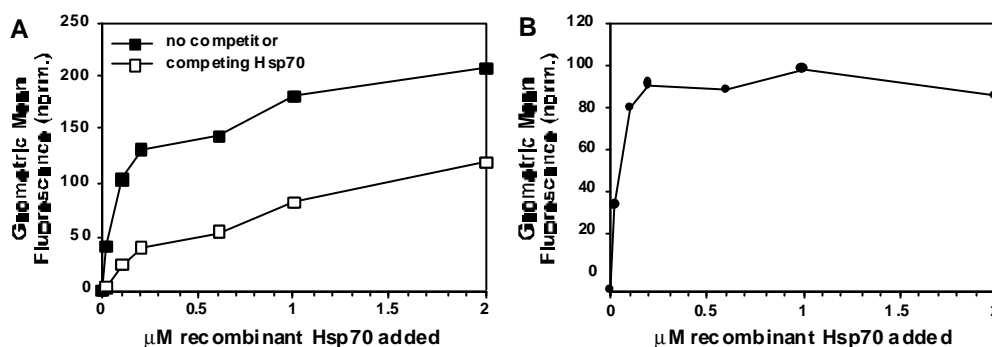


**Figure 32.** Concentration-dependent binding of Hsp70 to ANA-1 cells. (A)  $5 \times 10^5$  ANA-1 cells were incubated at 4°C for 45 min in PBA with increasing concentrations of Alexa488-labeled Hsp70 (0-2 μM) in the absence (filled squares) or presence (open squares) of unlabeled Hsp70 (20-fold molar excess). Fluorescence intensities were analyzed by flow cytometry and plotted against the concentration of Alexa488-Hsp70 in the binding assay. (B) Difference binding curve obtained by subtracting non-specific binding (open squares) from total binding (filled squares) in (A). Representative results of three independent experiments are shown.

### D.3.3 Specific binding of mammalian but not bacterial Hsp70 to ANA-1 cells

The specificity of the Hsp70 receptor on ANA-1 cells for Hsp70 proteins from various sources was analyzed. Cells were incubated with fluorescently labeled human Hsp70 at 4°C in the presence of different Hsp70s as competitors and subsequently analyzed by flow cytometry. For comparison, the control reactions as described above are repeated here (Figure 33). Bovine Hsc70, either from brain or liver, was as efficient as

competitor as unlabeled human Hsp70 (Figure 33A and B). In contrast, the *E. coli* homologue of Hsp70, DnaK, did not compete the binding of labeled human Hsp70 (Figure 33B), despite the high homology in primary sequence between both species (63% similarity, 49% identity). Mammalian Hsp70s and *E. Coli* DnaK recognize as chaperones a similar range of hydrophobic peptides (Blond-Elguindi et al., 1993; Flynn et al., 1983; Rüdiger et al., 1997). Thus, the absence of a specific association of DnaK with the cell surface supports the conclusion that Hsp70 binding is not mediated by a chaperone-like interaction. The ER paralogue BiP competed only poorly for the binding of labeled Hsp70 (Figure 33B), and fluorescent-labeled BiP showed only weak binding (data not shown). Grp94 from bovine liver did not compete the binding of Hsp70, indicating that the sites mediating Grp94 binding (Arnold et al., 1999; Wassenberg et al., 1999) differ from those for Hsp70 (data not shown).

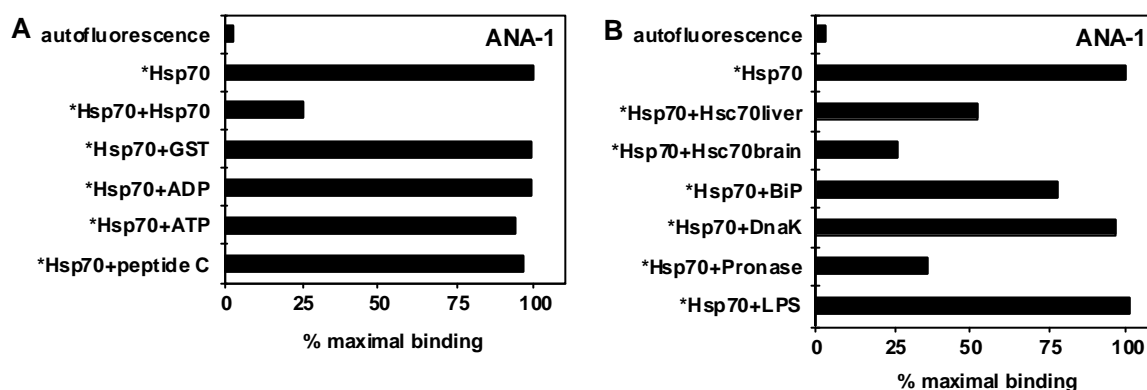


**Figure 33.** Properties of Hsp70 binding to the cell surface of ANA-1 macrophages and ligand specificity.  $5 \times 10^5$  cells were incubated for 45 min at  $4^\circ\text{C}$  in PBA with Alexa488-labeled Hsp70 ( $1 \mu\text{M}$ ; \*Hsp70) in the presence or absence of competitor proteins ( $20 \mu\text{M}$ ), nucleotides ( $2 \text{ mM}$ ), peptide C ( $100 \mu\text{M}$ ), or lipopolysaccharide (LPS) ( $100 \mu\text{M}$ ). Fluorescence intensities were analyzed by flow cytometry and quantified by gating with 2 to 5% of gated cells in the autofluorescence control. Values were normalized to 100% binding of labeled Hsp70 without subtraction of the autofluorescence value. Similar results were obtained in at least three independent experiments. **(A)** Unlabeled human Hsp70, GST, nucleotides, or peptide C (KLIGVLSSLFRPK) were present in the binding reaction. **(B)** Binding reactions contained, in addition to labeled Hsp70, Hsc70, purified from bovine liver or brain, BiP, *E. coli* DnaK, or LPS. Binding of labeled Hsp70 remaining after Pronase treatment of cells is shown to indicate the level of non-specific, i.e. non-competable, Hsp70 binding. Representative results of three independent experiments are shown. The deviation between the experiments was less than 5%.

Specific binding of Hsp70 was not mediated by a contamination of the protein with lipopolysaccharide (LPS), a ligand of the toll-like receptors and CD14 on monocytes and macrophages, because a 100-fold molar excess of LPS did not reduce the binding of Hsp70 (Figure 33B). Furthermore, all proteins used in this study were found to contain similar amounts of endotoxin in the range of  $10^3$  EU/mg protein (data not shown) as based on quantitative Limulus Amebocyte lysate assay.

In summary, these results indicate the existence of proteinaceous receptor sites for mammalian but not bacterial Hsp70 on the surface of ANA-1 macrophages. Such receptor sites are not found on Jurkat T lymphocytes and other cell lines tested (see Materials and Methods and D.3.1).

#### D.3.4 Localization of bound and internalized Hsp70 by confocal microscopy

In collaboration with Felix Wieland and Thalia Becker (*BZH*, Heidelberg), confocal microscopy was used to confirm the specific binding of Hsp70 to the cell surface of ANA-1 cells and the subsequent internalization of the bound protein. ANA-1 cells were incubated at 4°C with either Cy3-labeled Hsp70 or GST. FITC-labeled transferrin served as a positive control. At low concentrations of labeled Hsp70 (100 nM) or transferrin (20 nM) predominantly specific binding was observed. All cells showed clear surface binding of transferrin but no binding of GST (Figure 34A). Upon merging both fluorescence channels, only the FITC-transferrin staining was detected. Incubation with Hsp70 also resulted in a clear cell surface labeling which showed significant colocalization with the transferrin signal (Figure 34B). In both cases, punctate staining suggested a clustering of receptors.

In a second series of experiments cells were shifted to 37°C after protein binding and removal of unbound material at 4°C. Whereas no binding and uptake was seen with Cy3-GST (Figure 34C), both Hsp70 and transferrin were internalized by the cells upon incubation for 30 min at 37°C, resulting in an intracellular, vesicular staining with partial co-localization of the two proteins (Figure 34D).

These experiments corroborate the specificity of the flow cytometry-based binding assay and demonstrate that Hsp70 bound at 4°C is competent to undergo receptor-mediated endocytosis at 37°C.



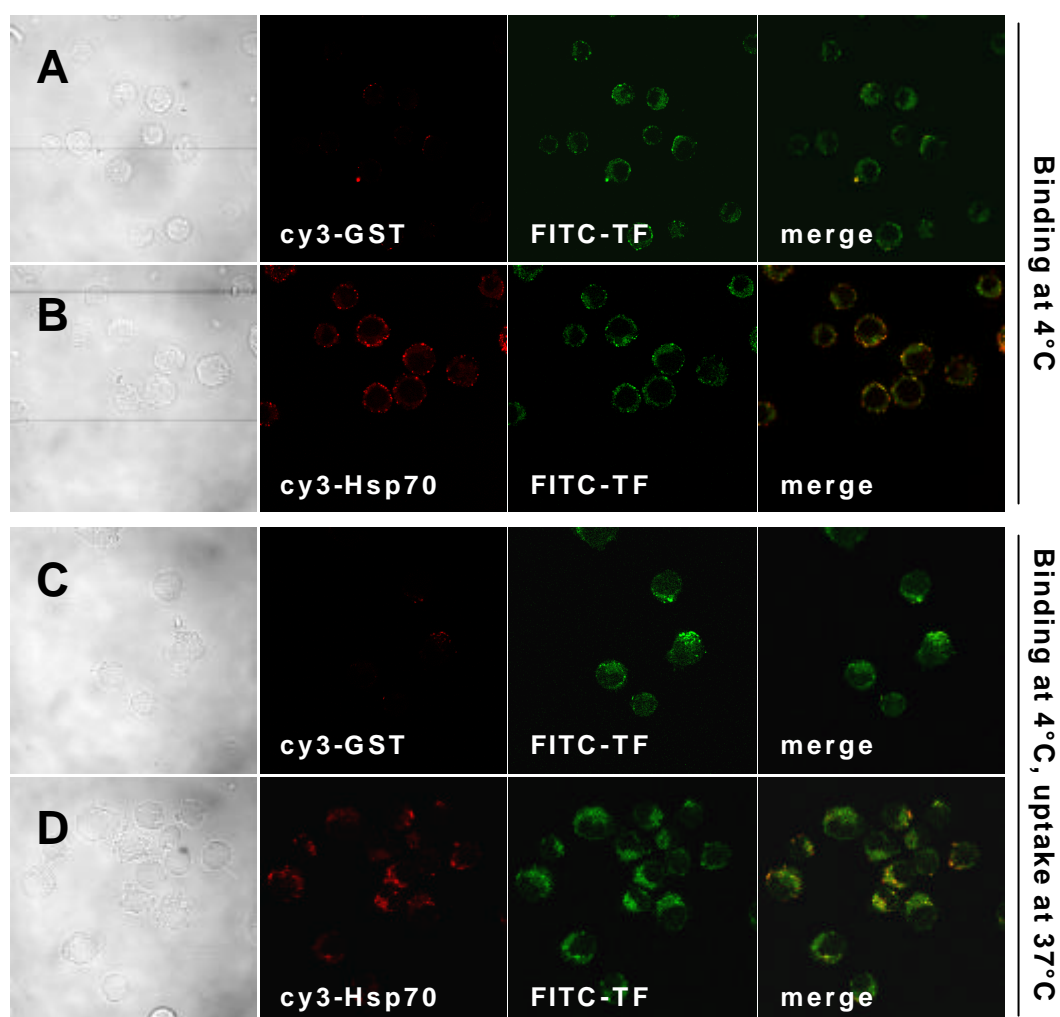


**Figure 34.** Surface binding and uptake of Hsp70 by ANA-1 macrophages. **(A, B)** Localization of Hsp70 at the cell surface upon binding at 4°C. ANA-1 cells were incubated in the presence of 20 nM FITC-labeled Transferrin and either 100 nM Cy3-labeled GST (A) or Hsp70 (B) for 45 min at 4°C in medium containing 10% FCS, washed as described in Material and Methods, and then analyzed by confocal microscopy. **(C, D)** Uptake of Hsp70 at 37°C after specific binding at 4°C. Following binding as in (A, B), cells were incubated for an additional 20 min at 37°C, and analyzed as above. Microscopic studies were performed by Thalia Becker in the group of Felix Wieland (BZH, Heidelberg).

#### D.3.5 Receptor-mediated binding of Hsp70 to PBMCs but not PBLs

The experiments described thus far analyzed the binding of Hsp70 to transformed and immortalized cell lines. Only one cell line, the macrophage cell line ANA-1, was observed to bind Hsp70 specifically. Therefore, an analysis of the overall expression

pattern of such a receptor on primary human blood cells was performed, which in addition would avoid any complications arising from the transformation process. To this end a mixture of peripheral blood lymphocytes (PBLs) and peripheral blood monocytes (PBMCs) was isolated from fresh blood by Ficoll gradient separation. Binding of fluorescence-labeled human Hsp70 was analyzed by flow cytometry as above. Co-staining of CD14 was used as a specific marker for PBMCs.

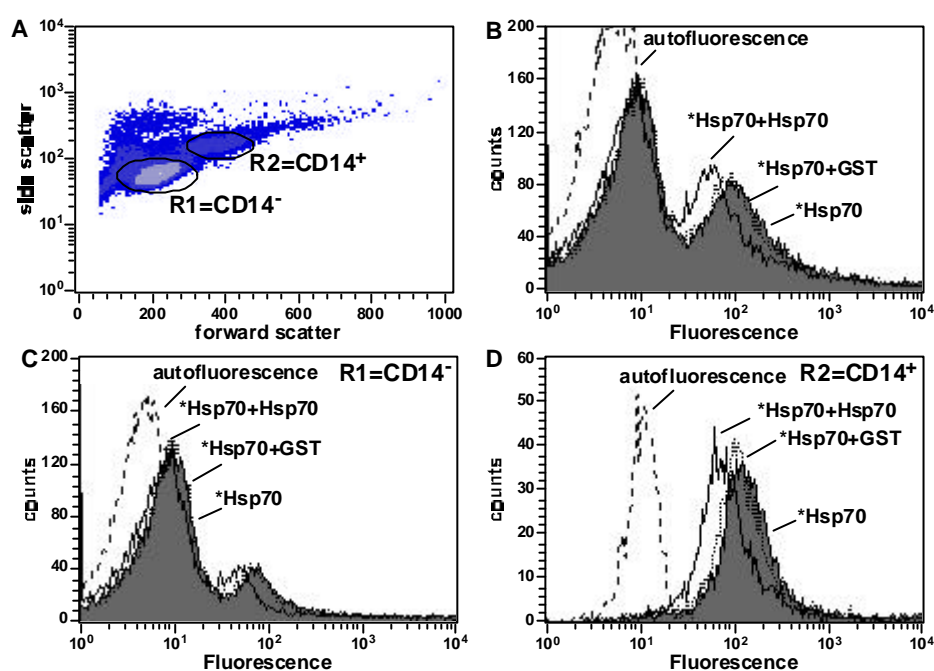


**Figure 35.** Specific binding of Hsp70 to peripheral blood monocytes (PBMCs) but not lymphocytes (PBLs) in human blood. Cells freshly isolated from peripheral blood were incubated at 4°C for 45 min with 1  $\mu$ M Alexa488-labeled Hsp70 (\*Hsp70) in the presence or absence of 20  $\mu$ M unlabeled Hsp70 or GST. Cells were analyzed by flow cytometry. (A) Forward-site-scatter plot of isolated peripheral blood cells showing the regions used for separate analysis of fluorescence intensities. (B) Fluorescence intensities of the whole cell population after incubation with \*Hsp70 in the presence of unlabeled Hsp70 as specific competitor or GST as unspecific competitor. (C) Hsp70 binding analysis of CD14-negative cells in region R2. (D) Hsp70 binding analysis of CD14-positive cells in region R2. Representative results of at least three independent experiments are shown.

Upon binding of Hsp70 to the unfractionated mixture of PBLs and PBMCs (Figure 35A and B), a biphasic distribution of fluorescence intensity was observed. However, specific binding, as judged by competition with unlabeled Hsp70, was only detected in the cell population which was labeled more intensely (Figure 35B). Based on

co-staining for CD14, these cells were identified as monocytic (Figure 35D). In contrast, the CD14-negative cells showed little or no specific Hsp70 binding (Figure 35C). The CD14 positive monocytic cells showed the same properties of Hsp70 binding established for ANA-1 cells regarding specificity and saturation of binding (data not shown).

To confirm these findings, a cell fraction enriched in PBMCs and depleted in PBLs and erythrocytes was prepared by the Nycoprep gradient technique. Figure 36A shows the CD14 positive surface staining of the final preparation of cells and the gating used to restrict the flow cytometry analysis to the CD14-positive cells. The forward/side scatter density plot in Figure 36B demonstrates the physical homogeneity of the preparation. These parameters were used to further restrict the binding analysis to a homogenous population of PBMCs. Efficient specific binding of Hsp70 was observed with these cells as based on the criteria established above (Figure 36C).

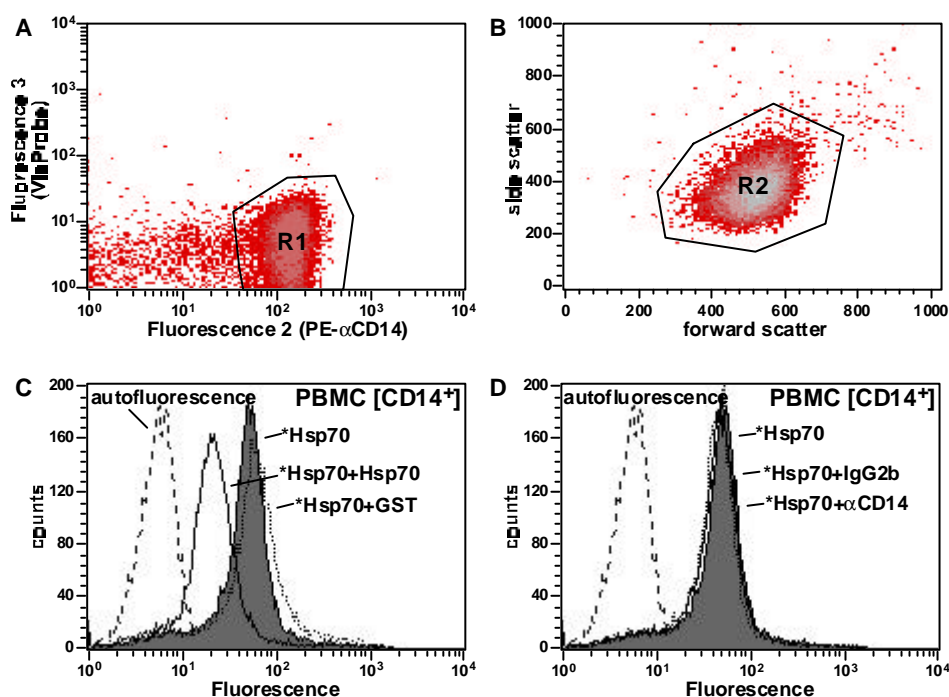


**Figure 36.** Specific binding of Hsp70 to PBMCs isolated by a combined ficoll/osmotic gradient. (A) Analysis of freshly isolated PBMCs was restricted to viable cells (ViaProbe; fluorescence 3) which were CD14-positive as judged by binding of a CD14-specific, PE-labeled antibody (fluorescence 2) (R1). (B) Restriction to a cell population with homogeneous physical properties (forward/side scatter; R2). (C) PBMCs were incubated at 4°C for 45 min with 1  $\mu$ M Alexa488-labeled Hsp70 (\*Hsp70) in the presence or absence of 20  $\mu$ M unlabeled Hsp70 or GST. Cells were analyzed by flow cytometry. (D) An  $\alpha$ CD14 antibody (clone MY4; Beckman-Coulter) or an isotype control (IgG<sub>2</sub>b) was used as competitor (20  $\mu$ M). Representative results of at least three independent experiments are shown.

Following recent reports that the monocyte-specific receptor CD14 is involved in the activation of these cells by Hsp70 and Hsp60 (Asea et al., 2000; Kol et al., 2000), we examined whether CD14 directly mediates Hsp70 binding. To address this question, binding assays were performed in the presence of a 10-fold molar excess of a CD14-specific monoclonal antibody, clone My4, which is known to block the CD14-mediated activation of monocytes by LPS and to inhibit the activation of human PBMCs by Hsp70 and Hsp60 (Asea et al., 2000; Kol et al., 2000). However, no competition of Hsp70 binding by this antibody was observed (Figure 36D). Additionally, pre-incubation of PBMCs with anti-CD14 antibodies also failed to reduce the specific binding of Hsp70 (data not shown). Taken together with the finding that an excess of LPS did not compete the binding of Hsp70 (Figure 33B), it appears unlikely that CD14 represents the binding site for Hsp70 on the surface of PBMCs.

#### D.3.6 Loss of Hsp70 binding properties upon differentiation to dendritic cells

To test whether Hsp70 binding was only restricted to monocytes or also to other specialized antigen presenting cells, primary dendritic cells were generated by treatment of PBMCs with GM-CSF and IL-4. Differentiation was monitored by expression of CD1a on the cell surface. Mature dendritic cells, monitored by expression of CD83, were obtained by treatment with LPS and/or TNF $\alpha$ .

Although a homogeneous population of differentiated cells was obtained, no cell surface binding of Hsp70 was detected either to immature or to mature dendritic cells (Figure 37A-D). This is due to a loss of the receptor since PBMCs used for generation of dendritic cells showed expression of a Hsp70-specific cell surface receptor, as seen in Figure 35 and 36.

Thus, specific Hsp70 cell surface binding was only detected on macrophages and primary monocytes, but was not observed on lymphocytes or primary dendritic cells. In the latter case, down-regulated expression of the Hsp70-specific receptor is the cause for the lack of binding. Hsp70-binding is apparently not directly mediated by CD14, the LPS-receptor on monocytes/macrophages known to be involved in the Hsp70-mediated activation of these cells.

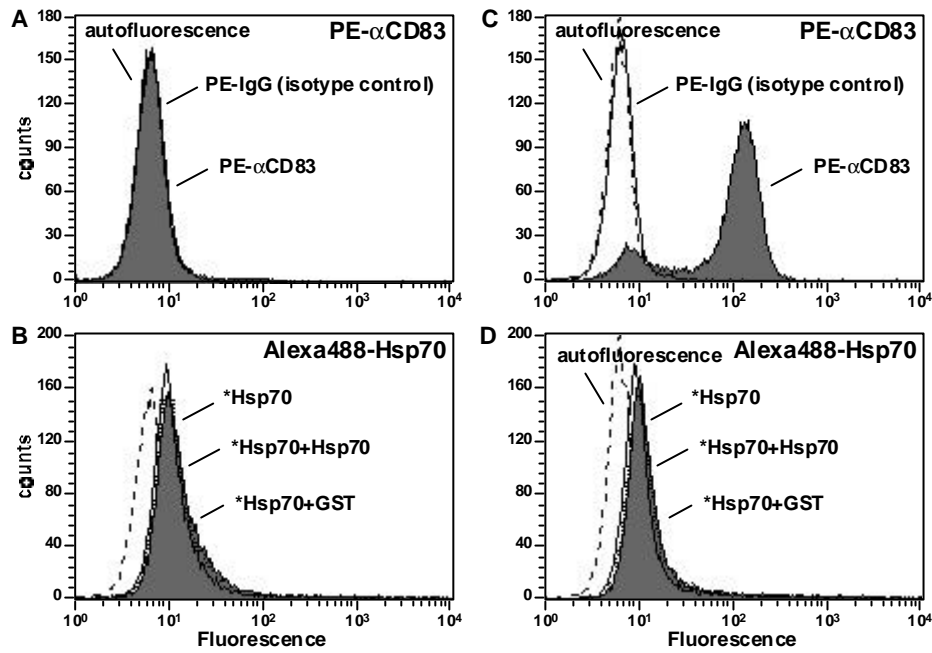


**Figure 37.** Loss of Hsp70 binding upon differentiation from PBMCs to dendritic cells. Analysis of primary dendritic cells was restricted to viable cells which were CD1a-positive as judged by binding of a CD1a-specific, PE-labeled antibody (data not shown) (A) An PE-conjugated  $\alpha$ CD83 antibody or an isotype control (IgG<sub>1</sub>) was used to detect cell surface expression of CD83. (B) CD1a-positive, but CD83-negative cells were incubated at 4°C for 45 min with 1  $\mu$ M Alexa488-labeled Hsp70 (\*Hsp70) in the presence or absence of 20  $\mu$ M unlabeled Hsp70 or GST. Cells were analyzed by flow cytometry. (C) An PE-conjugated  $\alpha$ CD83 antibody or an isotype control (IgG<sub>1</sub>) was used to detect cell surface expression of CD83. (D) CD1a-positive, CD83-positive cells were incubated at 4°C for 45 min with 1  $\mu$ M Alexa488-labeled Hsp70 (\*Hsp70) in the presence or absence of 20  $\mu$ M unlabeled Hsp70 or GST. Cells were analyzed by flow cytometry. Representative results of three independent experiments are shown.

## D.4 Discussion

Several reports appeared recently describing various functions of Hsp70 and other molecular chaperones in immunity. Their potential for tumor rejection therapy is particularly attractive since such an activity is not due to an adjuvant effect (MHC class II-mediated B-cell responses). The MHC class I response mediated by chaperones is specific for a certain subset of molecules leading to antigen-selective killing of cells, and the chaperone itself does not serve as an antigen. Therefore, the clinical application of a therapy based on vaccination with complexes of Hsps and tumor-associated antigenic peptides may provide advantages over conventional, less specific treatments like chemotherapy or radiation-based therapies once the main tumor mass has been surgically removed. Identification of the receptor and the dissection of the pathway of Hsp70-mediated immunity may lead to new strategies for the development of Hsp-based vaccines.

The basic role of an Hsp70-specific receptor would be to capture Hsp70 with bound antigenic peptide for eventual cross-presentation of the latter by MHC class I. The three proteins most active in eliciting this activity, Hsp70, Grp94, and calreticulin, would be expected to use similar mechanisms. Indeed, a receptor for Grp94 has recently been detected on the surface of APCs and has been shown to mediate the uptake of Grp94 into clathrin-coated pits and the co-localization with MHC class I components in vesicular structures (Arnold-Schild et al., 1999). Because Grp94 is structurally unrelated to Hsp70, it seems likely that both proteins bind to different receptors, or at least at different sites of a single receptor. This is consistent with our finding that Grp94 is unable to compete the binding of Hsp70. However, uptake of Hsp70-peptide complexes followed by peptide presentation on MHC class I has also been observed recently, suggesting a similar mechanism of receptor-mediated endocytosis (Castellino et al., 2000).

The expression of a Hsp70-specific receptor on the surface of monocytes and macrophages, which are professional APCs, is in agreement with such a function in antigen delivery. On the other hand, the observed down-regulation of receptor expression on mature and immature dendritic cells, the most potent cells in antigen presentation by cross-priming, may suggest a different function or mode of action of the receptor described here.

Recently, it has been shown that Hsp70 released during tumor cell killing recruits T cells, macrophages and dendritic cells into the tumor, resulting in the expression of proinflammatory cytokines (Todryk et al., 1999). It is possible that one function of the Hsp70-receptor is to mediate this activation response. Interestingly, this stimulatory effect was shown to depend on the expression of CD14 on monocytes and Toll-like receptor 4 on mouse macrophages (Asea et al., 2000; Kol et al. 2000; Ohashi et al., 2000). Whereas the activation of APCs by Hsp70 was inhibited by antibodies against CD14, neither the same antibody nor a natural ligand of CD14, LPS, was able to inhibit cell surface binding of Hsp70 to monocytes and macrophages analyzed in this study. Thus, the CD14-dependent activation of APCs by Hsp70 may occur downstream of specific receptor binding and/or uptake of Hsp70. Although CD14 seems not to be the Hsp70-specific receptor, it is noteworthy that the expression of the actual receptor coincides with the expression of CD14 on the surface of various cell lines as well as the primary cells analyzed. Additionally, preliminary results obtained in this study confirmed the potency of Hsp70 in activation of the CD14-positive PBMCs and ANA-1 cells, but not the CD14-negative cell lines tested (data not shown). The immunostimulatory activation of macrophages and monocytes by Hsp70, as measured by cytokine release, is not incompatible with uptake and processing of Hsp70/peptide complexes for the purpose of antigen presentation. Indeed, activation of cells by Hsp70/peptide complexes may be part of their tumor rejection activity. The Hsp70-receptor may thus have a dual role in the immune response, serving as a receptor for endocytosis as well as for signal transduction resulting in activation of antigen presenting cells.

In addition to their therapeutic potential, Hsp/peptide complexes may play a role as endogenous anti-tumor and anti-viral vaccines. In principle, two routes may be envisioned by which Hsps can reach the extracellular space. In the first, Hsps may be released into the extracellular space by apoptotic or necrotic cells. In the second route, small amounts of antigenic peptide-binding Hsps of the ER lumen, such as BiP and Grp94, may constantly be secreted from cells, acting as part of the normal immune surveillance system. Based on our finding that BiP binds only weakly to APCs, Grp94 may be the predominant agent in such a process.

## E References

Agashe, V. R., M. C. Shastry, and J. B. Udgaonkar. (1995). Initial hydrophobic collapse in the folding of barstar. *Nature* 377, 754-7.

Altmeyer, A., R. G. Maki, A. M. Feldweg, M. Heike, V. P. Protopopov, S. K. Masur, and P. K. Srivastava. (1996). Tumor-specific cell surface expression of the-KDEL containing, endoplasmic reticular heat shock protein gp96. *Int J Cancer* 69, 340-349.

Anfinsen, C. B. (1972). The formation and stabilization of protein structure. *Biochem J* 128, 737-49.

Anfinsen, C. B. (1973). Principles that govern the folding of protein chains. *Science* 181, 223-30.

Ang D, and C. Georgopoulos. (1989). The heat-shock-regulated *grpE* gene of *Escherichia coli* is required for bacterial growth at all temperatures but is dispensable in certain mutant backgrounds. *J Bacteriol* 171, 2748-55.

Arnold-Schild, D., D. Hanau, D. Spehner, C. Schmid, H. G. Rammensee, de la, Salle, H, and H. Schild. (1999). Cutting edge: receptor-mediated endocytosis of heat shock proteins by professional antigen-presenting cells. *J Immunol* 162, 3757-3760.

Asea, A., S. K. Kraeft, E. A. Kurt-Jones, M. A. Stevenson, L. B. Chen, R. W. Finberg, G. C. Koo, and S. K. Calderwood. (2000). Hsp70 stimulates cytokine production through a CD14-dependent pathway, demonstrating its dual role as a chaperone and cytokine. *Nat Med* 6, 435-442.

Bach, F.H. (1979). T and B lymphocytes. Academic Press, New York, 143.

Baldwin, R. L. (1995). The nature of protein folding pathways: the classical versus the new view. *J Biomol NMR* 5, 103-9.

Baldwin, R. L.. (1996). On-pathway versus off-pathway folding intermediates. *Fold Des* 1, R1-8.

Ballinger, C. A., P. Connell, Y. Wu, Z. Hu, L. J. Thompson, L. Y. Yin, and C. Patterson. (1999). Identification of CHIP, a novel tetratricopeptide repeat-containing protein that interacts with heat shock proteins and negatively regulates chaperone functions. *Mol Cell Biol* 19, 4535-45.

Bardelli, A., P. Longati, D. Albero, S. Goruppi, C. Schneider, C. Ponzetto, and P. M. Comoglio. (1996). HGF receptor associates with the anti-apoptotic protein BAG-1 and prevents cell death. *EMBO J* 15, 6205-6212.

Barrick, D., and R. L. Baldwin. (1993). Three-state analysis of sperm whale apomyoglobin folding. *Biochemistry* 32, 3790-6.



- Basu, S., and P. K. Srivastava. (1999). Calreticulin, a peptide-binding chaperone of the endoplasmic reticulum, elicits tumor- and peptide-specific immunity. *J Exp Med* 189, 797-802.
- Beere, H. M., B. B. Wolf, K. Cain, D. D. Mosser, A. Mahboubi, T. Kuwana, P. Taylor, R. I. Morimoto, G. M. Cohen, and D. R. Green. (2000). Heat-shock protein 70 inhibits apoptosis by preventing recruitment of procaspase-9 to the Apaf-1 apoptosome. *Nat Cell Biol* 2, 469-75.
- Bellmann, K., M. Jaattela, D. Wissing, V. Burkart, and H. Kolb. (1996). Heat shock protein hsp70 overexpression confers resistance against nitric oxide. *FEBS Lett* 391, 185-8.
- Bimston, D., J. Song, D. Winchester, S. Takayama, J. C. Reed, and R. I. Morimoto. (1998). BAG-1, a negative regulator of Hsp70 chaperone activity, uncouples nucleotide hydrolysis from substrate release. *EMBO J* 17, 6871-6878.
- Binder, R. J., D. K. Han, and P. K. Srivastava. (2000). CD91: a receptor for heat shock protein gp96. *Nature Immunol* 1, 151-155.
- Blachere, N.E., Z. Li, R. Y. Chandawarkar, R. Suto, N. S. Jaikaria, S. Basu, H. Udono, and P. K. Srivastava. (1997). Heat shock protein-peptide complexes, reconstituted in vitro, elicit peptide-specific cytotoxic T lymphocyte response and tumor immunity. *J Exp Med* 186, 1315-22.
- Blond-Elguindi, S., S. E. Cwirla, W. J. Dower, R. J. Lipshutz, S. R. Sprang, J. F. Sambrook, and M. J. Gething. (1993). Affinity panning of a library of peptides displayed on bacteriophages reveals the binding specificity of BiP. *Cell* 75, 717-728.
- Blundell, T. L. and L. N. Johnson. (1976). Protein Crystallography. Academic Press, London.
- Bork, P., and M. Sudol. (1994). The WW domain: a signalling site in dystrophin? *Trends Biochem Sci* 19, 531-3.
- Boriack-Sjodin, P. A., S. M. Margarit, D. Bar-Sagi, and J. Kuriyan. (1998). The structural basis of the activation of Ras by Sos. *Nature* 394, 337-343.
- Bradford, M. M. (1976). A rapid and sensitive method for the quantitation of microgram quantities of protein utilizing the principle of protein-dye binding. *Anal Biochem* 72, 248-54.
- Braig, K., Z. Otwinowski, R. Hegde, D. C. Bisvert, A. Joachimiak, A. L. Horwich, and P. B. Sigler. (1994). The Crystallographic structure of the bacterial chaperonin GroEL at 2.8 Å. *Nature* 371, 578-86.
- Banchereau, J., and R. M. Steinman. (1998). Dendritic cells and the control of immunity. *Nature* 392, 245-52.

Bränden, C.I. and T. A. Jones. (1990). Between Objectivity and Subjectivity. *Nature* 343, 687-698.

Branden, C., and J. Tooze. (1991). Introduction to Protein Structure. Garland Publishing Inc., New York and London.

Briknarová, K., S. Takayama, L. Brive, M. L. Havert, D. A. Knee, J. Velasco, S. Homma, E. Cabezas, J. Stuart, D. W. Hoyt, A. C. Satterthwait, M. Llinas, J. C. Reed, and K. R. Ely. (2001). Structural analysis of BAG1 cochaperone and its interactions with Hsc70 heat shock protein. *Nat Struct Biol* 8, 349-352.

Brünger, A.T. (1992). Free R Value: A novel Statistical Quantity for Assessing the Accuracy of Crystallogral Structures. *Nature* 355, 472-475.

Brünger, A. T., P. D. Adams, G. M. Clore, W. L. DeLano, P. Gros, R. W. Grosse-Kunstleve, J. S. Jiang, J. Kuszewski, M. Nilges, N. S. Pannu, R. J. Read, L. M. Rice, T. Simonson, and G. L. Warren. (1998). Crystallograllography & NMR system: A new software suite for macromolecular structure determination. *Acta Crystallograllogr D* 54, 905-921.

Buchberger, A., H. Schroder, T. Hesterkamp, H. J. Schonfeld, and B. Bukau. (1996). Substrate shuttling between the DnaK and GroEL systems indicates a chaperone network promoting protein folding. *J Mol Biol* 261, 328-33.

Buerger, M.J. (1977). Kristallographie. de Gruyter, New York.

Bukau, B., E. Deuerling, C. Pfund, and E. A. Craig. (2000). Getting newly synthesized proteins into shape. *Cell* 101, 119-122.

Bukau B., and A. L. Horwich. (1998). The Hsp70 and Hsp60 chaperone machines. *Cell* 92, 351-366.

Carbone, F. R., C. Kurts, S. R. Bennett, J. F. Miller, and W. R. Heath. (1998). Cross-presentation: a general mechanism for CTL immunity and tolerance. *Immunol Today* 19, 368-73.

Castellino, F., P. E. Boucher, K. Eichelberg, M. Mayhew, J. E. Rothman, A. Houghton, and R. N. Germain. (2000). Receptor-mediated uptake of antigen/heat shock protein complexes results in major histocompatibility complex class I antigen presentation via two distinct processing pathways. *J Exp Med* 191, 1957-1964.

Chandawarkar, R. Y., M. S. Wagh, and P. K. Srivastava. (1999). The dual nature of specific activity of tumor-derived gp96 preparations. *J Exp Med* 189, 1437-1442.

Cheetham, M. E., J. P. Brion, and B. H. Anderton. (1992). Human homologues of the bacterial heat-shock protein DnaJ are preferentially expressed in neurons. *Biochem J* 284, 469-476.

- Chen, W., U. Syldath, K. Bellmann, V. Burkart, and H. Kolb. (1999). Human 60-kDa heat-shock protein: a danger signal to the innate immune system. *J Immunol* 162, 3212-3219.
- Chirico, W. J., M. G. Waters, and G. Blobel. (1988). 70K heat shock related proteins stimulate protein translocation into microsomes. *Nature* 332, 805-10.
- Collaborative Computational Project Number 4. (1994). *Acta Crystallogr D* 50, 760-3.
- Cohen, F. E. (2000). Prions, peptides and protein misfolding. *Mol Med Today* 6, 292-3.
- Connell, P., C. A. Ballinger, J. Jiang, Y. Wu, L. J. Thompson, J. Höhfeld, and C. Patterson. (2001). The co-chaperone CHIP regulates protein triage decisions mediated by heat-shock proteins. *Nat Cell Biol* 3, 93-96.
- Cowtan, K. D. and P. Main. (1993). Improvement of Macromolecular Electron-Density Maps by the Simultaneous Application of Real and Reciprocal Space Constrains. *Acta Crystallogr D* 50, 760-763.
- Cox, G. W., B. J. Mathieson, L. Gandino, E. Blasi, D. Radzioch, and L. Varesio. (1989). Heterogeneity of hematopoietic cells immortalized by v-myc/v-raf recombinant retrovirus infection of bone marrow or fetal liver. *J Natl Cancer Inst* 81, 1492-6.
- Cresswell, P., N. Bangia, T. Dick, and G. Diedrich. (1999). The nature of the MHC class I peptide loading complex. *Immunol Rev* 172, 21-8.
- Cyr, D. M., X. Lu, and M. G. Douglas. (1992). Regulation of Hsp70 function by a eukaryotic DnaJ homolog. *J Biol Chem* 267, 20927-20931.
- Dekker, P. J., and N. Pfanner. (1997). Role of mitochondrial GrpE and phosphate in the ATPase cycle of matrix Hsp70. *J Mol Biol* 270, 321-7.
- Deshaies, R. J., B. D. Koch, M. Werner-Washburne, E. A. Craig, and R. Schekman. (1988). A subfamily of stress proteins facilitates translocation of secretory and mitochondrial precursor polypeptides. *Nature* 332, 800-5.
- Deuerling, E., A. Schulze-Specking, T. Tomoyasu, A. Mogk A, and B. Bukau. (1999). Trigger factor and DnaK cooperate in folding of newly synthesized proteins. *Nature* 400, 693-6.
- Dobson, C. M. (1999). Protein misfolding, evolution and disease. *Trends Biochem Sci* 24, 329-32.
- Dobson, C. M., A. Sali, and M. Karplus. (1998). Proteinfaltung aus theoretischer und experimenteller Sicht. *Angewandte Chemie* 110, 908-935.
- Dodson, E., G. J. Kleywegt, and K. Wilson. (1996). Report of a Workshop on the Use of Statistical Validators in Protein X-Ray Crystallography. *Acta Crystallogr D* 52, 228-234.

- Doong, H., J. Price, Y. S. Kim, C. Gasbarre, J. Probst, L. A. Liotta, J. Blanchette, K. Rizzo, and E. Kohn. (2000). CAIR-1/BAG-3 forms an EGF-regulated ternary complex with phospholipase C-gamma and Hsp70/Hsc70. *Oncogene* 19, 4385-95.
- Drenth, J. (1994). Principles of Protein X-ray Crystallography. Springer-Verlag, New York.
- Ducruix, A., and R. Grige. (1992). Crystallograllization of Nucleic Acids and Proteins. A Practical Approach. Oxford University Press, Oxford.
- Ellis, R. J. (1997). Molecular chaperones: avoiding the crowd. *Curr Biol* 7, R531-3.
- Ellis, R. J. (2000). Chaperone substrates inside the cell. *Trends Biochem Sci* 25, 210-2.
- Engh, R.A., and R. Huber. (1991). Accurate Bond and Angle Parameters for X-ray Protein Structure Refinement. *Acta Crystallogr A* 47, 392-400.
- Esnouf, R. M. (1999). Further additions to MolScript version 1.4, including reading and contouring of electron-density maps. *Acta Crystallogr D* 55, 938-940.
- Ewalt, K. L., J. P. Hendrick, W. A. Houry, and F. U. Hartl. (1997). In vivo observation of polypeptide flux through the bacterial chaperonin system. *Cell* 90, 491-500.
- Fisher, E. A., M. Zhou, D. M. Mitchell, X. Wu, S. Omura, H. Wang, A. L. Goldberg, and H. N. Ginsberg. (1997). The degradation of apolipoprotein B100 is mediated by the ubiquitin-proteasome pathway and involves heat shock protein 70. *J Biol Chem* 272, 20427-34.
- Flaherty, K. M., C. DeLuca-Flaherty, and D. B. McKay. (1990). Three-dimensional structure of the ATPase fragment of a 70K heat-shock cognate protein. *Nature* 346, 623-628.
- Flaherty, K. M., D. B. McKay, W. Kabsch, and K. C. Holmes. (1991). Similarity of the three-dimensional structures of actin and the ATPase fragment of a 70-kDa heat shock cognate protein. *Proc Natl Acad Sci U S A* 88, 5041-5.
- Flynn, G. C., T. G. Chappell, and J. E. Rothman. (1989). Peptide binding and release by proteins implicated as catalysts of protein assembly. *Science* 245, 385-390.
- Frydman J., and J. Höhfeld. (1997). Chaperones get in touch: the Hip-Hop connection. *Trends Biochem Sci* 22, 87-92.
- Frydman J., E. Nimmesgern, K. Ohtsuka, and F. U. Hartl. (1994). Folding of nascent polypeptide chains in a high molecular mass assembly with molecular chaperones. *Nature* 370, 111-7.
- Fujihara, S. M., and S. G. Nadler. (1999). Intranuclear targeted delivery of functional NF-kappaB by 70 kDa heat shock protein. *EMBO J* 18, 411-9.

- Gabai, V. L., A. B. Meriin, D. D. Mosser, A. W. Caron, S. Rits, V. I. Shifrin, and M. Y. Sherman. (1997). Hsp70 prevents activation of stress kinases. A novel pathway of cellular thermotolerance. *J Biol Chem* 272, 18033-7.
- Gamer, J., G. Multhaup, T. Tomoyasu, J. S. McCarty, S. Rudiger, H. J. Schonfeld, C. Schirra, H. Bujard, and B. Bukau. (1996). A cycle of binding and release of the DnaK, DnaJ and GrpE chaperones regulates activity of the Escherichia coli heat shock transcription factor sigma32. *EMBO J* 15, 607-17.
- Gao, B., Y. Emoto, L. Greene, and E. Eisenberg. (1993). Nucleotide binding properties of bovine brain uncoating ATPase. *J Biol Chem* 268, 8507-13.
- Gao, B., L. Greene, and E. Eisenberg. (1994). Characterization of nucleotide-free uncoating ATPase and its binding to ATP, ADP, and ATP analogues. *Biochemistry* 33, 2048-54.
- Gebauer, M., M. Zeiner, and U. Gehring. (1997). Proteins interacting with the molecular chaperone hsp70/hsc70: physical associations and effects on refolding activity. *FEBS Lett* 417, 109-13.
- Germain, R. N. (1994). MHC-dependent antigen processing and peptide presentation: providing ligands for T lymphocyte activation. *Cell* 76, 287-99.
- Gething, M. J., and J. Sambrook. (1992). Protein folding in the cell. *Nature* 355, 33-45.
- Giacovazzo, C. (Editor). (1992). *Fundamentals of Crystallography*. Oxford University Press, Oxford.
- Glover, J. R., and S. Lindquist. (1998). Hsp104, Hsp70, and Hsp40: a novel chaperone system that rescues previously aggregated proteins. *Cell* 94, 73-82.
- Goodsell, D. S. (1991). Inside a living cell. *Trends Biochem Sci* 16, 203-6.
- Graham, F. L., J. Smiley, W. C. Russell, and R. Nairn. (1977). Characteristics of a human cell line transformed by DNA from human adenovirus type 5. *J Gen Virol* 36, 59-74.
- Guex, N. and M. C. Peitsch. (1997). Swiss-Model and the Swiss-Pdb Viewer: An environment for comparative protein modeling. *Electrophoresis* 18, 2714-2723.
- Ha, J.-H., and D. B. McKay. (1994). ATPase kinetics of recombinant bovine 70 kDa heat shock cognate protein and its amino-terminal ATPase domain. *Biochemistry* 33, 14625-14635.
- Ha, J.-H., and D.B. McKay. (1995). Kinetics of nucleotide-induced changes in the tryptophan fluorescence of the molecular chaperone Hsc70 and its subfragments suggest the ATP-induced conformational change follows initial ATP binding. *Biochemistry* 34, 11635-11644.

- Hanahan D. (1983). Studies on transformation of *Escherichia coli* with plasmids. *J Mol Biol* 166, 557-80.
- Hannan, L. A., S. L. Newmyer, and S. L. Schmid. (1998). ATP- and cytosol-dependent release of adaptor proteins from clathrin-coated vesicles: A dual role for Hsc70. *Mol Biol Cell* 9, 2217-29.
- Harker, D. and J. S. Kasper. (1948). Phases of fourier coefficients directly from Crystallogral diffraction data. *Acta Crystallogr* 1, 70-5.
- Harp, J. M., D. E. Timm, and G. J. Bunick. (1998). Macromolecular Crystallogral annealing: overcoming increased mosaicity associated with cryoCrystallograllography. *Acta Crystallogr D* 54, 622-8.
- Harrison, C. J., M. Hayer-Hartl, M. Di Liberto F. Hartl, and J. Kuriyan. (1997). Crystallogral structure of the nucleotide exchange factor GrpE bound to the ATPase domain of the molecular chaperone DnaK. *Science* 276, 431-435.
- Hartl, F. U. (1996). Molecular chaperones in cellular protein folding. *Nature* 381, 571-579.
- Hartley, A. D., M. A. Santos, D. R. Colthurst, and M. F. Tuite. (1996). Preparation and use of yeast cell-free translation lysate. *Methods Mol Biol* 53, 249-57.
- Hayer-Hartl, M. K., J. J. Ewbank, T. E. Creighton, and F. U. Hartl. (1994). Conformational specificity of the chaperonin GroEL for the compact folding intermediates of alpha-lactalbumin. *EMBO J* 13, 3192-202.
- Herendeen, S. L., R. A. VanBogelen, and F. C. Neidhardt. (1979). Levels of major proteins of *Escherichia coli* during growth at different temperatures. *J Bacteriol* 139, 185-94.
- Ho, A. K., G. A. Raczniak, E. B. Ives, and S. R. Wentz. (1998). The integral membrane protein snl1p is genetically linked to yeast nuclear pore complex function. *Mol Biol Cell* 9, 355-73.
- Höhfeld, J., and S. Jentsch. (1997). GrpE-like regulation of the hsc70 chaperone by the anti-apoptotic protein BAG-1. *EMBO J* 16, 6209-6216.
- Höhfeld, J., Y. Minami, and F. U. Hartl. (1995). Hip, a novel cochaperone involved in the eukaryotic Hsc70/Hsp40 reaction cycle. *Cell* 83, 589-98.
- Honing, S., G. Kreimer, H. Robenek, and B. M. Jockusch. (1994). Receptor-mediated endocytosis is sensitive to antibodies against the uncoating ATPase (hsc70). *J Cell Sci* 107, 1185-96.

- Honore, B., H. Leffers, P. Madsen, H. H. Rasmussen, J. Vandekerckhove, and J. E. Celis. (1992). Molecular cloning and expression of a transformation-sensitive human protein containing the TPR motif and sharing identity to the stress-inducible yeast protein STI1. *J Biol Chem* 267, 8485-91.
- Hoppe, W. (1957). Die Faltmolekülmethode: Eine neue Methode zur Bestimmung der Kristallstruktur bei ganz oder teilweise bekannten Molekülstrukturen. *Acta Crystallogr* 10, 750-751.
- Horwich, A. L., K. B. Low, W. A. Fenton, I. N. Hirshfield, and K. Furtak. (1993). Folding in vivo of bacterial cytoplasmic proteins: role of GroEL. *Cell* 74, 909-17.
- Huber, R. (1965) Die automatisierte Faltmolekülmethode. *Acta Crystallogr A* 19, 353-356.
- Huebers, H. A., and C. A. Finch. (1987). The physiology of transferrin and transferrin receptors. *Physiol Rev* 67, 520-582.
- Irmer, H., and J. Höhfeld. (1997). Characterization of functional domains of the eukaryotic co-chaperone Hip. *J Biol Chem* 272, 2230-5.
- Jaattela, M. (1993). Overexpression of major heat shock protein hsp70 inhibits tumor necrosis factor-induced activation of phospholipase A2. *J Immunol* 151, 4286-94.
- Jaattela, M., D. Wissing, K. Kokholm, T. Kallunki, and M. Egeblad. (1998). Hsp70 exerts its anti-apoptotic function downstream of caspase-3-like proteases. *EMBO J* 17, 6124-34.
- Jack, A. and M. Levitt. (1978). Refinement of large structures by simultaneous minimization of energy and R factor. *Acta Crystallogr. A* 34, 931-935.
- Jamin, M., and R. L. Baldwin. (1996). Refolding and unfolding kinetics of the equilibrium folding intermediate of apomyoglobin. *Nat Struct Biol* 3, 613-8.
- Jancarik, J. and S. K. Kim. (1991). Sparse matrix sampling: a screening method for Crystallograllization of proteins. *J. Appl. Crystallogr* 24, 409-11.
- Jensen, R. E., and A. E. Johnson. (1999). Protein translocation: is Hsp70 pulling my chain? *Curr Biol* 9, R779-82.
- Johnson, L. J., and E. A. Craig. (1997). Protein folding in vivo: unraveling complex pathways. *Cell* 90, 201-204.
- Jones, T.A., J. Y. Zou, S. W. Cowan, and M. Kjeldgaard. (1991). Improved Methods For Building Protein Models in Electron-Density Maps and the Location of Errors in These Models. *Acta Crystallogr A* 47, 110-119.
- Jordan, R., and R. McMacken. (1995). Modulation of the ATPase activity of the molecular chaperone DnaK by peptides and the DnaJ and GrpE heat shock proteins. *J Biol Chem* 270, 4563-9.

- Kang, P. J., J. Ostermann, J. Shilling, W. Neupert, E. A. Craig, and N. Pfanner. (1990). Requirement for hsp70 in the mitochondrial matrix for translocation and folding of precursor proteins. *Nature* 348, 137-43.
- Kanelakis, K. C., Y. Morishima, K. D. Dittmar, M. D. Galigniana, S. Takayama S, J. C. Reed, and W. B. Pratt. (1999). Differential effects of the hsp70-binding protein BAG-1 on glucocorticoid receptor folding by the hsp90-based chaperone machinery. *J Biol Chem* 274, 34134-40.
- Kanelakis, K. C., P. J. Murphy, M. D. Galigniana, Y. Morishima, S. Takayama, J. C. Reed, D. O. Toft, and W. B. Pratt. (2000). hsp70 interacting protein Hip does not affect glucocorticoid receptor folding by the hsp90-based chaperone machinery except to oppose the effect of BAG-1. *Biochemistry* 39, 14314-21.
- Karle, J., and H. Hauptmann. (1950). The phases and magnitudes of structure factors. *Acta Crystallogr* 3, 181-7.
- Karzai, A. W., and R. McMacken. (1996). A bipartite signalling mechanism involved in DnaJ-mediated activation of the Escherichia coli DnaK protein. *J Biol Chem* 271, 11236-46.
- Kleywegt, G. J. and A. T. Brünger. (1996). Checking Your Imagination: Applications of the Free R Value. *Structure* 4, 897-904.
- Klumpp, M., W. Baumeister, and L. O. Essen. (1997). Structure of the substrate binding domain of the thermosome, an archaeal group II chaperonin. *Cell* 91, 263-70.
- Kol, A., A. H. Lichtman, R. W. Finberg, P. Libby, and E. A. Kurt-Jones. (2000). Cutting edge: Heat shock protein (Hsp) 60 activates the innate immune response: CD14 is an essential receptor for Hsp60 activation of mononuclear cells. *J Immunol* 164, 13-17.
- Konnert, J.H., and W. A. Hendrickson. (1980). A restrained-parameter thermal factor refinement procedure. *Acta Crystallogr A* 36, 344-349.
- Kullmann, M., J. Schneikert, J. Moll, S. Heck, M. Zeiner, U. Gehring, and A. C. Cato. (1998). RAP46 is a negative regulator of glucocorticoid receptor action and hormone-induced apoptosis. *J Biol Chem* 273, 14620-5.
- Laemmli, U. K. (1970). Cleavage of structural proteins during the assembly of the head of bacteriophage T4. *Nature* 227, 680-5.
- Lamb, J. R., S. Tugendreich, and P. Hieter. (1995). Tetratricopeptide repeat interactions: to TPR or not to TPR? *Trends Biochem Sci* 20, 257-9.
- Lammert, E., D. Arnold, M. Nijenhuis, F. Momburg, G. J. Hammerling, J. Brunner, S. Stevanovic, H. G. Rammensee, and H. Schild. (1997). The endoplasmic reticulum-resident stress protein gp96 binds peptides translocated by TAP. *Eur J Immunol* 27, 923-7.



- Langer, T., G. Pfeifer, J. Martin, W. Baumeister, and F. U. Hartl. (1992). Chaperonin-mediated protein folding: GroES binds to one end of the GroEL cylinder, which accommodates the protein substrate within its central cavity. *EMBO J* 11, 4757-65.
- Langer, T., C. Lu, H. Echols, J. Flanagan, M. K. Hayer, and F. U. Hartl. (1992). Successive action of DnaK, DnaJ and GroEL along the pathway of chaperone-mediated protein folding. *Nature* 356, 683-9.
- Laskowski, R.A., M. W. McArthur, D. S. Moss, and J. M. Thornton. (1993). Procheck. A program to produce both detailed and schematic plots of protein structures. *J Appl Crystallogr* 26, 283-291.
- Lee, J. H., T. Takahashi, N. Yasuhara, J. Inazawa, S. Kamada, and Y. Tsujimoto. (1999). Bis, a Bcl-2-binding protein that synergizes with Bcl-2 in preventing cell death. *Oncogene* 18, 6183-90.
- Lehner, P. J., and P. Cresswell. (1996). Processing and delivery of peptides presented by MHC class I molecules. *Curr Opin Immunol* 8, 59-67.
- Leroux, M. R., and F. U. Hartl. (2000). Protein folding: versatility of the cytosolic chaperonin TRiC/CCT. *Curr Biol* 10, R260-4.
- Levinthal, C. (1968). *J Chim Phys* 65, 44-45.
- Levinthal, C. (1969). Mossbauer Spectroscopy in Biological Systems. Allerton House, Monticello, Illinois, University of Illinois Press, Urbana, 22.
- Li, C. Y., J. S. Lee, Y. G. Ko, J. I. Kim, and J. S. Seo. (2000). Heat shock protein 70 inhibits apoptosis downstream of cytochrome c release and upstream of caspase-3 activation. *J Biol Chem* 275, 25665-71.
- Liberek, K., J. Marszalek, D. Ang, C. Georgopoulos, and M. Zylicz. (1991). Escherichia coli DnaJ and GrpE heat shock proteins jointly stimulate ATPase activity of DnaK. *Proc Natl Acad Sci U S A* 88, 2874-2878.
- Liberek, K., D. Skowyra, M. Zylicz, C. Johnson, and C. Georgopoulos. (1991). The Escherichia coli DnaK chaperone, the 70-kDa heat shock protein eukaryotic equivalent, changes conformation upon ATP hydrolysis, thus triggering its dissociation from a bound target protein. *J Biol Chem* 266, 14491-14496.
- Liossis, S. N., X. Z. Ding, J. G. Kiang, and G. C. Tsokos. (1997). Overexpression of the heat shock protein 70 enhances the TCR/CD3- and Fas/Apo-1/CD95-mediated apoptotic cell death in Jurkat T cells. *J Immunol* 158, 5668-75.
- Liu, R., S. Takayama, Y. Zheng, B. Froesch, G. Q. Chen, X. Zhang, J. C. Reed, and X. K. Zhang. (1998). Interaction of BAG-1 with retinoic acid receptor and its inhibition of retinoic acid-induced apoptosis in cancer cells. *J Biol Chem* 273, 16985-16992.

- Lopez-Buesa, P., C. Pfund, and E. A. Craig. (1998). The biochemical properties of the ATPase activity of a 70-kDa heat shock protein (Hsp70) are governed by the C-terminal domains. *Proc Natl Acad Sci U S A* 95, 15253-8.
- Lüders, J., J. Demand, and J. Höhfeld. (2000). The ubiquitin-related BAG-1 provides a link between the molecular chaperones Hsc70/Hsp70 and the proteasome. *J Biol Chem* 275, 4613-4617.
- Lüders, J., J. Demand, O. Papp, and J. Höhfeld. (2000). Distinct isoforms of the cofactor BAG-1 differentially affect Hsc70 chaperone function. *J Biol Chem* 275, 14817-23.
- Martin, J., M. Mayhew, T. Langer, and F. U. Hartl. (1993). The reaction cycle of GroEL and GroES in chaperonin-assisted protein folding. *Nature* 366, 228-33.
- Maruya, M., M. Sameshima, T. Nemoto, and I. Yahara. (1999). Monomer arrangement in HSP90 dimer as determined by decoration with N and C-terminal region specific antibodies. *J Mol Biol* 285, 903-7.
- Massa, W. (1994). Kristallstrukturbestimmung. Teubner Studienbücher Chemie, Stuttgart.
- Matagne, A., S. E. Radford, and C. M. Dobson. (1997). Fast and slow tracks in lysozyme folding: insight into the role of domains in the folding process. *J Mol Biol* 267, 1068-74.
- Mayer, M. P., H. Schroder, S. Rudiger, K. Paal, T. Laufen, and B. Bukau. (2000). Multistep mechanism of substrate binding determines chaperone activity of Hsp70. *Nat Struct Biol* 7, 586-93.
- Mayhew, M., A. C. da Silva, J. Martin, H. Erdjument-Bromage, P. Tempst, and F. U. Hartl. (1996). Protein folding in the central cavity of the GroEL-GroES chaperonin complex. *Nature* 379, 420-6.
- McCarty, J. S., A. Buchberger, J. Reinstein, and B. Bukau. (1995). The role of ATP in the functional cycle of the DnaK chaperone system. *J Mol Biol* 249, 126-137.
- McClellan, A. J., and J. Frydman. (2001). Molecular chaperones and the art of recognizing a lost cause. *Nat Cell Biol* 3, E51-E53.
- McPherson, A. (1990). Current approaches to macromolecular Crystallograllization. *Eur J Biochem* 189, 1-23.
- McPherson, A. (1982). Preparation and analysis of protein Crystallograls. John Wiley & Sons, New York.
- McRee, D.E. (1993). Practical Protein Crystallogralligraphy. Academic Press, London.
- Meacham, G. C., C. Patterson, W. Zhang, J. M. Younger, and D. M. Cyr. (2001). The Hsc70 co-chaperone CHIP targets immature CFTR for proteasomal degradation. *Nat Cell Biol* 3, 100-105.

- Meriin, A. B., V. L. Gabai, J. Yaglom, V. I. Shifrin, and M. Y. Sherman. (1998). Proteasome inhibitors activate stress kinases and induce Hsp72. Diverse effects on apoptosis. *J Biol Chem* 273, 6373-9.
- Merritt, E.A. and D. J. Bacon. (1997). Raster3D: Photorealistic molecular graphics. *Meth Enzym* 276, 505-524.
- Miao, B., J. E. Davis, and E. A. Craig. (1997). Mge1 functions as a nucleotide release factor for Ssc1, a mitochondrial Hsp70 of *Saccharomyces cerevisiae*. *J Mol Biol* 265, 541-52.
- Minami, Y., J. Höhfeld, K. Ohtsuka, and F. U. Hartl. (1996). Regulation of the heat-shock protein 70 reaction cycle by the mammalian DnaJ homolog, Hsp40. *J Biol Chem* 271, 19617-19624.
- Morishima, Y., K. C. Kanelakis, A. M. Silverstein, K. D. Dittmar, L. Estrada, and W. B. Pratt. (2000). The Hsp organizer protein hop enhances the rate of but is not essential for glucocorticoid receptor folding by the multiprotein Hsp90-based chaperone system. *J Biol Chem* 275, 6894-900.
- Moroi, Y., M. Mayhew, J. Trcka, M. H. Hoe, Y. Takechi, F. U. Hartl, J. E. Rothman, and A. N. Houghton. (2000). Induction of cellular immunity by immunization with novel hybrid peptides complexed to heat shock protein 70. *Proc Natl Acad Sci U S A* 97, 3485-3490.
- Mosser, D. D., A. W. Caron, L. Bourget, C. Denis-Larose, and B. Massie. (1997). Role of the human heat shock protein hsp70 in protection against stress-induced apoptosis. *Mol Cell Biol* 17, 5317-27.
- Multhoff, G., C. Botzler, L. Jennen, J. Schmidt, J. Ellwart, and R. Issels. (1997). Heat shock protein 72 on tumor cells: a recognition structure for natural killer cells. *J Immunol* 158, 4341-4350.
- Multhoff, G., C. Botzler, M. Wiesnet, E. Muller, T. Meier, W. Wilmanns, and R. D. Issels. (1995). A stress-inducible 72-kDa heat-shock protein (HSP72) is expressed on the surface of human tumor cells, but not on normal cells. *Int J Cancer* 61, 272-279.
- Murakami, H., D. Pain, and G. Blobel. (1988). 70-kD heat shock-related protein is one of at least two distinct cytosolic factors stimulating protein import into mitochondria. *J Cell Biol* 107, 2051-7.
- Nagata, H., W. J. Hansen, B. Freeman, and W. J. Welch WJ. (1998). Mammalian cytosolic DnaJ homologues affect the hsp70 chaperone-substrate reaction cycle, but do not interact directly with nascent or newly synthesized proteins. *Biochemistry* 37, 6924-38.
- Nair, S., P. A. Wearsch, D. A. Mitchell, J. J. Wassenberg, E. Gilboa, and C. V. Nicchitta. (1999). Calreticulin displays in vivo peptide-binding activity and can elicit CTL responses against bound peptides. *J Immunol* 162, 6426-6432.

Nathan, D. F., M. H. Vos, and S. Lindquist. (1997). In vivo functions of the *Saccharomyces cerevisiae* Hsp90 chaperone. *Proc Natl Acad Sci U S A* 94, 12949-56.

Netzer, W. J., and F. U. Hartl. (1998). Protein folding in the cytosol: chaperonin-dependent and -independent mechanisms. *Trends Biochem Sci* 23, 68-73.

Newmyer, S. L., and S. L. Schmid. (2001). Dominant-interfering Hsc70 Mutants Disrupt Multiple Stages of the Clathrin-coated Vesicle Cycle In Vivo. *J Cell Biol* 152, 607-620.

Nguyen, T. H., D. T. Law, and D. B. Williams. (1991). Binding protein BiP is required for translocation of secretory proteins into the endoplasmic reticulum in *Saccharomyces cerevisiae*. *Proc Natl Acad Sci U S A* 88, 1565-9.

Nicchitta, C. V. (1998). Biochemical, cell biological and immunological issues surrounding the endoplasmic reticulum chaperone GRP94/gp96. *Curr Opin Immunol* 10, 103-9.

Nicholls, A., R. Bharadwaj, and B. Honig. (1993). Grasp – graphical representation and analysis of surface properties. *Biophys J* 64, A166.

Nieland, T. J. F., M. C. A. A. Tan, M. Monnee-van Muijen, F. Koning, A. M. Kruisbeek, and G. M. van Bleek. (1996). Isolation of an immunodominant viral peptide that is endogenously bound to the stress protein GP96/GRP94. *Proc Natl Acad Sci U S A* 93, 6135-6139.

Nollen, E. A., A. E. Kabakov, J. F. Brunsting, B. Kanon, J. Höhfeld, and H. H. Kampinga. (2001). Modulation of in Vivo HSP70 Chaperone Activity by Hip and Bag-1. *J Biol Chem* 276, 4677-4682.

Nollen, E. A., J. F. Brunsting, J. Song, H. H. Kampinga, and R. I. Morimoto. (2000). Bag1 functions in vivo as a negative regulator of Hsp70 chaperone activity. *Mol Cell Biol* 20, 1083-8.

O'Brien, M. C., and D. B. McKay. (1995). How potassium affects the activity of the molecular chaperone Hsc70. I. Potassium is required for optimal ATPase activity. *J Biol Chem* 270, 2247-50.

Obermann, W. M., H. Sonderrmann, A. A. Russo, N. P. Pavletich, and F. U. Hartl. (1998). In vivo function of Hsp90 is dependent on ATP binding and ATP hydrolysis. *J Cell Biol* 143, 901-10.

Oh, S., A. Iwahori, and S. Kato. (1993). Human cDNA encoding DnaJ protein homologue. *Biochim Biophys Acta* 1174, 114-116.

Ohashi, K., V. Burkat, S. Flohe, and H. Kolb. (2000). Cutting edge: Heat shock protein 60 is a putative endogenous ligand of the toll-like receptor-4 complex. *J Immunol* 164, 558-561.

- Ohtsuka, K. (1993). Cloning of a cDNA for heat-shock protein hsp40, a human homologue of bacterial DnaJ. *Biochem Biophys Res Commun* 197, 235-240.
- Otwinowski, Z., and W. Minor. (1997). Processing of X-ray diffraction data collected in oscillation mode. *Methods Enzymol* 276, 307-326.
- Pace, C. N., F. Vajdos, L. Fee, G. Grimsley, and T. Gray. (1995). How to measure and predict the molar absorption coefficient of a protein. *Protein Sci* 4, 2411-23.
- Packschies, L., H. Theyssen, A. Buchberger, B. Bukau, R. S. Goody, and J. Reinstein. (1997). GrpE accelerates nucleotide exchange of the molecular chaperone DnaK with an associative displacement mechanism. *Biochemistry* 36, 3417-3422.
- Palleros D. R., K .L Reid, L. Shi, W. J. Welch, and A. L Fink. (1993). ATP-induced protein-Hsp70 complex dissociation requires K<sup>+</sup> but not ATP hydrolysis. *Nature* 365, 664-666.
- Palleros, D. R., W. J. Welch, and A. L. Fink. (1991). Interaction of hsp70 with unfolded proteins: Effects of temperature and nucleotides on the kinetics of binding. *Proc Natl Acad Sci U S A* 88, 5719-5723.
- Pamer, E., and P. Cresswell. (1998). Mechanisms of MHC class I-restricted antigen processing. *Annu Rev Immunol* 16, 323-58.
- Panaretou, B., C. Prodromou, S. M. Roe, R. O'Brien, L. E. Ladbury, P. W. Piper, and L. H. Pearl. (1998). ATP binding and hydrolysis are essential to the function of the Hsp90 molecular chaperone in vivo. *EMBO J* 17, 4829-36.
- Panjwani, N., O. Akbari, S. Garcia, M. Brazil, and B. Stockinger. (1999). The HSC73 molecular chaperone: involvement in MHC class II antigen presentation. *J Immunol* 163, 1936-42.
- Parks, T. D., K. K. Leuther, E. D. Howard, S. A. Johnston, and W. G. Dougherty. (1994). Release of proteins and peptides from fusion proteins using a recombinant plant virus proteinase. *Anal Biochem* 216, 413-7.
- Patterson, A. L. (1934). A fourier series method for the determination of components of interatomic distances in Crystallograls. *Phys Rev* 46, 372-6.
- Patterson, A. L. (1935). A direct method for the determination of the components of interatomic distances in Crystallograls. *Z Kris* 90, 517-42.
- Pellecchia M., T. Szyperski, D. Wall, C. Georgopoulos, and K. Wuthrich. (1996). NMR structure of the J-domain and the Gly/Phe-rich region of the Escherichia coli DnaJ chaperone. *J Mol Biol* 260,236-50.
- Pellecchia M., D. L. Montgomery, S. Y. Stevens, C. W. Vander Kooi, H. P. Feng, L. M. Gierasch, and E. R. Zuiderweg. (2000). Structural insights into substrate binding by the molecular chaperone DnaK. *Nature Struct Biol* 7, 298-203.

- Perrakis, A., T. K. Sixma, K. S. Wilson, and V. S. Lamzin. (1997). wARP: improvement and extension of Crystallographic phases by weighted averaging of multiple refined dummy atomic models. *Acta Crystallog. D* 53, 448-455.
- Petersen, G., C. Hahn, and U. Gehring. (2001). Dissection of the ATP binding domain of the chaperone hsc70 for interaction with the cofactor Hsp46. *J Biol Chem* 276, 10178-84.
- Pfund, C., N. Lopez-Hoyo, T. Ziegelhoffer, B. A. Schilke, P. Lopez-Buesa, W. A. Walter, M. Wiedmann, and E. A. Craig. (1998). The molecular chaperone Ssb from *Saccharomyces cerevisiae* is a component of the ribosome-nascent chain complex. *EMBO J* 17, 3981-9.
- Pierce, M. M., C. S. Raman, and B. T. Nall. (1999). Isothermal titration calorimetry of protein-protein interactions. *Methods* 19, 213-21.
- Pilon, M., and R. Schekman. (1999). Protein translocation: how Hsp70 pulls it off. *Cell* 97, 679-682.
- Pratt, W. B., and D. O. Toft. (1997). Steroid receptor interactions with heat shock protein and immunophilin chaperones. *Endocr Rev* 18, 306-60.
- Pratt, W. B., A. M. Silverstein, and M. D. Galigniana. (1996). A model for the cytoplasmic trafficking of signalling proteins involving the hsp90-binding immunophilins and p50cdc37. *Cell Signal* 11, 839-51.
- Privalov, P. L. (1996). Intermediate states in protein folding. *J Mol Biol* 258, 707-25.
- Prodromou, C., B. Panaretou, S. Chohan, G. Siligardi, R. O'Brien, J. E. Ladbury, S. M. Roe, P. W. Piper, and L. H. Pearl. (2000). The ATPase cycle of Hsp90 drives a molecular 'clamp' via transient dimerization of the N-terminal domains. *EMBO J* 19, 4383-92.
- Przepiorka, D., and P. K. Srivastava. (1998). Heat shock protein-peptide complexes as immunotherapy for human cancer. *Mol Med Today* 4, 478-484.
- Ptitsyn, O. B. (1998). Protein folding: nucleation and compact intermediates. *Biochemistry (Mosc)* 63, 367-73.
- Qian, Y. Q., D. Patel, F. U. Hartl, and D. J. McColl. (1996). Nuclear magnetic resonance solution structure of the human Hsp40 (HDJ-1) J-domain. *J Mol Biol* 260, 224-35.
- Radford, S. E. (2000). Protein folding: progress made and promises ahead. *Trends Biochem Sci* 25, 611-618.
- Radford, S. E., C. M. Dobson, and P. A. Evans. (1992). The folding of hen lysozyme involves partially structured intermediates and multiple pathways. *Nature* 358, 302-7.
- Ralph, P., and I. Nakoinz. (1977). Antibody-dependent killing of erythrocyte and tumor targets by macrophage-related cell lines: enhancement by PPD and LPS. *J Immunol* 119, 950-954.

- Ramachandran, G. N., and V. Sasisekharan. (1968). Conformation of polypeptides and proteins. *Adv Protein Chem* 23, 283-438.
- Raynes, D. A., and V. Guerrier. (1998). Inhibition of Hsp70 ATPase activity and protein renaturation by a novel Hsp70-binding protein. *J Biol Chem* 273, 32883-8.
- Reed, R. C., and C. V. Nicchitta. (2000). Chaperone-mediated cross-priming: a hitchhiker's guide to vesicle transport. *Int J Mol Med* 6, 259-64.
- Rock, K. L. (1996). A new foreign policy: MHC class I molecules monitor the outside world. *Immunol Today* 17, 131-7.
- Rock, K. L., and A. L. Goldberg. (1999). Degradation of cell proteins and the generation of MHC class I-presented peptides. *Annu Rev Immunol* 17, 739-79.
- Rodriguez, A., A. Regnault, M. Kleijmeer, P. Ricciardi-Castagnoli, and S. Amigorena. (1999). Selective transport of internalized antigens to the cytosol for MHC class I presentation in dendritic cells. *Nat Cell Biol* 1, 362-8.
- Rossmann, M. G. (1972). The molecular replacement method. Gordon and Breach, New York.
- Rossmann, M.G. and D. M. Blow. (1962). The detection of subunits within the Crystallographic asymmetric unit. *Acta Crystallogr A* 15, 24-31.
- Rüdiger, S., L. Germeroth, S. Schneider-Mergener, and B. Bukau. (1997). Substrate specificity of the DnaK chaperone determined by screening cellulose-bound peptide libraries. *EMBO J* 16, 1501-1507.
- Saleh, A., S. M. Srinivasula, L. Balkir, P. D. Robbins, and E. S. Alnemri. (2000). Negative regulation of the Apaf-1 apoptosome by Hsp70. *Nat Cell Biol* 2, 476-83.
- Samali, A., and T. G. Cotter. (1996). Heat shock proteins increase resistance to apoptosis. *Exp Cell Res* 223, 163-70.
- Scheibel, T., T. Weikl, and J. Buchner. (1998). Two chaperone sites in Hsp90 differing in substrate specificity and ATP dependence. *Proc Natl Acad Sci U S A* 95, 1495-9.
- Scheraga, H. A., Y. Konishi, and T. Ooi. (1984). Multiple pathways for regenerating ribonuclease A. *Adv Biophys* 18, 21-41.
- Schild, H., D. Arnold-Schild, E. Lammert, and H.-G. Rammensee. (1999). Stress proteins and immunity mediated by cytotoxic T lymphocytes. *Curr Opin Immunol* 11, 109-113.
- Schechter, A.N., R. F. Chen, and C. B. Anfinsen. (1970). Kinetics of folding of staphylococcal nuclease. *Science* 167, 886-7.

- Scheufler, C., A. Brinker, G. Bourenkov, S. Pegoraro, L. Moroder, H. Bartunik, F. U. Hartl, and I. Moarefi. (2000). Structure of TPR domain-peptide complexes: critical elements in the assembly of the Hsp70-Hsp90 multichaperone machine. *Cell* 101, 199-210.
- Schirmer, E. C., J. R. Glover, M. A. Singer, and S. Lindquist. (1996) HSP100/Clp proteins: a common mechanism explains diverse functions. *Trends Biochem Sci* 21, 289-96.
- Schlossman, D. M., S. L. Schmid, W. A. Braell, and J. E. Rothman. (1984). An enzyme that removes clathrin coats: purification of an uncoating ATPase. *J Cell Biol* 99, 723-33.
- Schmid, D., A. Baici, H. Gehring, and P. Christen. (1994). Kinetics of molecular chaperone action. *Science* 263, 971-3.
- Schneider, U., H. U. Schwenk, and G. Bornkamm. (1977). Characterization of EBV-genome negative "null" and "T" cell lines derived from children with acute lymphoblastic leukemia and leukemic transformed non-Hodgkin lymphoma. *Int J Cancer* 19, 621-626.
- Schneikert, J., S. Hubner, E. Martin, and A. C. Cato. (1999). A nuclear action of the eukaryotic cochaperone RAP46 in downregulation of glucocorticoid receptor activity. *J Cell Biol* 146, 929-40.
- Schroder, H., T. Langer, F. U. Hartl, and B. Bukau. (1993). DnaK, DnaJ and GrpE form a cellular chaperone machinery capable of repairing heat-induced protein damage. *EMBO J* 12, 4137-44.
- Schultz, C. P. (2000). Illuminating folding intermediates. *Nat Struct Biol* 7, 7-10.
- Sharp, F. R., S. M. Massa, and R. A. Swanson. (1999). Heat-shock protein protection. *Trends Neurosci* 22, 97-9.
- Shen, Z., G. Reznikoff, G. Dranoff, and K. L. Rock. (1997). Cloned dendritic cells can present exogenous antigens on both MHC class I and class II molecules. *J Immunol* 158, 2723-30.
- Silverstein, A. M., M. D. Galigniana, M. S. Chen, J. K. Owens-Grillo, M. Chinkers, and W. B. Pratt. (1997). Protein phosphatase 5 is a major component of glucocorticoid receptor.hsp90 complexes with properties of an FK506-binding immunophilin. *J Biol Chem* 272, 16224-30.
- Simon, M. M., A. Reikerstorfer, A. Schwarz, C. Krone, T. A. Luger, M. Jaattela, and T. Schwarz. (1995). Heat shock protein 70 overexpression affects the response to ultraviolet light in murine fibroblasts. Evidence for increased cell viability and suppression of cytokine release. *J Clin Invest* 95, 926-33.
- Singh-Jasuja, H., H. U. Scherer, N. Hilf, D. Arnold-Schild, H. G. Rammensee, R. E. Toes, H. Schild. (2000). The heat shock protein gp96 induces maturation of dendritic cells and down-regulation of its receptor. *Eur J Immunol* 30, 2211-2215.



- Singh-Jasuja, H., R. E. Toes, P. Spee, C. Munz, N. Hilf, S. P. Schoenberger, P. Ricciardi-Castagnoli, J. Neefjes, H. G. Rammensee, D. Arnold-Schild, and H. Schild. (2000). Cross-presentation of glycoprotein 96-associated antigens on major histocompatibility complex class I molecules requires receptor-mediated endocytosis. *J Exp Med* 191, 1965-74.
- Smith, D. F. (2000). Chaperones in progesterone receptor complexes. *Semin Cell Dev Biol* 11, 45-52.
- Smith, D. F., W. P. Sullivan, T. N. Marion, K. Zaitsev, B. Madden, D. J. McCormick, D. O. Toft. (1993). Identification of a 60-kilodalton stress-related protein, p60, which interacts with hsp90 and hsp70. *Mol Cell Biol* 13, 869-76.
- Song, J. , M. Takeda, and R. I. Morimoto. (2001). Bag1-Hsp70 mediates a physiological stress signalling pathway that regulates Raf-1/ERK and cell growth. *Nature Cell Biol* 3, 276-82.
- Sondermann, H., C. Scheufler, C. Schneider, J. Höhfeld, F. U. Hartl, and I. Moarefi. (2001). Structure of a Bag/Hsc70 Complex: Convergent Functional Evolution of Hsp70 Nucleotide Exchange Factors. *Science* 291, 1553-1557.
- Spee, P., and J. Neefjes. (1997). TAP-translocated peptides specifically bind proteins in the endoplasmic reticulum, including gp96, protein disulfide isomerase and calreticulin. *Eur J Immunol* 27, 2441-9.
- Srivastava, P. K., A. B. DeLeo, and L. J. Old. (1986). Tumor rejection antigens of chemically induced sarcomas of inbred mice. *Proc Natl Acad Sci U S A* 83, 3407-3411.
- Srivastava, P. K., A. Menoret, S. Basu, R. J. Binder, and K. L. McQuade. (1998). Heat shock proteins come of age: Primitive functions acquire new roles in an adaptive world. *Immunity* 8, 657-665.
- Stebbins, C. E., A. A. Russo, C. Schneider, N. Rosen, F. U. Hartl, and N. P. Pavletich. (1997). Crystal structure of an Hsp90-geldanamycin complex: targeting of a protein chaperone by an antitumor agent. *Cell* 89, 239-50.
- Stuart, J. K., D. G. Myszka, L. Joss, R. S. Mitchell, S. M. McDonald, Z. Xie, S. Takayama, J. C. Reed, and K. R. Ely. (1998). Characterization of interactions between the anti-apoptotic protein BAG-1 and Hsc70 molecular chaperones. *J Biol Chem* 273, 22506-22514.
- Sundstrom, C., and K. Nilsson. (1976). Establishment and characterization of a human histiocytic lymphoma cell line (U-937). *Int J Cancer* 17, 565-77.
- Suto, R., and P. K. Srivastava. (1995). A mechanism for the specific immunogenicity of heat shock protein- chaperoned peptides. *Science* 269, 1585-1588.

- Szabo, A., T. Langer, H. Schroder, J. Flanagan, B. Bukau, and F. U. Hartl. (1994). The ATP hydrolysis-dependent reaction cycle of the Escherichia coli Hsp70 system DnaK, DnaJ, and GrpE., *Proc Natl Acad Sci U S A* 91, 10345-10349.
- Szabo, A., R. Korszun, F. U. Hartl, and J. Flanagan. (1996). A zinc finger-like domain of the molecular chaperone DnaJ is involved in binding to denatured protein substrates. *EMBO J* 15, 408-17.
- Szyperski, T., M. Pellicchia, D. Wall, C. Georgopoulos, and K. Wuthrich. (1994). NMR structure determination of the Escherichia coli DnaJ molecular chaperone: secondary structure and backbone fold of the N-terminal region (residues 2-108) containing the highly conserved J domain. *Proc Natl Acad Sci U S A* 91, 11343-7.
- Takayama, S., T. Sato, S. Krajewski, K. Kochel, S. Irie, J. A. Millan, and J. C. Reed. (1995). Cloning and functional analysis of BAG-1: a novel Bcl-2-binding protein with anti-cell death activity. *Cell* 80, 279-284.
- Takayama, S., D. N. Bimston, S. Matsuzawa, B. C. Freeman, C. Aime-Sempe, Z. Xie, R. I. Morimoto, and J. C. Reed. (1997). BAG-1 modulates the chaperone activity of Hsp70/Hsc70. *EMBO J* 16, 4887-4896.
- Takayama, S., Z. Xie, and J. C. Reed. (1999). An evolutionarily conserved family of Hsp70/Hsc70 molecular chaperone regulators. *J Biol Chem* 274, 781-786.
- Takeda, S., and D. B. McKay. (1996). Kinetics of peptide binding to the bovine 70 kDa heat shock cognate protein, a molecular chaperone. *Biochemistry* 35, 4636-44.
- Taniuchi, H., and C. B. Anfinsen. (1969). An experimental approach to the study of the folding of staphylococcal nuclease. *J Biol Chem* 244, 3864-75.
- Terada, K., and M. Mori. (2000). Human DnaJ homologs dj2 and dj3, and bag-1 are positive cochaperones of hsc70. *J Biol Chem* 275, 24728-34.
- Terwilliger, T. C., and J. Berendzen. (1999). Automated MAD and MIR structure solution. *Acta Crystallogr D* 55, 849-861.
- Teter, S. A., W. A. Houry, D. Ang, T. Tradler, D. Rockabrand, G. Fischer, P. Blum, C. Georgopoulos, and F. U. Hartl. (1999). Polypeptide flux through bacterial Hsp70: DnaK cooperates with trigger factor in chaperoning nascent chains. *Cell* 97, 755-65.
- They, C., A. Regnault, J. Garin, J. Wolfers, L. Zitvogel, P. Ricciardi-Castagnoli, G. Raposo, and S. Amigorena. (1999). Molecular characterization of dendritic cell-derived exosomes. Selective accumulation of the heat shock protein hsc73. *J Cell Biol* 147, 599-610.
- Theysen, H., H. P. Schuster, L. Packschies, B. Bukau, and J. Reinstein. (1996). The second step of ATP binding to DnaK induces peptide release. *J Mol Biol* 263, 657-670.

- Todryk, S., A. A. Melcher, N. Hardwick, E. Linardakis, A. Bateman, M. P. Colombo, A. Stoppacciaro, and R. G. Vile. 1999. Heat shock protein 70 induced during tumor cell killing induces Th1 cytokines and targets immature dendritic cell precursors to enhance antigen uptake. *J Immunol* 163, 1398-1408.
- Towbin, H., T. Staehelin, and J. Gordon. (1979). Electrophoretic transfer of proteins from polyacrylamide gels to nitrocellulose sheets: procedure and some applications. *Proc Natl Acad Sci U S A* 76, 4350-4.
- Tsuchiya, S., M. Yamabe, Y. Yamaguchi, Y. Kobayashi, T. Konno, and K. Tada. (1980). Establishment and characterization of a human acute monocytic leukemia cell line (THP-1). *J Cancer* 26, 171-6.
- Udgaonkar, J. B., and R. L. Baldwin. (1990). Early folding intermediate of ribonuclease A. *Proc Natl Acad Sci U S A* 87, 8197-201.
- Udono, H., and P. K. Srivastava. (1994). Comparison of tumor-specific immunogenicities of stress-induced proteins gp96, hsp90, and hsp70. *J Immunol* 152, 5398-5403.
- Vainberg, I. E., S. A. Lewis, H. Rommelaere, C. Ampe, J. Vandekerckhove, H. L. Klein, and N. J. Cowan. (1998). Prefoldin, a chaperone that delivers unfolded proteins to cytosolic chaperonin. *Cell* 93, 863-73.
- van den IJssel, P., D. G. Norman, and R. A. Quinlan. (1999). Molecular chaperones: small heat shock proteins in the limelight. *Curr Biol* 9, R103-5.
- Velten, M., B. O. Villoutreix, M. M. Ladjimi. (2000). Quaternary structure of the HSC70 cochaperone HIP. *Biochemistry* 39, 307-15.
- Wall, D., M. Zylicz, and C. Georgopoulos. (1994). The NH<sub>2</sub>-terminal 108 amino acids of the Escherichia coli DnaJ protein stimulate the ATPase activity of DnaK and are sufficient for lambda replication. *J Biol Chem* 269, 5446-51.
- Wallace, A. C., R. A. Laskowski, and J. M. Thornton. (1995). LIGPLOT: a program to generate schematic diagrams of protein-ligand interactions. *Protein Eng* 8, 127-134.
- Wang, H.-G., S. Takayama, U. R. Rapp, and J. C Reed. (1996). Bcl-2 interacting protein, BAG-1, binds to and activates the kinase Raf-1. *Proc Natl Acad Sci U S A* 93, 7063-7068.
- Wanker, E. E. (2000). Protein aggregation in Huntington's and Parkinson's disease: implications for therapy. *Mol Med Today* 6, 387-91.
- Wassenberg, J. J., C. Dezfalian, and C. V. Nicchitta. (1999). Receptor mediated and fluid phase pathways for internalization of the ER hsp90 chaperone GRP94 in murine macrophages. *J Cell Sci* 112, 2167-2175.
- Watts, C. (1997). Capture and processing of exogenous antigens for presentation on MHC molecules. *Annu Rev Immunol* 15, 821-50.

Weaver, A. J., W. P. Sullivan, S. J. Felts, B. A. Owen, and D. O. Toft. (2000). Crystal structure and activity of human p23, a heat shock protein 90 co-chaperone. *J Biol Chem* 275, 23045-52.

Weber, F., F. Keppel, C. Georgopoulos, M. K. Hayer-Hartl, and F. U. Hartl. (1998). The oligomeric structure of GroEL/GroES is required for biologically significant chaperonin function in protein folding. *Nat Struct Biol* 5, 977-85.

Wetlaufer, D. B. (1962). Ultraviolet spectra of proteins and amino acids. *Advanced Protein Chemistry* 17, 303-91.

Wilbanks, S. M., D. B. McKay. (1995). How potassium affects the activity of the molecular chaperone Hsc70. II. Potassium binds specifically in the ATPase active site. *J Biol Chem* 270, 2251-7.

Wildegger, G., and T. Kiefhaber. (1997). Three-state model for lysozyme folding: triangular folding mechanism with an energetically trapped intermediate. *J Mol Biol* 270, 294-304.

Wiseman, T., S. Williston, J. F. Brandts, and L. N. Lin. (1989). Rapid measurement of binding constants and heats of binding using a new titration calorimeter. *Anal Biochem* 179, 131-7.

Woolfson, M. M. (1970). X-Ray Crystallography. Cambridge University Press, London.

Yan, W., B. Schilke, C. Pfund, W. Walter, S. Kim, and E. A. Craig. (1998). Zuotin, a ribosome-associated DnaJ molecular chaperone. *EMBO J* 17, 4809-17.

Yang, X., G. Chernenko, Y. Hao, Z. Ding, M. M. Pater, A. Pater, and S. C. Tang . (1998). Human BAG-1/RAP46 protein is generated as four isoforms by alternative translation initiation and overexpressed in cancer cells. *Oncogene* 17, 981-9.

Yewdell, J. W., C. C. Norbury, and J. R. Bennink. (1999). Mechanisms of exogenous antigen presentation by MHC class I molecules in vitro and in vivo: implications for generating CD8+ T cell responses to infectious agents, tumors, transplants, and vaccines. *Adv Immunol* 73, 1-77.

Young, J. C., C. Schneider, and F. U. Hartl. (1997). In vitro evidence that hsp90 contains two independent chaperone sites. *FEBS Lett* 418, 139-43.

Young, J. C., W. M. Obermann, and F. U. Hartl. (1998). Specific binding of tetratricopeptide repeat proteins to the C-terminal 12-kDa domain of hsp90. *J Biol Chem* 273, 18007-10.

Young, J. C., and F. U. Hartl. (2000). Polypeptide release by Hsp90 involves ATP hydrolysis and is enhanced by the co-chaperone p23. *EMBO J* 19, 5930-5940.

Zarrinpar, A., and W. A. Lim. (2000). Converging on proline: the mechanism of WW domain peptide recognition. *Nat Struct Biol* 7, 611-3.

Zeiner, M., Y. Niyaz, and U. Gehring. (1999). The hsp70-associating protein Hap46 binds to DNA and stimulates transcription. *Proc Natl Acad Sci U S A* 96, 10194-9.

Zeiner, M., M. Gebauer, and U. Gehring. (1997). Mammalian protein RAP46: an interaction partner and modulator of 70 kDa heat shock proteins. *EMBO J* 16, 5483-5490.

Zhu, X., X. Zhao, W. F. Burkholder, A. Gragerov, C. M. Ogata, M. E. Gottesman, and W. A. Hendrickson. (1996). Structural analysis of substrate binding by the molecular chaperone DnaK. *Science* 272, 1606-14.

## F Appendix

### F.1 Amino acid sequences of Hsc70 and Bag-1M

#### F.1.1 Amino acid sequence of rat Hsc70

```

1  mskgpavgid  lggtyscvgv  fqhgkveiia  ndqgnrttps  yvaftdterl  igdaaknqva
61  mnptntvfda  krligrrfdd  avvqsdmkhw  pfmvvdagr  pkvqveykge  tksfypeevs
121 smvltkmkei  aeaylgktvt  navvtvpayf  ndsqrqatkd  agtiaglnvl  riineptaaa
181 iaygldkkvg  aernvlifdl  gggtfdvsil  tiedgifevk  stagdthlgg  edfdnrmvnh
241 fiaefkrkhk  kdisenkrav  rrlrtacera  krtlssstqa  sieidslyeg  idfytsitra
301 rfeelnadlf  rgtldpveka  lrdakldksq  ihdivlvggs  tripkiqkll  qdffngkeln
361 ksinpdeava  ygaavqaail  sgdksenvqd  lllldvtpls  lgietaggvm  tvlikrntti
421 ptkqtqftt  ysdnqpgvli  qvyegeramt  kdnllgkfe  ltgippaprg  vpqievtfdi
481 dangilnvsa  vdkstgkenk  ititndkgrl  skediermvq  eaekykaede  kqrdkvsskn
541 slesyafnmk  atvedeklqg  kindedkqki  ldkcneiisw  ldknqtaeke  efehqqkele
601 kvcnpiitkl  yqsaggmpgg  mppggfpgga  ppsggassgp  tieevd

```

**Figure 38.** Amino acid sequence of Hsc70 from *rattus norvegicus* (Accession number: S07197). The fragment used for crystallization (residues 5-381) is indicated in bold.

#### F.1.2 Amino acid sequence of human Bag-1M

```

1  mkkktrrrst  rseeltrsee  ltlseeatws  eeatqseeat  qgeemnrsqe  vtrdeestr
61  eevtreema  agltvtvths  nekhdhvt  qqgssepvvq  dlaqvveevi  gvpqsfqli
121 fkgkslkeme  tplsalmiqd  gcrvmligk  nspqeevelk  klkhleksve  kiadqleeln
181 keltgiqqgf  lpkdlqaeal  ckldrrvkat  ieqfmkilee  idtlilpenf  kdsrlkrkgl
241 vkqvqaflae  cdtveqnicq  eterlqstnf  alae

```

**Figure 39.** Amino acid sequence of Bag-1M from *rattus norvegicus* (Accession number: XP\_005538). The fragment used for crystallization (residues 151-263) is indicated in bold.

## F.2 Abbreviations

$\mu$	micro ( $10^{-6}$ )
(v/v)	volume/volume
(w/v)	weight/volume
Å	Angström (=0.1 nm)
<i>A. thaliana</i>	<i>Arabidopsis thaliana</i>
AA/BisAA	acrylamide/Bis-acrylamide
Ac	acetate
ADP	adenosine 5'-diphosphate
APC	antigen presenting cell
ATP	adenosine 5'-triphosphate
Bag	Bcl2-associated athanogene
BiP	binding protein
<i>C. elegans</i>	<i>Caenorhabditis elegans</i>
CCT	chaperonin-containing TCP-1
cdc	cell division cycle
CHIP	carboxyl-terminus Hsc70-interacting protein
CTL	cytotoxic T lymphocyte
<i>D. melanogaster</i>	<i>Drosophila melanogaster</i>
Da	dalton
ddH <sub>2</sub> O	double-distilled water
DDT	Dithiothreitol
DNA	deoxyribonucleic acid
dNTP	dideoxy-nucleoside triphosphate
<i>E. coli</i>	<i>Escherichia coli</i>
EDTA	ethylenediaminetetraacetic acid
ER	endoplasmic reticulum
FACS	fluorescence-activated cell sorting
FCS	fetal calf serum
FITC	fluorescein-isothiocyanate
FPLC	fast performance liquid chromatography

---

g	gram
GM-CSF	granulocyte/macrophage-colony stimulating factor
Grp78	glucose-regulated protein 78 kDa
Grp94	glucose-regulated protein 94 kDa
GST	glutathione-S-transferase
GTP	guanosine 5'-triphosphate
HEPES	N-(2-hydroxyethyl)piperazine-N'-(2-ethanesulfonic acid)
HGF	hepatocyte growth factor
Hip	Hsc70 interacting protein
Hop	heat shock organizing protein
Hsc	heat shock cognate protein
Hsp	heat shock protein
HspBP1	heat shock protein binding protein 1
Ibp	inclusion body binding protein
IL-4	interleukine 4
IPTG	isopropyl- $\beta$ -D-thiogalactopyranoside
ITC	isothermal titration calorimetry
k	kilo ( $=10^3$ )
$K_D$	thermodynamical binding constant
l	liter
LB	Luria-Bertani
LBD	ligand-binding domain
LPS	lipopolysaccharide
M	molar
m	milli ( $10^{-3}$ )
MAD	multiple anomalous dispersion
MHC	major histocompatibility complex
min	minutes
MIR	multiple isomorphous replacement
MR	molecular replacement
n	nano ( $=10^{-9}$ )
OD	optical density
$P_i$	inorganic phosphate



---

PAGE	polyacrylamide gelelectrophoresis
PBL	peripheral blood lymphocytes
PBMC	peripheral blood monocytes
PBS	phosphate-buffered saline
PCR	polymerase chain reaction
PDB	Protein Data Base
PDGF	platelet-derived growth factor
PE	R-phycoerythrin
PEG	polyethylene glycol
rmsd	route mean square deviation
<i>S. cerevisiae</i>	<i>Saccharomyces cerevisiae</i>
<i>S. pombe</i>	<i>Schizosaccharomyces pombe</i>
SDS	sodium dodecylsulfate
sec	seconds
SeMet	selenomethionine
$t_{1/2}$	half time
TAP	transporter in antigen processing
TB	terrific broth
TCP-1	T-complex contained protein 1
TEMED	N,N,N',N'-tetramethylethylenediamine
TEV	tobacco etch virus
TLC	thin layer chromatography
TNF $\alpha$	tumor necrosis factor $\alpha$
TPR	tetratrico peptide repeat
TriC	TCP-1 ring complax
Tris	Tris(hydroxymethyl)aminomethane
U	Unit
WB	Western blot

### F.3 Publications

- **Sondermann, H.**, C. Scheufler, C. Schneider, J. Höhfeld, F. U. Hartl, and Ismail Moarefi. (2001). Structure of a Bag/Hsc70 complex: convergent functional evolution of Hsp70 nucleotide exchange factors. *Science* 291: 1553-1557.
- **Sondermann, H.**, T. Becker, M. Mayhew, F. Wieland, and F. U. Hartl. 2000. Characterization of a Receptor for Heat Shock Protein 70 on Macrophages and Monocytes. *Biol Chem* 381: 1165-1174.
- Obermann W. M. J., **H. Sondermann**, A. A. Russo, N. P. Paveletich, and F. U. Hartl. (1998). In vivo function of Hsp90 is dependent on ATP binding and ATP hydrolysis. *J Cell Biol* 143(4): 901-910.

### F.4 Published Meeting Abstracts

- **Sondermann, H.**, T. Becker, M. Mayhew, F. Wieland, and F. U. Hartl. (2000). Characterization of a monocyte/macrophage-specific receptor for heat shock protein 70. FALL MEETING OF THE GESELLSCHAFT FÜR BIOCHEMIE UND MOLEKULARBIOLOGIE. Munich, October 10-13, 2000. *Biol Chem* 381(Supplement Issue): S219.

### F.5 Unpublished Meeting Abstracts

- **Sondermann H.**, C. Scheufler, C. Schneider, J. Höhfeld, F. U. Hartl, and I. Moarefi. (2001). Structure of a Bag domain/Hsc70 ATPase domain Complex: Convergent Functional Evolution of Hsp70 Nucleotide Exchange Factors. EuroConference /EMBO workshop "Mechanisms and Cellular Functions of Molecular Chaperones": May 26 - 31, 2001.
- **Sondermann H.**, T. Becker, F. Wieland, and F. U. Hartl. (2000). Receptor-mediated Binding and Uptake of Heat Shock Protein 70 by Antigen Presenting Cells. COLD SPRING HARBOR MEETING "Molecular Chaperones & Heat Shock Response": May 3-7, 2000.
- **Sondermann H.**, W. M. J. Obermann, A. A. Russo, N. P. Paveletich, and F. U. Hartl. (1999). In vivo function of Hsp90 is dependent on ATP binding and ATP hydrolysis. KEYSTONE SYMPOSIUM "Protein Folding, Degradation and Molecular Chaperones": April 10-16, 1999.

Danksagung:

Die vorliegende Arbeit wurde in der Zeit von Dezember 1997 bis März 2001 am Max-Planck-Institut für Biochemie, Abteilung Zelluläre Biochemie, in Martinsried angefertigt.

Mein besonderer Dank gilt Prof. Dr. F.-Ulrich Hartl für seine freundschaftliche Kollegialität, seine intensive Förderung und Unterstützung, weiterhin für die Bereitstellung des spannenden Themas und der hervorragenden Arbeitsbedingungen.

Ebenfalls möchte ich Herrn Dr. Ismail Moarefi meinen Dank aussprechen für seine uneingeschränkte Unterstützung und seinen grenzenlosen Optimismus, die wesentlich zum Gelingen dieser Arbeit beitrugen. Ich danke ihm besonders für die hervorragende Anleitung bei den kristallographischen Arbeiten und der Strukturanalyse.

Dr. Sabine Waffenschmidt, Institut für Biochemie der Universität zu Köln, danke ich für die freundliche Übernahme der Betreuung dieser extern durchgeführten Arbeit und für die Übernahme der Begutachtung.

Prof. Dr. Thomas Langer möchte ich danken für die Übernahme des Zweitgutachtens.

Meinen Kollegen Peter Breuer, Achim Brinker, Matt Tector, Sarah Teter und Jason Young danke ich für zahllose Stunden interessanter Diskussionen, uneingeschränkter Hilfestellung, und für das sehr motivierende Arbeitsumfeld.

Für seine fachliche Unterstützung bei der Datensammlung und Strukturlösung danke ich Dr. Clemens Scheufler.

Allen Mitarbeitern der Abteilung Zelluläre Biochemie danke ich für die freundschaftliche Atmosphäre.

## *Curriculum vitae*

Holger Sondermann  
geboren am 12. Oktober 1972 in Köln-Porz

### **Wissenschaftlicher Werdegang**

#### **Dissertation**

Nov, 1997-heute Experimentelle Doktorarbeit im Labor von Prof. Dr. Franz-Ulrich Hartl am Max-Planck-Institut für Biochemie (Abteilung Zelluläre Biochemie).  
Themen: 1. Charakterisierung eines Monozyten/Makrophagen-spezifischen Rezeptors für Hsp70.  
2. Struktur-Funktions-Analyse des Hsp70-Kochaperons Bag-1 (in Kolaboration mit Dr. Ismail Moarefi).

#### **Studium**

Jan, 1997-Okt, 1997 Diplomarbeit am Institut für Biochemie II der Medizinischen Fakultät an der Universität zu Köln im Labor von Prof. Mats Paulsson unter Anleitung von Dr. Monique Aumailley.  
Thema: Biochemische Analyse verschiedener Zelladhäsionsverbindungen.  
Dez, 1996 Diplomhauptprüfung  
Fächer: Biochemie (Hauptfach)  
Entwicklungsbiologie  
Organische Chemie  
Okt, 1995-Feb, 1996 Forschungspraktikum am Institut für Biochemie II der Medizinischen Fakultät an der Universität zu Köln unter Anleitung von Prof. Mats Paulsson.  
Thema: Reinigung und biochemische Charakterisierung von Laminin-Isoformen gereinigt aus verschiedenen Geweben.  
April, 1995 Diplomvorprüfung  
Fächer: Botanik, Zoologie, Chemie und Physik  
Okt, 1993-Okt, 1997 Studium der Biologie an der Universität zu Köln (Wintersemester 1993/94 bis Sommersemester 1997/98)  
Okt, 1992-Okt, 1993 Studium der Chemie an der Universität zu Köln (Wintersemester 1992/93 und Sommersemester 1993)

#### **Hochschulreife**

12. Juni 1992 Kaiserin-Theophanu Gymnasium (Köln-Kalk)

Ich versichere, daß ich die von mir vorgelegte Dissertation selbständig angefertigt, die benutzten Quellen und Hilfsmittel vollständig angegeben und die Stellen der Arbeit - einschließlich Tabellen, Karten und Abbildungen -, die anderen Werken im Wortlaut oder dem Sinn nach entnommen sind, in jedem Einzelfall als Entlehnung kenntlich gemacht habe; daß diese Dissertation noch keiner anderen Fakultät oder Universität zur Prüfung vorgelegen hat; daß sie - abgesehen von oben angegebenen Teilpublikationen - noch nicht veröffentlicht worden ist sowie, daß ich eine solche Veröffentlichung vor Abschluß des Promotionsverfahrens nicht vornehmen werde. Die Bestimmungen dieser Promotionsordnung sind mir bekannt. Die von mir vorgelegte Dissertation ist von Dr. Sabine Waffenschmidt (Köln) und Prof. Dr. F.-Ulrich Hartl (Martinsried) betreut worden.

Holger Sondermann